High performance ductile and pseudo-ductile polymer matrix composites
A review

Wisnom, M. R.; Pimenta, S.; Shaffer, M. S.P.; Robinson, P.; Potter, K. D.; Hamerton, I.; Czél, G.; Jalalvand, M.; Fotouhi, M.; More Authors

DOI
10.1016/j.compositesa.2024.108029

Publication date
2024

Document Version
Final published version

Published in
Composites Part A: Applied Science and Manufacturing

Composites: Part A 181 (2024) 108029

Contents lists available at ScienceDirect

Composites Part A

journal homepage: www.elsevier.com/locate/compositesa

Review

High performance ductile and pseudo-ductile polymer matrix composites: A review

M.R. Wisnom [a,*], S. Pimenta [b], M.S.P. Shaffer [b], P. Robinson [b], K.D. Potter [a], I. Hamerton [a], G. Czél [c,d], M. Jalalvand [e], M. Fotouhi [f], D.B. Anthony [b], H. Yu [g], M.L. Longana [h], X. Wu [a], A. Bismarck [b,i]

[a] Bristol Composites Institute, University of Bristol, United Kingdom
[b] Imperial College, London, United Kingdom
[c] Budapest University of Technology and Economics, Faculty of Mechanical Engineering, Department of Polymer Engineering, Hungary
[d] MTA-BME Lendület Sustainable Polymers Research Group, Budapest, Hungary
[e] Engineering Materials, School of Engineering, University of Southampton, United Kingdom
[f] Technical University of Delft, Netherlands
[g] University of Bath, United Kingdom
[h] Polytechnic of Milan, Italy
[i] University of Vienna, Austria

A B S T R A C T

The ability of fibre reinforced composites to deform with a non-linear stress–strain response and gradual, rather than sudden, catastrophic failure is reviewed. The principal mechanisms by which this behaviour can be achieved are discussed, including ductile fibres, progressive fibre fracture and fragmentation, fibre reorientation, and slip between discontinuous elements. It is shown that all these mechanisms allow additional strain to be achieved, enabling a yield-like behaviour to be generated. In some cases, the response is ductile and in others pseudo-ductile. Mechanisms can also be combined, and composites which give significant pseudo-ductile strain can be produced. Notch sensitivity is reduced, and there is the prospect of increasing design strains whilst also improving damage tolerance. The change in stiffness or visual indications of damage can be exploited to give warning that strain limits have been exceeded. Load carrying capacity is still maintained, allowing continued operation until repairs can be made. Areas for further work are identified which can contribute to creating structures made from high performance ductile or pseudo-ductile composites that fail gradually.

1. Introduction

Fibre-reinforced polymer (FRP) composites offer exceptional strength, stiffness, and durability. When combined with their low density, excellent corrosion and environmental resistance, they are increasingly the materials of choice for many high-performance applications. However, a major drawback is that they normally exhibit sudden brittle failure, with a linear elastic response right up to the point of final fracture. Although some analyses suggest the possibility of gradual degradation in laminates as a result of successive ply failures, such behaviour is rarely observed experimentally, and failure is normally catastrophic with little prior indication that it is about to occur. The severe consequences of such abrupt failures have sparked the quest to create materials and architectures that give a more gradual failure with indications of damage whilst retaining the other excellent properties of composites.

Ductility is normally defined as the ability to sustain plastic deformation under load before failure, typically with a plateau in the stress–strain response and no loss of modulus on reloading. It is very important in achieving progressive rather than sudden failure, increasing toughness and absorbing energy. It is also crucial in redistributing load at stress concentrations, thus reducing notch sensitivity that often leads to catastrophic structural failure. Truly ductile response is very difficult to achieve with current high-performance composites, such as carbon fibre / epoxy, where both constituents are themselves brittle. Using a ductile matrix such as a thermoplastic polymer does not normally help, because the matrix only carries a small proportion of the load, and failure is controlled by the brittle fibres.

An alternative phenomenon is pseudo-ductility, which may be defined as the ability to deform significantly with a softening response but without complete fracture, while maintaining load carrying capability. Pseudo-ductility can be achieved with non-linearity or “pseudo-

* Corresponding author.
E-mail address: M.Wisnom@Bristol.ac.uk (M.R. Wisnom).

https://doi.org/10.1016/j.compositesa.2024.108029
Received 2 June 2023; Received in revised form 12 January 2024; Accepted 13 January 2024
Available online 19 January 2024

yielding" via elastic deformation and macroscopic damage rather than mechanisms at the microscopic or molecular level. Although damage results in a loss of modulus on reloading, it can allow load redistribution around stress concentrations, and potentially increases damage tolerance. Furthermore, the reduced stiffness can also be exploited in detecting or monitoring damage. A long plateau on the stress–strain curve is desirable, preferably with a positive slope. Such "work hardening" avoids localization of failure which could otherwise occur once strain increases at a certain point without a corresponding increase in the stress to stop further localised deformation. A schematic pseudo-ductile response is illustrated in Fig. 1.1.

Ductility is usually related to the failure strain of a material in tension. Since the elastic contribution is normally small proportionately, the failure strain is similar to the plastic strain, i.e. the length of the yielding plateau, or the permanent strain in the sample if unloaded just before failure. Pseudo-ductile strain can be defined analogously, although there may or may not be any permanent deformation in the material. Pseudo-ductile strain can be used as a measure to compare different materials and architectures and is taken here as the difference between the final failure strain, and the elastic strain at the same stress based on the initial modulus E_0, as shown in Fig. 1.1. In some cases, a sharp "yield" point (often referred to as "knee-point") is observed, but in others there is a gradual non-linearity with smooth transition between the elastic and plateau parts of the stress–strain curves. To account for this gradual transition, the stress σ_y at an offset "plastic strain" ε_p can be used, analogous to the proof stress in metals, with corresponding pseudo-yield strain, ε_y. A value of 0.1 % is shown in Fig. 1.1, but may be chosen to be appropriate for the particular material. Depending on the mechanism, some pseudo-ductility may be associated with minor load drops as damage accumulates. To be usable, the composite should retain integrity; although it is difficult to apply a universal, absolute criterion, where there is substantial damage that limits important characteristics of the composite, it should no longer be considered as pseudo-ductile.

This paper reviews research on polymer matrix fibre-reinforced composite materials that exhibit ductile or pseudo-ductile response. The topic has not been reviewed previously except for the 2013 paper by Bank, on progressive failure and ductility of FRP composites related to the construction sector [1]. Its focus was mainly on structural response and on crushing of composite tubes, where progressive destruction leads to a plateau in the load–deflection response, which is also good for crashworthiness in transport applications. In contrast, the current paper focuses rather on the basic material behaviour at a coupon rather than component or structural level, and summarises the large amount of research that has been conducted more recently. This paper does not cover materials with high stiffness metallic or ceramic matrices where the matrix carries a substantial proportion of the load, and which have significantly different failure mechanisms from polymer matrix composites. Laminates of composites and metallic layers such as GLARE are also out of the scope of this review, but both continuous and discontinuous fibre composites are considered, with a range of different fibres. The main focus is on research reported on fundamental tensile behaviour, and responses observed under other loading conditions including

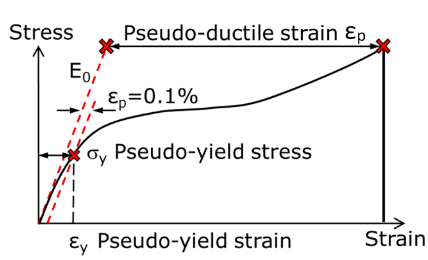

Fig. 1.1. Typical response and definition of pseudo-ductile strain.

compression and bending are also considered where available. The different mechanisms by which ductile or pseudo-ductile response can be created are discussed. Section 2 deals with ductile fibres and their composites, including polymeric, metallic, and natural fibres, as well as those based on carbon nanotubes. Section 3 covers ductility and pseudo-ductility created via fibre reorientation, where the architectures allow additional strain to be achieved over and above that in the fibres themselves. Section 4 discusses pseudo-ductility via progressive fibre or ply fracture in continuous FRPs, covering both single-fibre materials and hybrids, with a particular focus on fragmentation, which is a very important and promising mechanism for generating gradual failure. Section 5 presents work on ductility and pseudo-ductility in discontinuous composites, including fragmentation and the additional mechanisms of matrix deformation and slip between reinforcing elements. Section 6 reviews notched response, and Section 7 summarises the different approaches, considers the trade-offs between strength, stiffness and ductility, and discusses remaining challenges and future perspectives.

2. Ductile fibres and their composites

2.1. Introduction

The ideal way to produce ductile composites would be to embed fully ductile reinforcing fibres in a ductile matrix. However, traditional high-performance fibres, such as carbon, glass and even polymer fibres, are brittle. On the whole, there is a well-recognised materials trade-off between strength, modulus and ductility. Some more ductile fibres do exist and research, as reviewed below, has addressed polymer fibres (Section 2.1), natural and cellulose based fibres (Section 2.2), ductile carbon-based fibres exploiting spun carbon nanotubes (Section 2.3) and steel fibres (Section 2.4).

2.2. Polymer fibres and composites

Polymers with random molecular chains often show high ductility, and fibres can be created by drawing either in the melt or gel phases. With increasing draw ratio (and hence molecular alignment), the fibre tensile strength and modulus increase, but the strain at failure decreases and the fibres tend to become more and more brittle, as exemplified by the response of cold-drawn isotactic polypropylene (iPP) fibres at different values of the draw ratio, λ, in Fig. 2.1.

Self-reinforced polypropylene (SRPP) composites can be produced by a variety of processing strategies. One classic example incorporates highly stretched iPP fibres possessing a high degree of crystallinity in an amorphous polypropylene (PP) copolymer matrix, with a lower melting temperature [3]. Alternatively SRPP can be prepared by hot compaction

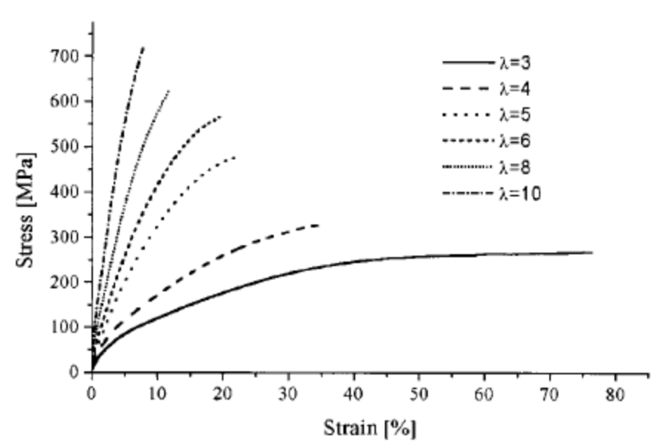

Fig. 2.1. Effect of draw ratio λ on stress–strain response of single polypropylene fibres [2].

of woven aligned PP tapes during which fractions of the PP melt and fuse [4]. SRPP materials were first commercialised under the tradenames Curv™ or Pure™, but the concept has been considered for a number of polymers [5], and is attracting current interest for recyclability [6]. This approach can indeed produce a ductile response for SRPP, as shown in Fig. 2.2, but the strength and modulus of such composites are low compared with high-performance fibre reinforced polymers. The properties are necessarily limited by the modest performance of the semi-crystalline PP fibres; better modulus can be obtained with more ordered polyethylene fibres, although the hot compaction process leads to a significant loss in strength [5]. The different commercially available materials have been reviewed in [7]. The properties of self-reinforced polymers can be significantly improved by hybridising with higher performance fibres such as glass or carbon, as discussed in Section 4.4, but usually at the expense of ductility.

Polyvinyl alcohol (PVOH) fibres, although not traditional reinforcements, have moduli and strengths up to 70 GPa and 2.3 GPa respectively [8]. Composites made from woven fabrics of PVOH fibres with a volume fraction of 30 % in the loading direction show a non-linear response, with a knee point at around 70 MPa, strength of 250 MPa, initial modulus of 10.7 GPa and failure strain over 7 % [9]. A variety of hybrid woven combinations of PVOH fibres and glass fibres produced composites which all showed similar non-linear responses, and strengths up to 350 GPa. All-glass balanced woven composites with a fibre volume fraction of 40 % also showed a non-linear response, despite the linearity of the fibres, suggesting that the woven architecture may have been the reason for the non-linearity. Very high strains of 5.7 % were reported, raising potential questions about the way the displacements were corrected for machine compliance.

Most other commercially available high performance polymer fibres, such as poly(paraphenylene terephthalamide) (Kevlar™), ultra-high molecular weight polyethylene (Dyneema™), or poly(p-phenylene-2,6-benzobisoxazole) (Zylon™) have excellent tensile strength (up to 5800 MPa) and energy absorption, but are brittle, with relatively low failure strains, generally up to 4 %. Composites made of polymer fibres such as aramid or PBO exhibit highly non-linear behaviour in compression. For example, Kevlar 49 / epoxy with a volume fraction of 49 % shows a stress–strain response with a plateau beyond 0.5 % strain and a pseudo-yield stress of about 210 MPa [10] due to defibrillation and kinking of the fibres. This value is low compared to the strength of about 1300 MPa and linear response in tension. However, in bending, substantial load can be carried with pseudo-ductility as the material "yields" progressively through the thickness, effectively forming a plastic hinge [10].

Aramid fibres have been consolidated, by partial dissolution, to form dense, high loading fraction composites with good strength and stiffness, but no expected increase in ductility [11]; similar approaches have been applied to consolidated, orientated films [12].

Improvement in truly ductile fibre matrix composites may rely on the development on new fibrous reinforcement, particularly exploiting

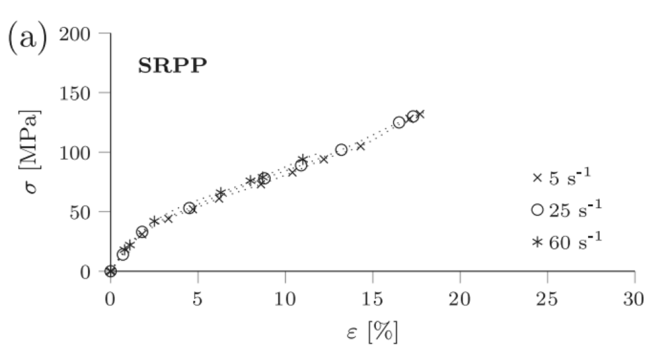

Fig. 2.2. Non-linear response of self-reinforced polypropylene loaded at different strain rates [13].

nanostructures (see also Section 2.4 below). The ultimate strength of highly oriented polymer fibres increases with decreasing diameter, consistent with the Griffith theory [14]. Beyond conventional polymer fibre spinning followed by further (cold) draw down, or bicomponent "islands-in-the-sea" spinning strategies, smaller diameter (nano)fibres can be produced by electrospinning. Non-linear stress–strain responses have been observed and the most impressive increases in tensile properties have been reported for atactic polyacrylonitrile nanofibres with diameters smaller than 200 – 250 nm. Elastic moduli of 48 GPa, tensile strengths of 1750 MPa and strains to failure of 60 %, as shown in Fig. 2.3 [15], highlight the potential to simultaneously increase fibre tensile properties and toughness. The reported increases in strength and elastic modulus are in line with the highest reported tensile properties of solution spun superdrawn ($\lambda = 80$) ultrahigh molecular weight PAN fibres with moduli of 35 GPa and strength of 1800 MPa [16], the highest PAN fibre properties reported so far [17]. Whilst these results are stimulating, there are considerable challenges, both in fundamental understanding, and scaling nanofibre production and integration, to produce composites at a meaningful scale.

2.3. Natural fibres and composites

Natural lignocellulose fibres often exhibit some non-linearity in part attributable to their internal nanocomposite or nanostructured architectures. For example, certain flax fibre types have a high strength of up to 1500 MPa [18] and show a reduction in stiffness at about 0.6 % strain followed at ~ 1.5 % by strain hardening response until final failure at ~ 2.2 %. The non-linear stress–strain behaviour is attributed to realignment of the helically wound microfibrils with the fibre axis enabled by rearrangement due to viscous flow of the amorphous matrix polymers, i.e. hemicellulose and pectin, linking the structural crystalline cellulose fibrils [18–21], although the effect is relatively small. Other natural fibres show greater ductility, but at the expense of stiffness and strength. For example, coir fibres show a knee point in the stress–strain curve, effectively representing a yield point, attributed to realignment of cellulose fibrils in the fibre direction at about 2 % strain. Typical failure strains are 17–47 %, depending on fibre diameter and initial elastic moduli range from 3 to 6 GPa, but mean strengths are normally only up to around 175 MPa [22]. Coir fibres fail by uncoiling of elementary cellulose microfibrils in the cell walls of the fibres. Properties of natural fibres vary significantly depending on botanical species and processing steps, such as scutching and the degree of retting [23], however, the irregular fibre geometries, and associated uncertainty determining cross-sectional area, have a strong influence on the scatter of reported

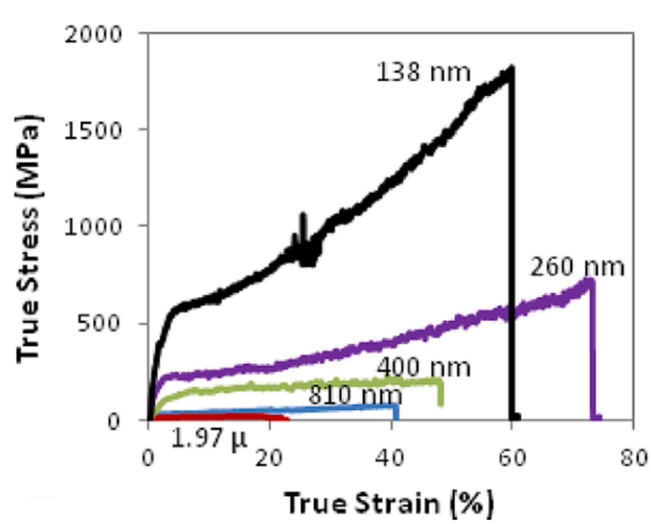

Fig. 2.3. Non-linear response of small diameter polyacrylonitrile (PAN) nanofibres [15].

tensile properties.

Silk (natural protein) fibres, such as those produced by the larvae of the mulberry silkworm (*Bombyx mori*), are superb textile fibres but have limited absolute strength and stiffness when compared with synthetic reinforcing fibres. However, the best silks provide the strongest natural fibres, exhibiting the highest tensile properties and strains to failure, with the most outstanding fibre properties displayed by small diameter dragline spider silk fibres (Fig. 2.4).

For instance, the dragline silk fibres produced by forced silking of red-legged golden orb-weaver spiders (*Trichonephila inaurata*) have an initial modulus of ~ 14 GPa, a strength of ~ 1500 MPa at strains to failure of ~ 40 % [24] with considerable non-linearity and outstanding toughness, even at low temperatures. The stress–strain curves of frame silk of the grey cross-spider (*Araneus sericatus*) (Fig. 2.5) exhibit ideal elastic behaviour up to strains of 2 % with relatively high initial modulus (10 GPa) tending towards a plateau before undergoing significant strain-hardening beyond strains of 8 % with a modulus of still 4 GPa [25]. An overview of the mechanical properties of various spider silks can be found in [26]. As for all polymer fibres, especially natural products, the tensile properties of spider silk fibres are dependent on many factors, such as strain rate, temperature, and humidity (Fig. 2.6), [27]. With increasing moisture content the fibre's elastic modulus and strength drop while their strain to failure increases. Unfortunately, it is not easy to produce significant amounts of natural spider silk fibres, because of the cannibalistic nature of spiders, but research (and significant commercial activity) focuses on biotechnological approaches to develop artificial spider silks [28]. Due to availability, silkworm silk is most explored both as a fibrous reinforcement [29], and as a matrix reinforcement for flax fibre composites [30], showing some ductility at strengths up to 300 MPa. Experiments with high performance (recombinant) protein fibres may prove a promising direction in the future [31].

Natural fibres, such as flax, used to make composites are discontinuous, with fibre lengths ranging from 30 to 100 mm, and heterogeneous, limiting the opportunities for high performance composites. Natural fibres as extracted from plant material can be converted into (twisted) yarns using conventional textile processes, and can in turn be woven into fabrics. Unimpregnated natural fibre yarns and textiles have a large

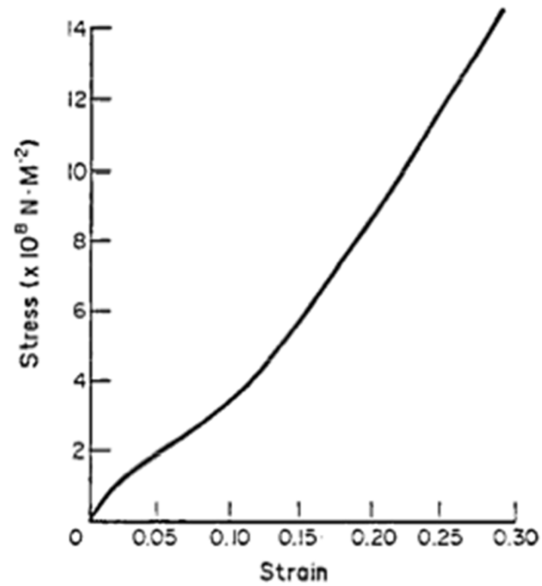

Fig. 2.5. Characteristic non-linear stress–strain curve of frame silk of Araneus sericatus determined at a rate of 140% extension/min [25].

variability in length, and processing induced defects [32]. Nevertheless, it has been shown that natural fibre reinforced composites could potentially replace glass fibre reinforced polymers in tensile stiffness-critical, though not strength-critical, applications [33]. Composites containing highly aligned textile preforms, such as interlaced woven fabrics and unidirectional fabrics produced from natural fibre yarns, possess considerably better properties than those made from random non-woven mats.

Some of the difficulties of using natural fibres can be avoided by converting bioderived precursors into synthetic fibres with less geometrical variability and more uniform properties. Cellulose for instance can be processed into continuous technical fibres by dissolution, spinning and regeneration. Regenerated cellulose fibres show a

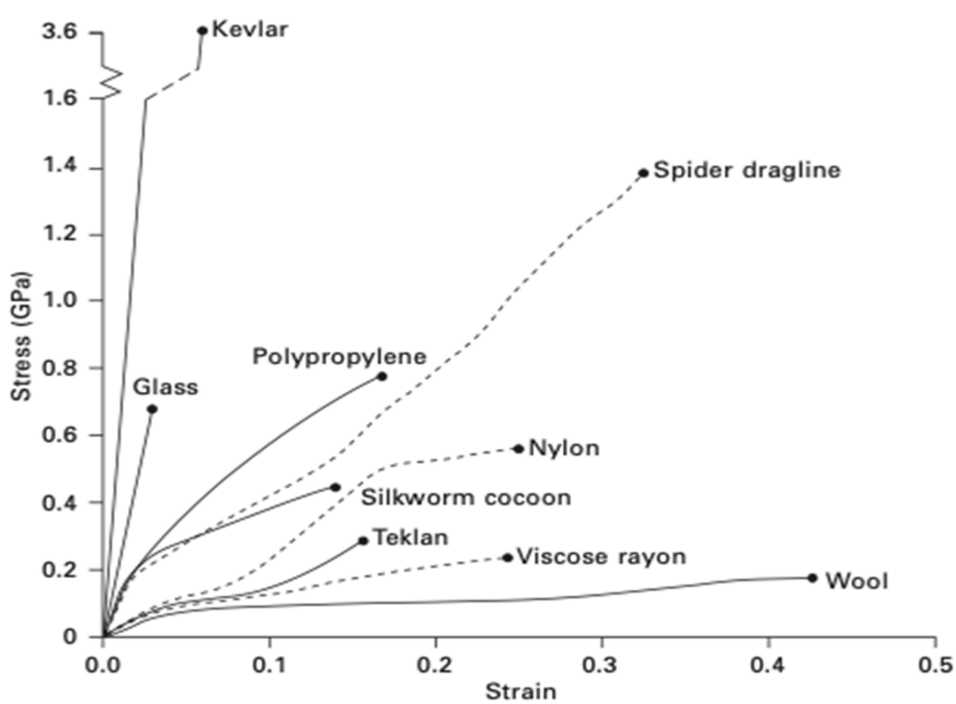

Fig. 2.4. Stress–strain curves of a range of bio/polymer and glass fibres. Teklan is a polyacrylonitrile fibre [24].

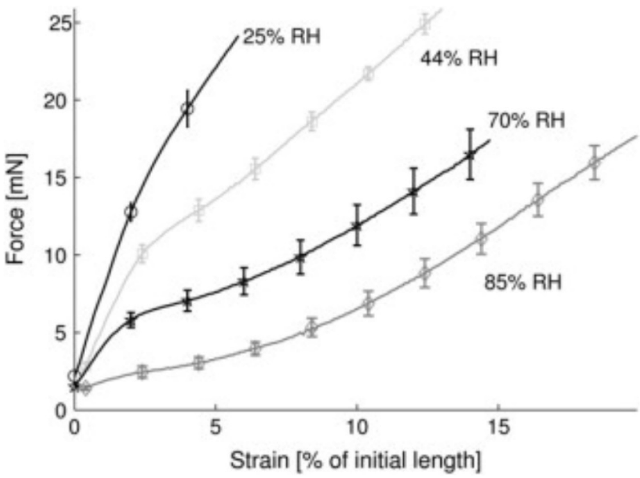

Fig. 2.6. Effect of humidity on the performance of dragline silk [27].

much greater degree of ductility than the original lignocellulosic fibres, with Cordenka™ (RT700) being one of the most promising examples. When twisted into fibre cords, Cordenka™ 700 (Super 3) has a modulus of 21 GPa, failure strain of 14 % and strength of 800 MPa, with a yield point at around 200 MPa at 1 % strain [34]. Cyclic tests show a high degree of viscoelasticity and plasticity (Fig. 2.7). Cordenka™ composites with EpoBioX resin and 40–50 % volume fraction have a tensile strength of around 300 MPa and 6 % strain. Fig. 2.8 compares the mechanical response with that for similar composites reinforced with flax fibres. The regenerated cellulose shows much greater ductility and strain, although lower modulus than flax fibre reinforced composites due to the much lower modulus of Cordenka fibres as compared with flax (21 GPa vs. 55 GPa). Shamsuddin et al. made composites with sized and unsized Cordenka™ fibres [35]. The matrix was inherently brittle polyhydroxybutyrate (PHB), neat or containing 2.5 wt% nano-fibrillated cellulose, having a fibre volume fraction of 50–55 %. Even higher ductility was achieved, with a failure strain of 12–15 %, as shown in Fig. 2.9.

2.4. Nanoreinforced ductile fibres

High aspect ratio one dimensional nanomaterials are well-suited reinforcements for structural fibres, because they match the dimensionality, pack effectively, and are small enough to be included within the fibre structure. A variety of building blocks have been explored, particularly carbon nanotubes, but including other species, such as nanocelluloses, and inorganic nanotubes (e.g. imogolite); 2D platelets have also been considered although less obviously suited to fibre geometries. At present, the focus remains on the processing and properties of the primary fibres, rather than their composites, but the successful creation of intrinsically ductile fibres with higher performance should

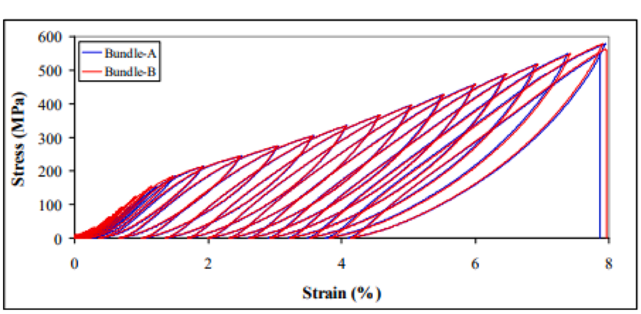

Fig. 2.7. Cyclic stress–strain curves from loading-unloading tests on twisted regenerated cellulose (Cordenka™) fibre bundles [34].

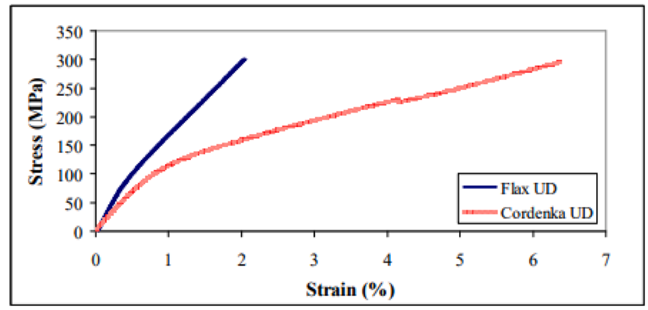

Fig. 2.8. Regenerated cellulose (Cordenka™) composites using predominantly bio-based epoxy (EpoBioX), show greater ductility than flax [34].

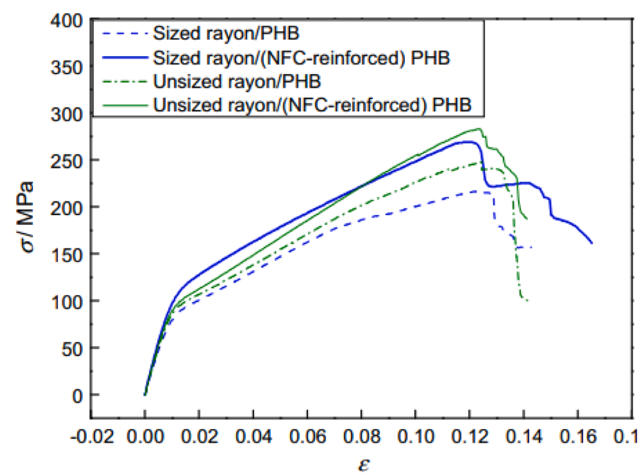

Fig. 2.9. High tensile strains with Cordenka™/ polyhydroxybutyrate (PHB) composites [35].

translate into useful ductile composites in the future. Two strategies can be considered. One is to improve the performance of an existing polymer fibre by using a nanoreinforcement, another is to build a new generation of fibres assembled entirely from nanomaterials. The former may be more straightforward to implement, the latter may offer greater benefits in the future.

An example of the former strategy, extending the natural fibre theme discussed above, uses bioderived nanomaterials incorporated in optionally renewable matrices. Lee et al. used uniform dispersions of cellulose nanocrystals (CNC) in polyvinyl alcohol (PVOH) solutions to prepare high CNC loading fraction high strength nanocomposite fibres by gel spinning, followed by hot-drawing [36]. These CNC/PVOH composite fibres contained 40 wt% CNC, offering a strength of almost 900 MPa and stiffness of ∼ 30 GPa, at a strain-to-failure of 5.6 %, Fig. 2.10. The improvements were quantitatively attributed both to the stiffening contribution of the CNCs though increased PVOH crystallinity (from 12.8 to 17.9 %) also contributes; further improvements could be expected using more regioregular (stereochemically homogeneous) PVOH and further optimisation of the spinning and drawing process. Ductile continuous fibres based purely on cellulose nanofibrils have been spun with strengths up to 300 MPa [37]. Even higher performance cellulose fibres were reported for nanostructured macroscopic cellulose fibres assembled from cellulose nanofibrils (CNF), with moduli up to 70 GPa, strength of 1100 MPa, a yield stress of 700 MPa and strain to failure of 6 % as shown in Fig. 2.11 [38]. Increasing the length of CNF from 390 nm (CNF-1360) to 680 nm (CNF-820) used for fibre production results in a significant increase in tensile strength but does not affect the knee point.

The most extensive and promising work on nanomaterials-based fibres explores the use of carbon nanotubes (CNT), due to the combination

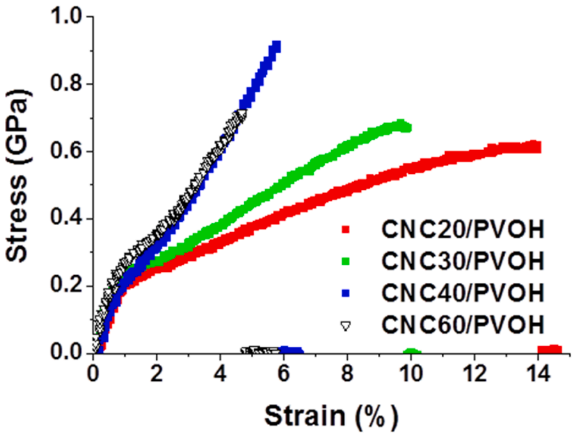

Fig. 2.10. Characteristic tensile stress–strain curves of different wt% CNC/PVOH composite fibres. All fibres have the same draw ratio of 6 [36].

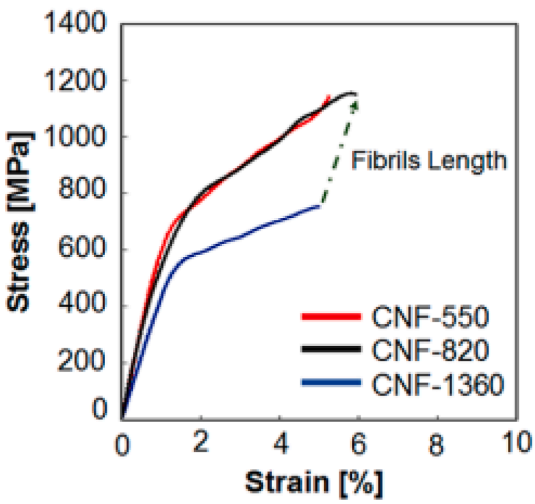

Fig. 2.11. Nanostructured cellulose nanofibre tensile response with different surface charge densities [38].

of excellent intrinsic properties and low density [39]. Full consideration is beyond the scope of this paper, especially because much of the field focusses on multifunctional applications [40], but a few results are reviewed here to highlight the potential for this approach to provide alternative high performance carbon-based fibres with a non-linear ductile response. Boncel et al. reported on CNT fibres that were continuously spun and then treated in hexadiene followed by UV initiated crosslinking [41]. A typical stress–strain response is shown in Fig. 2.12. A specific stiffness of about 75 GPa cm^3/g was reported, with a distinct change in slope and lower modulus from around 0.5 % strain.

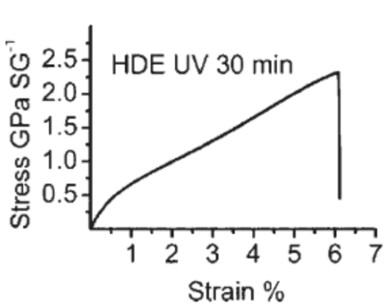

Fig. 2.12. Non-linear response of carbon nanotube fibre. The unit GPa/SG (SG = specific gravity) is equal to GPa cm^3/g [41].

The average failure strain was about 6 % and specific strength 2.3 GPa cm^3/g. These values are approximately equivalent to stiffnesses and strengths of over 100 GPa and 3 GPa, respectively. The maximum specific strength obtained was 3.5 GPa cm^3/g.

Lee et al. grafted PVOH of varying molecular weights to single-walled carbon nanotubes (SWCNTs) and produced PVOH-grafted single-walled carbon nanotube composite fibres with non-linear response, Fig. 2.13. Mean tensile strengths of up to 1100 MPa, stiffnesses up to 38.5 GPa and strains to failure of up to 23 % were obtained [42]. Cyclic loading–unloading data previously unpublished showed that the fibres are truly ductile, with elastic-perfectly plastic response and strains of up to 40 %, as shown in Fig. 2.14. Previous work by Miaudet et al. on nanotube/PVOH fibres showed even higher strains of up to 430 % [43]. The presence of the polymer, here, mediates the plastic response, whilst the CNTs provide the load bearing and stiffness.

An analogous system, using inorganic rather than carbon nanotubes simplifies processing, and enables in-situ observations, while exploring some key issues associated with packing and alignment. Interestingly, this system, based on double-walled aluminogermanate imogolite nanotubes and PVOH, demonstrates the potential to heal broken structural fibres [44]. Lyotropic imogolite nanotube suspensions were wet spun with PVOH into fibres with a tensile modulus of 24 GPa and strength of 800 MPa and strains to failure of 5.5 %. The fibres containing 8.1 wt% imogolite nanotubes exhibited a yield point at 0.5 % strain associated with the intrinsic PVOH response. Broken nanocomposite fibres (and only nanocomposite fibres) could be healed using water as a medium for evaporation-induced self-assembly at modest temperatures (~80 °C), yielding intact fibres with exceptionally high absolute strength and stiffness for a healed system.

The highest performance CNT-based fibres are generally prepared by superacid spinning of lyotropic solutions, analogous to polyaramid processing. Although the response tends to become more brittle as the order and absolute performance improve, as for polyaramids, some non-linearity can be retained. Combined with graphitisation treatment,

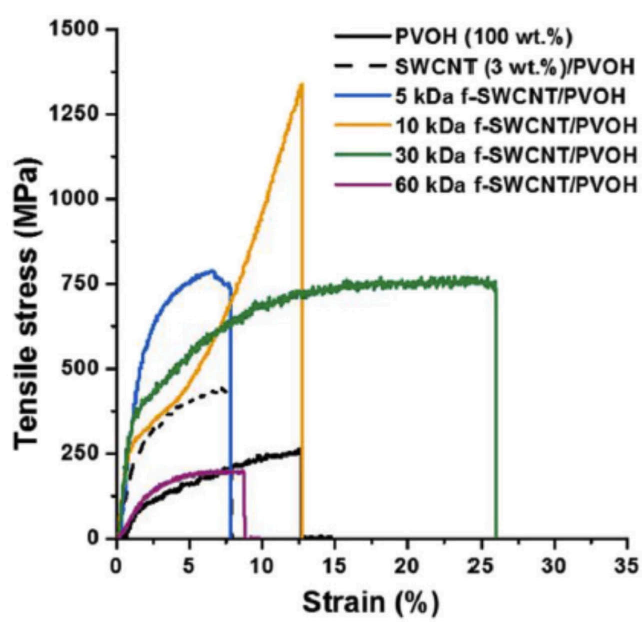

Fig. 2.13. Characteristic stress–strain curves of SWCNT/PVOH composite fibres. The traces show the effect of covalently grafting different molecular weights of polyvinyl alcohol (PVOH) side chains (5, 10, 30, 60 kDa) to the SWCNTs before incorporation in the PVOH matrix (40 wt% loading of grafted SWCNT). As controls, the results are compared with pure PVOH (100 wt%, matrix only) fibre and unfunctionalized SWCNT (3 wt%)/PVOH composite fibre (loading limited by the poor stability of unfunctionalized SWCNT dispersions).

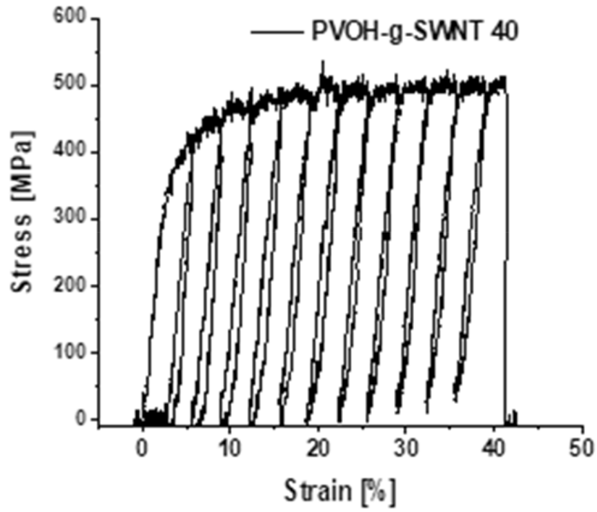

Fig. 2.14. Cyclic plastic response of CNT-PVOH composite fibre, demonstrating true plasticity, and large strain to failure over numerous loading cycles. The fibre contains around 40 wt% SWCNT grafted with 10 kDa-PVOH, similar to samples described in [42].

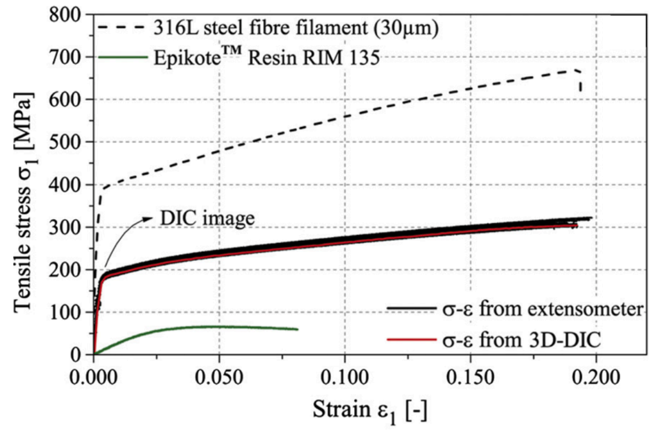

Fig. 2.15. Ductile steel/epoxy composite and its constituents [50].

recent results indicate a non-linear response in tension with strengths up to at least 5 GPa at 3 % elongation [45,46]. The major alternative approach relies on direct spinning from the gas phase, which offers an attractive reduction in overall process complexity, although production rates remain limiting. These fibres similarly offer promising specific strength, and some non-linearity particularly before densification; secondary densification with acid provides promising strengths although the strain to failure reduces [47]. Strengths can reach around 2.5 N/tex (equivalent to 2.5 GPa if specific density is one, or proportionately higher, if fibres are more effectively densified), with a non-linear response up to 6 % strain to failure [48]. Thermal annealing, can improve the performance further, providing fibres with high strengths (over 6 GPa), high modulus (600 GPa), and non-linear strain to failure (>1.5 %) [45]. Much work remains to be done to scale up production, but significant commercial progress is being made on both direct spun fibres (Huntsman, Qflo) and acid spun fibres (Dexmat), amongst others. The results suggest the potential to create truly ductile high performance fibre based composites in the medium term. Although again, there appears to be a trade-off between strength and strain to failure, macroscopic SWCNT based fibres already offer an improved balance of properties, with current rapid progress. Plenty of headroom remains before reaching the intrinsic strengths observed for bundles of small numbers of SWCNTs that approach 100GPa, with non-linear strains up to 15 % [49].

2.5. Metal fibre composites

Whilst steel, of course, has an undesirably high density compared to other fibre reinforcement materials, highly drawn steel wires have an interesting balance of strength, stiffness, and strain to failure, that may both be directly useful, and serve as a model system [14]. Polymer matrix composites reinforced with ductile steel fibres can produce a highly non-linear response by fibre yielding. Allaer et al. prepared Unidirectional (UD) 316L stainless steel fibre/epoxy composites (based on a low viscosity diglycidyl ether of bisphenol A, Epikote™ RIM 135) that yielded and achieved nearly 20 % strain and 300 MPa strength as shown in Fig. 2.15 [50]. Callens et al. reported similar properties for UD stainless steel / epoxy composites, with silane modification to improve adhesion, and tested cross-ply laminates as well [51]. They also used a PP matrix, which gave a ductile response with up to 13 % strain and 128 MPa strength [52]. Hybridisation with SRPP resulted in similar ductility with strains up to 12 % and strengths up to 145 MPa [53]. Hannemann et al. successfully produced hybrids with steel and carbon fibres in epoxy [54] although steel fibres (~30 μm) are typically significantly larger than carbon fibres (~5 μm). In tension, they showed a large load drop when the carbon fibres failed, but some configurations continued to carry substantial stress beyond that point. Layups with 0°, 90°, and ± 45° layers of carbon fibres comprising 53 % of the total volume fraction plus 11 % 0° steel fibres carried 150 MPa stress reducing to about 50 MPa up to about 12 % strain. McBride et al. hybridised E-glass and stainless-steel fibres in an epoxy matrix [55]. Yielding of the steel produced a non-linear response with ductility, with stresses depending on the proportion of glass to steel, but catastrophic failure occurred when the glass fibre failure strain was reached. The benefits of ductile metal fibres have also been explored by multi-scale modelling [56].

Metallic fibres are sometimes introduced into polymer matrix composites for multi-functional purposes such as actuation, de-icing or lightning strike protection, and may also add some ductility as a secondary benefit. For example, embedding steel fibres and meshes can aid thermographic non-destructive evaluation, and provide integrated ice protection [57], and embedding shape memory alloy wires has been shown to improve impact performance [58].

3. Ductility and pseudo-ductility via fibre reorientation

3.1. Introduction

The fibres in most modern composites are brittle, and so offer little opportunity for ductility or pseudo-ductility without fracture. However, additional strain beyond that in the fibres can be generated in a number of ways by reorientation of the fibres, enabled by deformation in the matrix. This can occur by angle-plies scissoring, and fibres becoming more aligned with the loading direction, as discussed in Section 3.2. Additional strain can also be generated by inherently wavy fibres undergoing straightening, reviewed in Section 3.3. Other possibilities exist to exploit hidden length to create extra strain as a result of the architecture, and some examples of this at the structural level are presented in Section 3.4. Depending on the matrix response, in some cases the composite's response may be recoverable, producing true ductility, as opposed to pseudo-ductility when damage or irreversible deformation occurs. Fibre reorientation contributes to the non-linearity exhibited by some 3D woven and braided composites, and is discussed in Section 4.6 as it is also related to fragmentation. A further possibility is non-linear response due to buckling. Gordon and Jeronimidis mimicked the structure of wood by creating hollow cylindrical tubes with helically wound fibre walls [59]. Pseudo-plasticity occurred under tensile loading due to buckling of the walls, with high energy absorption, and a maximum for a winding angle of 15°.

3.2. Angle-ply laminates

From the early days of composites, it was observed that angle-ply laminates could exhibit significant non-linearity due to the high shear strains the matrix may be able to reach and the lack of restriction from fibres in the loading or transverse directions. It was found that a single parameter flow rule plasticity model was able to represent the off-axis behaviour of epoxy composites even though thermoset polymers do not exhibit true plasticity, and the stress–strain responses for a range of off-axis angles could be fitted using the same plasticity parameter [60]. In particular, laminates with ± 45° plies exhibit substantially non-linear response. Fig. 3.1 shows typical results for scaled $[(+45/-45)_n]_s$ carbon/epoxy laminates with n = 1, 2, 3, 4 [61,62]. The strain at failure increased substantially as the number of plies increased, due to the reducing effect of damage starting with transverse cracks at the central double plies leading to delamination. For the 8-ply case these represent a quarter of the total thickness, leading rapidly to complete failure, whereas for the 32-ply laminates the damaged plies are a much smaller proportion of the total thickness. Even higher strains can be achieved with angle-plies with thermoplastic matrices, e.g. polycarbonate [63]. Pseudo-ductility in angle-ply laminates under flexural loading has been studied [64], and the mechanisms involved in the behaviour of angle-ply laminates in tension and compression have been investigated and modelled [65].

By using thin plies, matrix cracking and delamination can be suppressed in angle-ply laminates even with normally brittle matrices, allowing much higher strains to be achieved. For example, with a $(\pm45)_{5s}$ layup of high strength carbon/epoxy plies of only 0.03 mm thickness, strains of over 20 % and necking behaviour were obtained

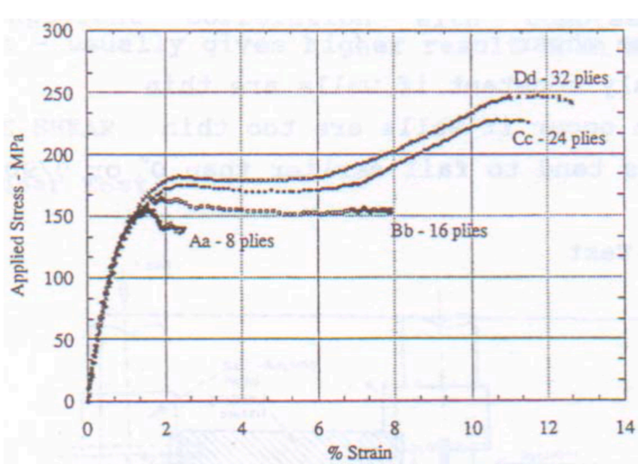

Fig. 3.1. Tensile behaviour of $[(+45/-45)_n]_s$ carbon/epoxy laminates, n = 1, 2, 3, 4 [61].

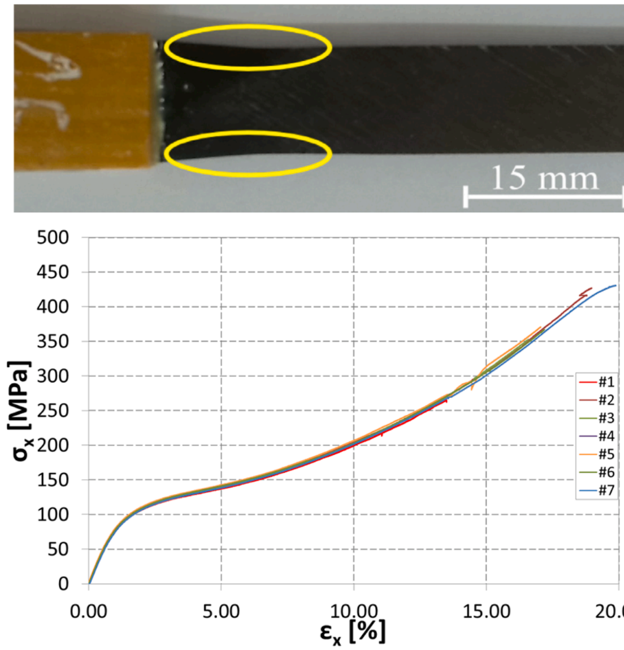

Fig. 3.2. Necking and non-linear tensile response of thin-ply ± 45 angle-ply carbon/epoxy laminates [66].

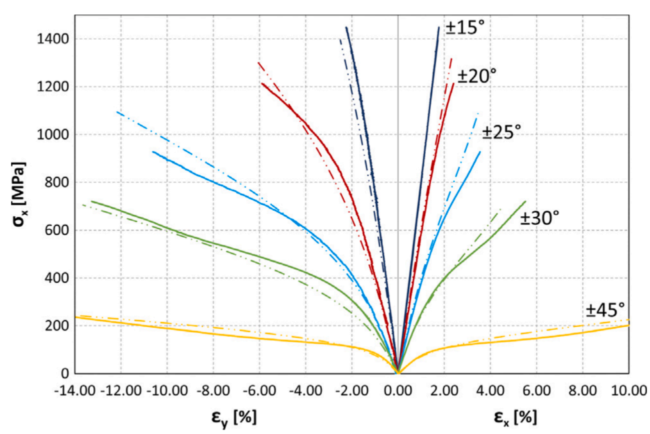

Fig. 3.3. Predicted (dot-dashed lines) and measured (full lines) response of thin-ply angle-ply carbon/epoxy laminates [68].

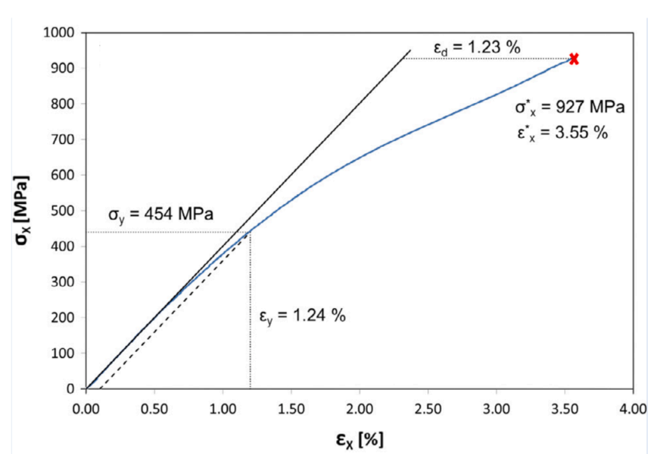

Fig. 3.4. Response of thin-ply ± 25° carbon/epoxy laminate [66].

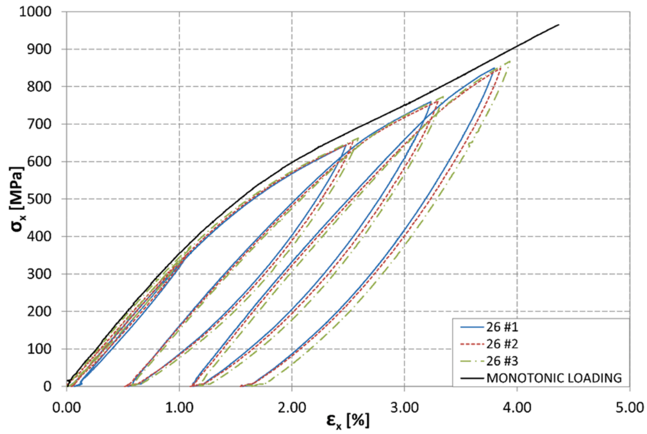

Fig. 3.5. Cyclic loading of $(\pm 26)_{5s}$ thin-ply carbon/epoxy laminate [71].

despite the brittle nature of the matrix, as shown in Fig. 3.2 [66]. A pseudo-ductile strain of about 14 % was achieved. The initial non-linearity is caused by the yielding of the matrix, but as the strains increase, the fibres start to reorient towards the loading direction, giving rise to an increase in stiffness [67].

There is a trade-off between the stresses and strains that can be achieved depending on the angle, as shown in Fig. 3.3, and this has been investigated in modelling studies [68,69]. High strains can only be reached for relatively high angles, leading to a reduction in modulus and strength. A good balance of properties can be achieved for example with ± 25° thin-ply carbon/epoxy laminates that were found experimentally to give a pseudo-ductile strain of 1.23 %, a maximum stress of 927 MPa and a modulus of 39 GPa, Fig. 3.4 [66]. Mizumoto et al. reported a failure strain of 8.7 % and stress of 340 MPa for ± 30° carbon/PP composites with 0.15 mm plies [70].

Tests involving loading, unloading, and then reloading have shown that the initial modulus is fully recovered, and so these laminates may be considered as ductile rather than pseudo-ductile, Fig. 3.5 [71].

Many other studies have shown pseudo-ductility in angle-plies, for example Vieille and Taleb for standard thickness plies woven carbon/epoxy and polyphenylene sulfide (PPS) at room temperature and 120 °C [72]. Moreno et al. [64] and Caminero et al. [73] showed pseudo-ductility in standard thickness ± 45° angle-ply carbon/epoxy laminates loaded in bending. Higher strains and greater pseudo-ductility were obtained for thicker laminates with more ply blocks. Yuan et al. studied ± 15°, ±30°, and ± 45° thin-ply carbon/epoxy laminates and the effect of ply block thickness, showing substantial pseudo-ductility [74]. Their model based on dividing the composite specimen into sub-cells was able to fit the data and separate the effects of material non-linearity and fibre reorientation.

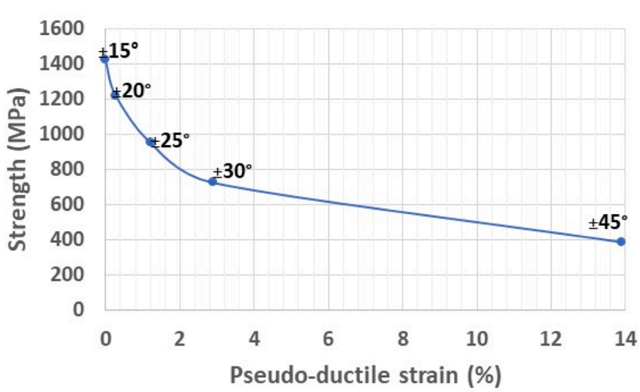

Fig. 3.6. Effect of angle on performance of thin-ply laminates.

Bergmann et al. showed extensive results for ± 45° woven ply composites with a range of different fibres, matrices and ply thicknesses and architectures [75]. Aramid, Dyneema™, and Vectran™ showed higher strains than glass and carbon, although with lower strengths in most cases. The effect of using a more ductile poly(ether ether ketone) (PEEK) versus epoxy matrix had much less effect. All materials showed a substantial strain rate effect, with larger strains at lower loading rates and generally lower strengths. Braided composites showed a more brittle response than woven ones.

Angle-ply composites inevitably have lower strength and modulus compared with the unidirectional material. The trade-offs are illustrated in Fig. 3.6 which shows the relation between pseudo-ductile strain and strength for the thin-ply laminates presented in Figs. 3.2-3.4. There are similar trade-offs for modulus. For example the ± 45° and ± 25° laminates have initial moduli of only 9 and 39 GPa compared with 102 GPa for the unidirectional material. Parametric studies have explored the relationship between strength, pseudo-yield stress and strain for a range of different material properties and laminates [68].

3.3. Wavy ply concepts

Kuo et al. demonstrated theoretically and experimentally that strains of over 6 % could be achieved using wavy carbon fibres with both parallel, in-phase and more random, out-of-phase waviness [76], although there was a stiffening rather than pseudo-ductile response. Stresses were very low because the matrix was a silicone elastomer, however similar effects can also be achieved with high stiffness matrices. For example, Chun et al. investigated the effect of waviness in the through thickness direction on in-plane response of carbon fibre/epoxy composites [77]. As the ratio of waviness amplitude to wavelength (a/λ) increased, a significant increase in non-linearity, additional strain and reducing stiffness were predicted and measured experimentally in compression tests, as shown in Fig. 3.7.

As well as offering additional strains due to reorientation, wavy fibres can also vary the overall strain at which fibres break, creating a more gradual failure. This was shown with non-constrained annealing of carbon fibre/Nylon (PA-12), which produced wavy fibre composites [78]. Also using a gas-flow-assisted process to spread fibres resulted in a broadening of the fibre alignment distribution albeit with a slight degradation of the fibres. Both the wavy and spread fibre composites gave a stepwise and more gradual tensile failure, with the wavy composites having an average ultimate failure strain of 2 %, at which the load-bearing capacity is fully lost, significantly higher than the 1.6 % of the control composite, Fig. 3.8.

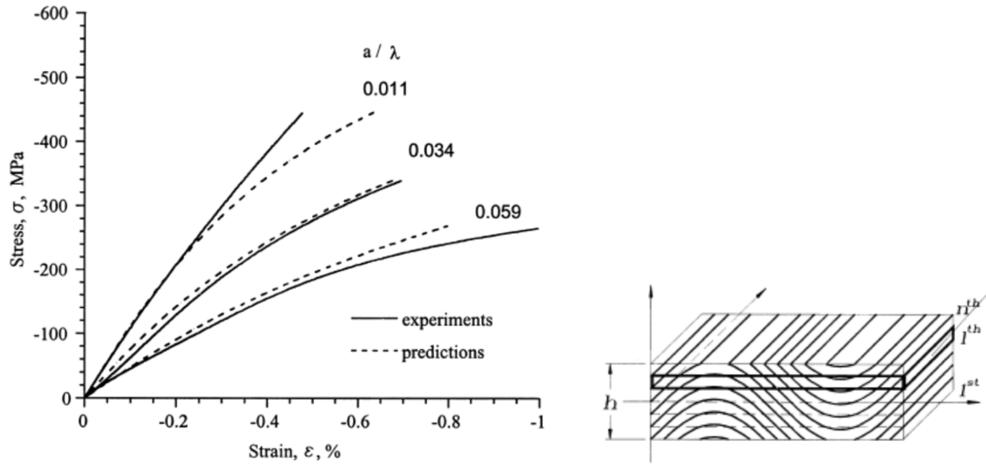

Fig. 3.7. Non-linear response due to through-thickness waviness in compression [77].

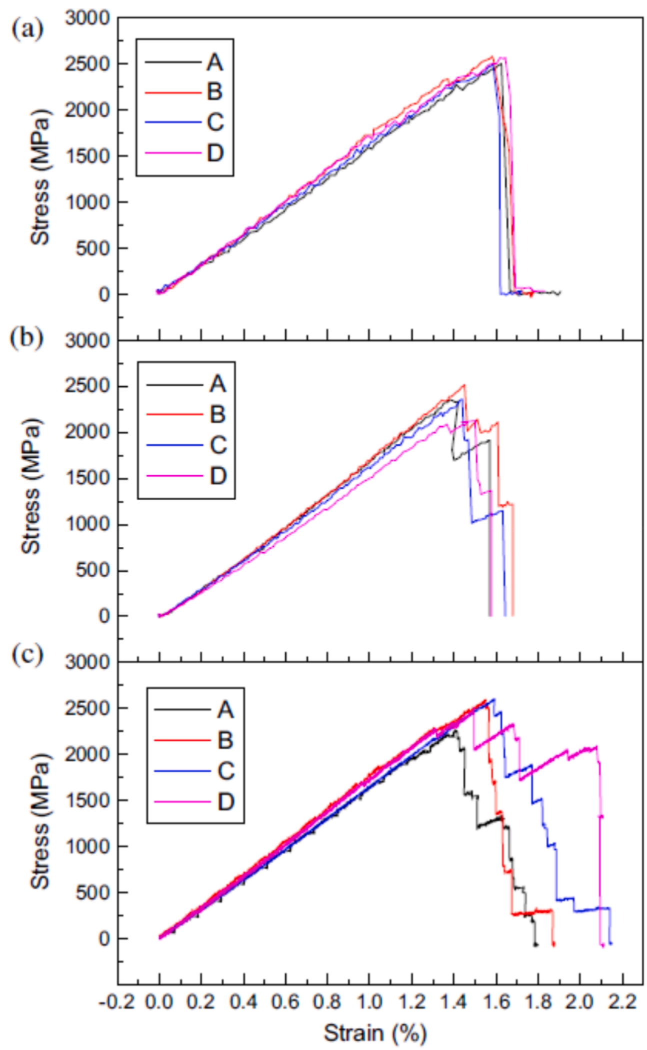

Fig. 3.8. Tensile stress–strain curves of (a) control, (b) gas-textured spread and (c) non-constrained annealed carbon fibre/PA-12 wavy tapes [78].

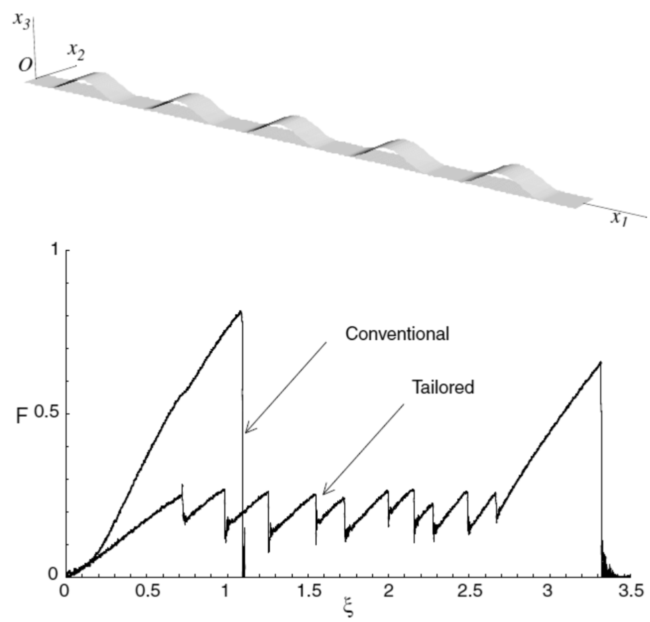

Fig. 3.9. Normalised load–displacement response of tailored undulating energy absorber concept versus conventional straight fibres [80].

3.4. *Structural concepts*

Dancila and Armanios developed an energy absorption concept consisting of undulating and straight sections of glass fibre reinforced rubber loaded in tension [79,80]. When the straight sections failed, the undulating portions underwent straightening, allowing additional deformation whilst still carrying load, resulting in a substantial increase in energy absorption, as shown in Fig. 3.9.

Pimenta and Robinson devised a wavy ply sandwich concept with symmetrical undulating skins and crushable foam cores [81]. The wave geometry, foam material, and shape of epoxy fillet were optimised through a combination of analytical modelling and FE simulations. Under tensile loading specimens exhibited large deformations, without the load drops observed in Fig. 3.9. This was achieved through

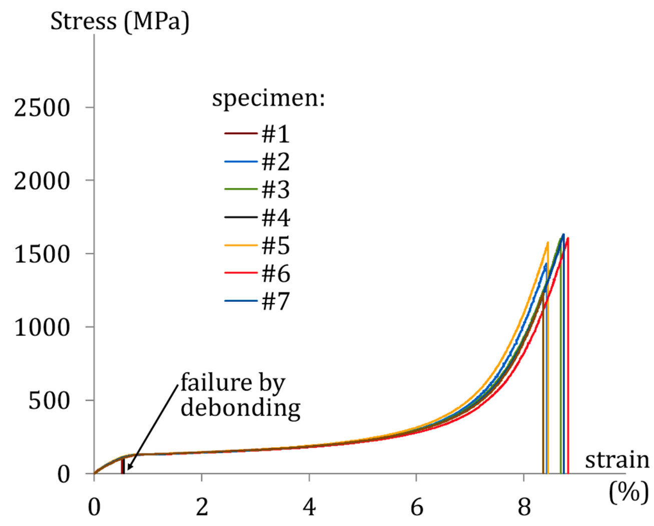

a) Experimental stress-strain curves.

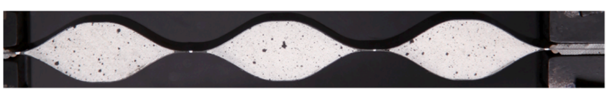

b) Untested specimen.

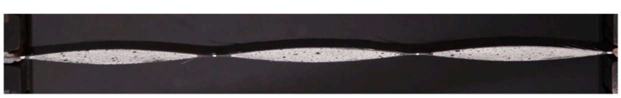

c) Immediately before final failure.

Fig. 3.10. Wavy ply sandwich concept and experimental results [81].

straightening of the wavy composite skins and high energy-absorption through crushing of the foam core cells, with a strength of 1570 MPa and "strains" of up to 9 %, as shown in Fig. 3.10. This concept gave high energy absorption of over 9 kJ/kg.

4. Pseudo-ductility via progressive fibre fracture in continuous fibre composites

4.1. Introduction

One of the earliest analyses of composite tensile failure was Rosen's cumulative weakening model [82]. This was based on statistical variation of fibre strengths due to defects and postulated that when fibres failed, load was redistributed equally on to the remaining continuous fibres. Fibre breaks were assumed to accumulate until complete failure occurred when one section was weakened to the point of no longer being able to carry the load. This model predicted gradual failure, with a large number of broken fibres throughout the composite, but in practice composites were found to fail suddenly, with much less cumulative damage than expected based on this early model. This discrepancy was explained by Zweben in terms of stress concentrations on fibres adjacent to breaks leading to a cascading failure, whereby once a critical cluster of fibres forms, adjacent fibres immediately break, leading to an unstable catastrophic failure [83]. More recent models capture the stress concentrations and interactions between fibres at different positions along the length more accurately, but similarly predict catastrophic failures e.g. [84], as is typically observed experimentally. However, in some circumstances it is possible to overcome this limitation and this section discusses mechanisms whereby globally stable tensile failure can

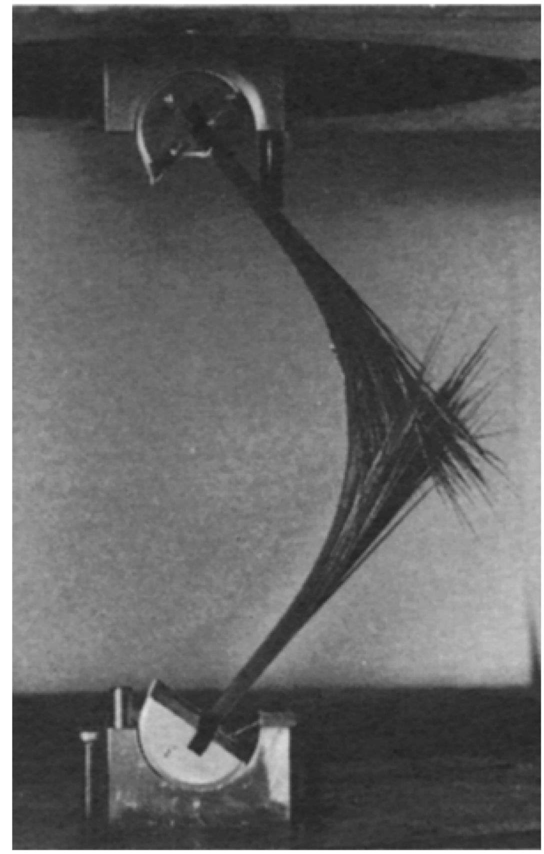

Fig. 4.1. Brush-like failure in UD carbon/epoxy specimen tested in bending [85].

be achieved, leading to pseudo-ductility. Gradual failure in conventional composites and hybrids is considered in Section 4.2, then fragmentation in thin-ply composites and hybrids in Section 4.3. Fragmentation in carbon – polypropylene hybrids is presented in Section 4.4, and finally combined fragmentation and reorientation of fibres in thin-ply composites (Section 4.5), and in 3D woven and braided architectures (Section 4.6).

4.2. Conventional Composites and Hybrids

Whilst conventional carbon fibre composites normally fail catastrophically, there are examples where gradual failure has been observed in bending. For example, Fig. 4.1 shows a picture of a XAS/913 high strength carbon/epoxy specimen loaded in compression in a pin-ended buckling rig that is failing gradually in tension through the thickness, producing a brush-like appearance, but without failure on the compression surface [85]. Gradual failure occurs because the stress gradient through the thickness promotes earlier failure of the highly stressed fibres on the surface, while the fibres away from the surface are less highly stressed. The fibres on the surface are only constrained on one side, and small bundles can separate from the rest of the composite via splitting and delamination, which relieves any stress concentrations on adjacent fibres that could cause the fracture to cascade, and reduces the bending stiffness. This behaviour can be explained by a bundle of bundles model where the composite is assumed to act as a number of small elements that can split and act independently. The model captures the mechanism and higher strains in bending compared to tension that are observed experimentally [86]. This type of gradual flexural failure can only occur if unstable compressive failure does not occur first, either because the material has a higher compressive than tensile strength or is sufficiently thin that microbuckling is suppressed by the strain gradient

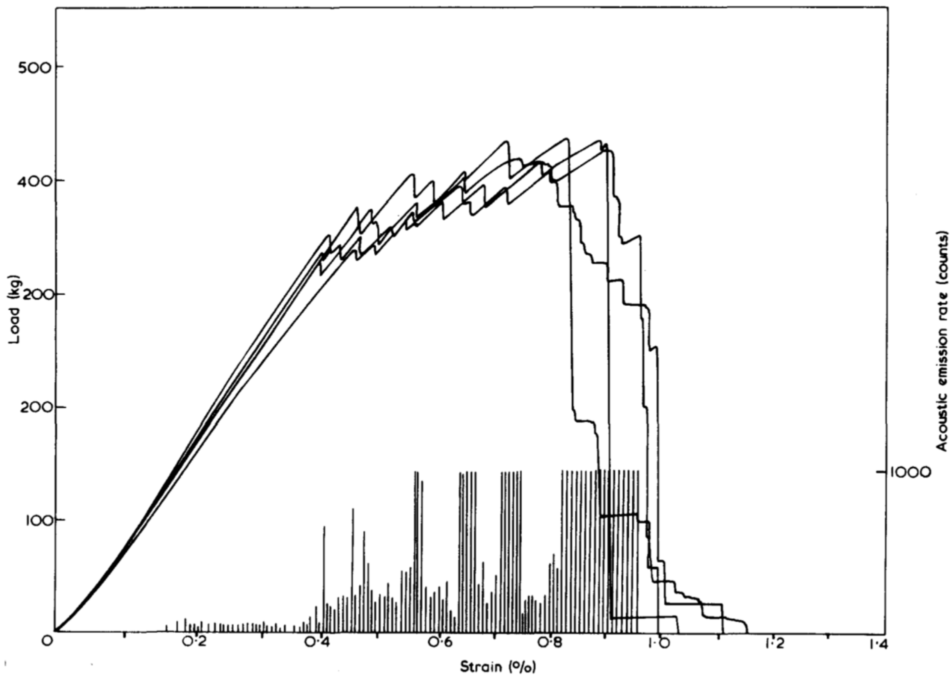

Fig. 4.2. Gradual failure in UD glass-carbon layered hybrid composite [95].

through the thickness [87]. Adequate roller sizes are also necessary to avoid local failures. Current carbon fibre composites tend to have a lower ratio of compressive to tensile strength than older systems such as XAS/913 and so are less likely to exhibit such gradual failure.

Another way that tensile failure may be made more gradual is by increasing the variability of fibre strengths. For example, the aforementioned gas-flow-assisted process to spread fibres (Section 3.3) developed by Diao et al., resulted in a broadening of the distribution of fibre strengths as well as of the alignment of the individual filaments, and this gave rise to a more gradual failure with several successive load drops compared to a sudden catastrophic failure with the baseline unspread material as shown in Fig. 3.8b [78]. Fibres with nacre-like layered interfaces have been produced which help to limit damage spreading from one fibre to another [88], leading to significantly increased number of fibre breaks before failure (as detected acoustically), higher failure strains and potentially more gradual failure [89]. More gradual failure has also been achieved in carbon fibre composites in flexure by printing a polycaprolactone grid on the surface of the fabric prior to infusion [90]. Cracks near the locally weakened inter-layered zones required more energy to propagate, delaying the onset of final failure. Introducing artificial delaminations in the layup created more gradual failure of cross-ply carbon laminates loaded in three-point bending [91], and models have also suggested that interleaving of unidirectional (UD) composites with a soft polymer has the potential for delaying catastrophic failure under tension [92].

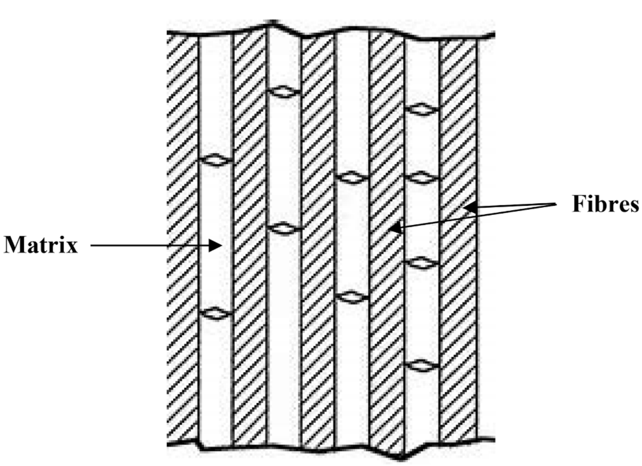

Fig. 4.3. Schematic of matrix fragmentation creating pseudo-ductility in ceramic matrix composites.

The distribution of fibre strengths can be greatly widened by mixing fibres of different types to create hybrid composites. Hayashi et al. showed the synergistic effects of mixing different fibres in their study on unidirectional layered glass/carbon hybrid composites [93]. They reported a "*hybrid effect*", referring to an enhanced strain to failure of the carbon fibres compared to that measured in an all-carbon/epoxy composite. However, the stress–strain response showed a sharp load drop after the failure of the carbon which had a lower strain to failure than the glass. This is indicative of substantial delamination between the fractured carbon and the glass, leading to a loss of integrity, and so the response cannot be considered as pseudo-ductile. There has been much controversy about this hybrid effect, clouded by underestimation of the difficulties of obtaining reliable test results. Some of the factors affecting the strength of hybrids have been reviewed by Swolfs [94].

Bunsell and Harris reported progressive failure in tests of a layer of carbon/epoxy between two layers of glass/epoxy, as shown in Fig. 4.2 [95]. The failure was more gradual than reported by Hayashi et al., with smaller load drops compared with similar specimens with a double layer of carbon, although the failure strains were quite low as a result of the fibres used. There was significant acoustic emission after the knee point due to the carbon fibre failure.

Aveston and Sillwood developed the theory of synergistic fibre strengthening in hybrid composites [96]. They noted the importance of spreading the brittle fibres thinly and evenly and created a composite with layers of carbon tows of 10,000 fibres spread to a width of 150 mm alternating with glass fibre layers, with overall fibre volume fractions of 3.5 % and 35 % respectively. The degree of non-linearity was modest, but very gradual failure of the carbon fibres was obtained, with multiple fibre fragmentations visible as small closely spaced cracks on the surface. This in-situ fragmentation is a very important mechanism for creating pseudo-ductility.

It is similar to the mechanism in fibre reinforced brittle matrix composites, where it is the matrix that fragments rather than the fibres

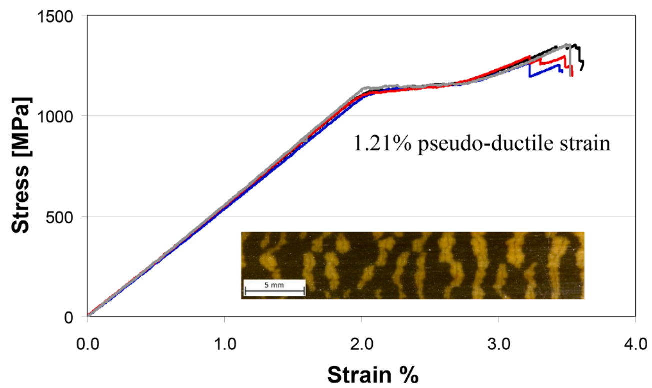

Fig. 4.4. Pseudo-ductile response of UD S-glass/high strength carbon hybrid (reproduced from [104,105]).

[97]. Fig. 4.3 illustrates this mechanism, which creates pseudo-ductility in ceramic matrix composites, e.g. [98]. Similarly pseudo-ductility has been created by sandwiching thin alumina plates between layers of carbon/epoxy, with the alumina fragmenting under tensile loading [99]. The ply fragmentation mechanism is discussed in more detail in Section 4.3 for thin plies. However, fibre level fragmentation may also give pseudo-ductility in a similar fashion, for example, with suitable hybridisation to ensure that multiple fragmentation dominates over localized failure. Aligned discontinuous hybrid composites discussed in Section 5 demonstrate that pseudo-ductility can be obtained in the limit where fibres are already broken. Initial work mentioned above with a nanonacre interface increased the number of fibre breaks before failure [89], and with further fragmentation, this mechanism should lead to non-linearity.

A number of authors have investigated the use of hybrid composites to produce reinforcing bars for concrete that fail gradually. For example, Bakis et al. presented results of hybrid pultruded rods with various combinations of glass, carbon, Kevlar and PVOH, reporting pseudo-ductile behaviour [100]. Cui and Tao tested rebars made combining fibres of steel, carbon, glass, and Twaron™ [101]. Yielding of the steel provided non-linearity before failure of the carbon fibres, and the bars were able to sustain load up to higher strains as the remaining fibres failed. These concepts produced gradual failure, but usually associated with load drops as the different fibres failed. Ali et al. later considered the role of delamination in the stress–strain response of basalt/carbon and glass/carbon hybrid rebars, and showed that the load drops could be controlled by appropriate design of the composite [102].

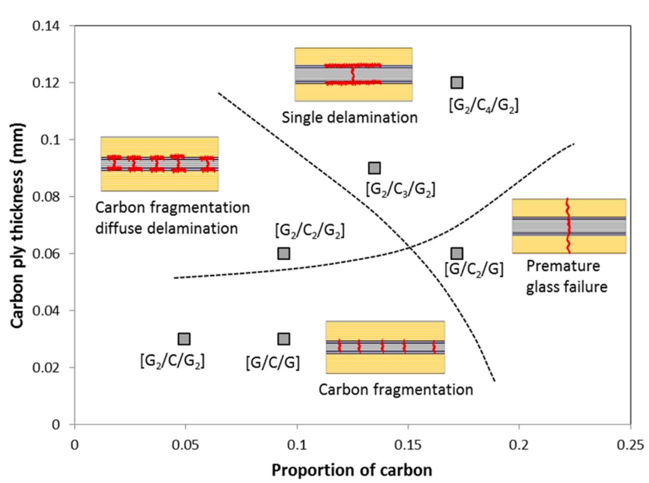

Fig. 4.5. Damage mode map for E-glass/thin carbon hybrid composite [106].

4.3. Ply fragmentation in thin-ply hybrids

Thin-ply composites have become widely available commercially with the development of tow spreading technology, and this has led to new opportunities to create pseudo-ductility via ply fragmentation. Thin plies of a single material tend to suppress matrix cracking and delamination, leading to a more brittle overall response [103]. However, in UD interply hybrid composites where one ply type has a significantly lower failure strain than the other type, a gradual failure can be produced. In this case the ply thickness is crucial, as explained by Czél and Wisnom. Thin plies avoid delamination, which can lead to undesirable load drops after failure of the low-strain layer, since the energy available to drive the delamination from the low-strain layer fracture is proportional to its thickness [104]. For typical epoxy-based high strength carbon/glass hybrid composites, a critical carbon layer thickness of about 0.06 mm was calculated, and it was shown that hybrid composites with carbon ply thicknesses below this limit did indeed fail by progressive fragmentation.

4.3.1. Pseudo-ductility in unidirectional tension

Fig. 4.4 shows the response for two 0.029 mm plies of high strength TR30 carbon fibre / epoxy with approximately 1.9 % failure strain creating a 0.058 mm low-strain ply-block sandwiched between single 0.155 mm thick S-glass epoxy plies (corresponding to the high-strain plies) on either side [105]. There is a broad and smooth plateau after the knee point due to the progressive fragmentation, with the amount of local delamination kept low, as a result of the thin carbon layers. Fragmentation started just before the knee point and continued, so that a pseudo-ductile strain of 1.23 % was obtained. There is also a striped pattern visible on the surface of the hybrid composites due to the translucence of the glass and the local damage at the ply interface associated with the fragmentation, which forms the basis for a strain overload sensor concept (see Section 4.3.3).

Modelling has shown that both the relative thickness (i.e. the proportion of carbon to total thickness) and absolute thickness of the carbon plies are important in controlling the hybrid response [106–108]. With the choice of the appropriate thicknesses, premature brittle failure of the whole hybrid specimen and catastrophic delamination can be avoided.

Damage mode maps can be produced such as Fig. 4.5, with the different failure mode regions in this case indicated approximately based on finite element (FE) analysis and compared with experimental results [106]. Ply tensile strength was represented stochastically, and cohesive elements were used to model delamination. This captures the different mechanisms of complete ply failure, fragmentation and delamination, and their interaction, and highlights the importance of the absolute as well as relative thickness of the low strain plies. Simplified analytical models allow the boundaries to be calculated

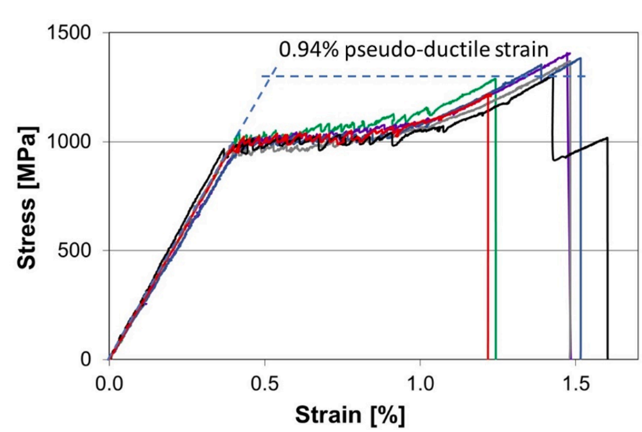

Fig. 4.6. Stress–strain response for UD [$T1000_2$/$XN80_2$/$T1000_2$] thin carbon hybrid. Replotted from results in [114].

explicitly, enabling parameter studies to be undertaken to understand what controls the failure mechanisms [107,108]. Tavares et al. investigated the mechanics of hybrid composites using analytical and computational models at the micromechanical rather than ply level, taking account of the variability of individual fibre strengths but not considering delamination. This gave further understanding of the factors controlling pseudo-ductility, showing in particular the need for continuity in the strength distributions of both fibre types [109]. Three dimensional progressive failure micro-mechanical modelling based on a chain of bundles has also been used to simulate the fragmentation mechanism, giving much faster solutions than FE [110]. Mesquita et al. presented a dual scale stochastic model linking the micromechanical and ply levels which was able to capture the experimental stress–strain behaviour and fragmentation lengths [111], although with some differences due to delamination which was not included in the model. A parametric study showed that a lower Weibull modulus for the low strain plies, indicating higher strength variability, predicted a more gradual development of failure. Conde et al. produced a micromechanical spring element model to analyse hybrid composites which was fast enough to be able to be used to optimise pseudo-ductility [112]. The model showed that high fibre dispersion favours pseudo-ductile behaviour. Ribeiro et al. applied an analytical model for the hybrid effect to predict pseudo-ductility and create damage mode maps for composites targeted at civil engineering applications [113].

There is a trade-off between pseudo-ductility on one hand, and pseudo-yield stress on the other [105,108]. A range of different glass-carbon hybrid configurations has been evaluated, and pseudo-ductile strains of up to 2.64 % have been obtained with a pseudo-yield stress of 520 MPa, or 0.80 % pseudo-ductile strain with a plateau stress of 1358 MPa [105], with moduli between 50 and 124 GPa depending on the type and fraction of carbon fibres.

Pseudo-ductile response has also been demonstrated with hybrids with different grades of carbon fibres. Fig. 4.6 shows the response of hybrid specimens made from 0.094 mm of Granoc XN80 ultra-high modulus pitch-based carbon fibres between 0.064 mm layers of T1000 intermediate modulus polyacrylonitrile-based carbon fibres, giving 0.94 % pseudo-ductile strain [114]. Pseudo-ductility for intermediate / high modulus carbon hybrids has also been reported by Danzi et al. [115].

Pseudo-ductility with standard thickness high modulus pitch / intermediate modulus carbon hybrids has been obtained where the carbon failed at a strain below that required to cause delamination [116]. Pseudo-ductile hybrids of intermediate modulus, high strain carbon / S-glass with about 0.1 mm carbon ply thickness have been created by toughening the glass/carbon interfaces using 0.03 or 0.06 mm thick epoxy films [117] or thinner electrospun nanofibrous polyamide PA6 mats of only 2–20 g/m^2 [118]. Pseudo-ductility was also achieved with the same intermediate modulus carbon and S-glass/epoxy composite layers, using thin PA12 film interleaves to toughen the interfaces [119]. Hybrids with tows of glass and carbon fibres laid side by side using tailored fibre placement showed pseudo-ductile response [120]. Glass/carbon hybrids manufactured by 3D printing can also show pseudo-ductility, with pseudo-ductile strains of up to 0.76 % reported depending on the ratio of materials [121]. Pseudo-ductile response of various interlayer hybrids of high strength carbon, high modulus carbon, basalt and E-glass for civil engineering applications were presented by Ribeiro et al. [122].

When the low strain plies in the hybrid laminates are very thin, it has been shown that there is an enhancement in the strain to failure of the plies which can be referred to as a hybrid effect [123]. For high strength carbon/glass hybrids this only occurs for plies less than 0.1 mm thick and can be as high as 20 % for a single 0.03 mm ply. The effect can be modelled, and has been shown to be due to the constraint on forming critical clusters of fibre breaks [123]. This means that as well as producing pseudo-ductile response, these hybrid laminates are able to take greater advantage of the intrinsic properties of the carbon fibres. Similar enhancements in the failure strain have also been measured with thin high modulus carbon sandwiched between intermediate modulus carbon plies [124]. It is interesting to compare this with the well known enhancement of transverse tensile cracking strain for thin plies, as reported by Parvizi et al. [125] and studied in detail more recently by Paris

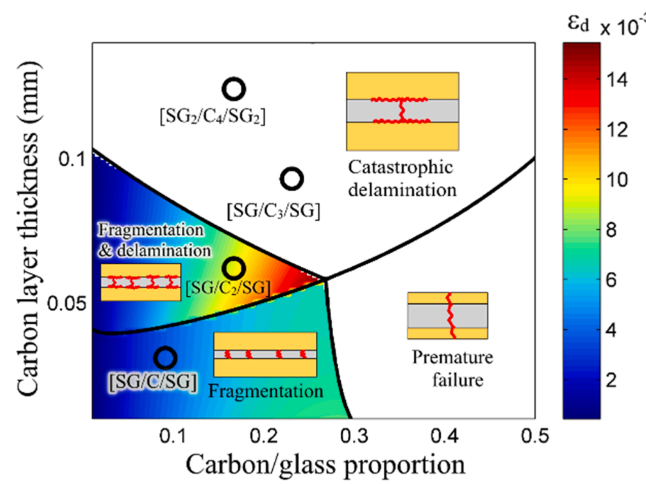

Fig. 4.8. Damage mode map for UD S-glass/carbon hybrid laminates illustrating optimal configuration for maximising pseudo-ductile strain ε_d [108].

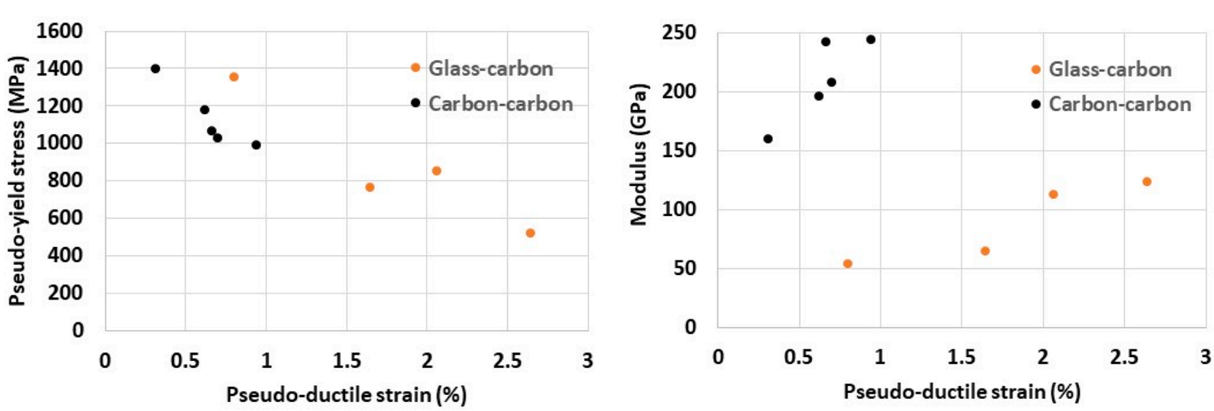

a) Pseudo-yield stress / strain trade-off b) Modulus and pseudo-ductile strain correlation

Fig. 4.7. Relation between key performance parameters for thin-ply hybrids.

et al. [126]. Although the mechanisms are different, in both cases there is constraint on the joining up of micro-scale damage, leading to an increase in failure strain when the plies are sufficiently thin.

Loading-unloading–reloading tests show a reduction in initial modulus due to the fragmentation damage and local delamination, so that such laminates are pseudo-ductile rather than truly ductile [127–129]. The reduction in the reloading modulus represents the amount of damaged carbon fibres no longer contributing or contributing less to carrying the load. When laminates are loaded in tension beyond the knee point and then loaded in compression, they may fail earlier than pristine laminates due to delamination of the fragmented carbon plies starting from the ply fractures [130].

It has been shown that acoustic emission can be used to detect fragmentation, with a direct correlation between acoustic and fragmentation events, allowing the technique to be used to detect fragmentation in opaque carbon/epoxy laminates [128,131]. It is also possible to separate the glass and carbon fibre breakages [132].

Introducing cuts into the low strain plies is an alternative means of producing pseudo-ductility via controlled local delamination of the discontinuous plies before they fragment [133]. A similar strategy can be used to produce pseudo-ductile behaviour in non-hybrid laminates by introducing cuts in selected plies. Layers of aligned short fibres can also be used for the low strain material [134]. Pseudo-ductility has been successfully introduced into the stiffeners of grid-stiffened structures by means of cut tows, giving increases of 30–50 % in maximum load carrying capacity and pseudo-ductile displacement under bending and tensile loading [135]. Discontinuous fibre approaches are discussed in detail in Section 5.

The trade-offs between pseudo-ductile strain, pseudo-yield stress and modulus are illustrated in Fig. 4.7 for various glass-carbon and carbon–carbon hybrids using the data from [105,114]. Fig. 4.7a shows the expected reduction in pseudo-yield stress with increasing pseudo-ductile strain for both types of hybrid. In contrast, Fig. 4.7b shows a positive correlation, with modulus and pseudo-ductile strain tending to increase together. The increasing proportion of high modulus fibres generates greater pseudo-ductility so long as the threshold is not exceeded that would cause a change to catastrophic failure. The trend is illustrated in the damage mode map in Fig. 4.8 for some of the same S-glass/carbon hybrids included in Fig. 4.7. The predicted pseudo-ductile strain is superimposed on the damage mode map. The maximum values are in the area where fragmentation and localized delamination both occur, increasing with greater proportion of carbon until the boundary is reached when the failure mode switches to catastrophic delamination or fibre failure. Optimal performance is close to the boundary, whilst leaving sufficient margin to avoid the risk of catastrophic failure. This trend shows the very beneficial effect of adding higher modulus fibres to a given material, simultaneously improving stiffness and creating more gradual failure. The trade-off then is between modulus and pseudo-yield stress, as higher modulus fibres tend to have lower failure strains, thus bringing the pseudo-yield (i.e. damage initiation) point earlier. Further parametric studies and discussion are presented in [108].

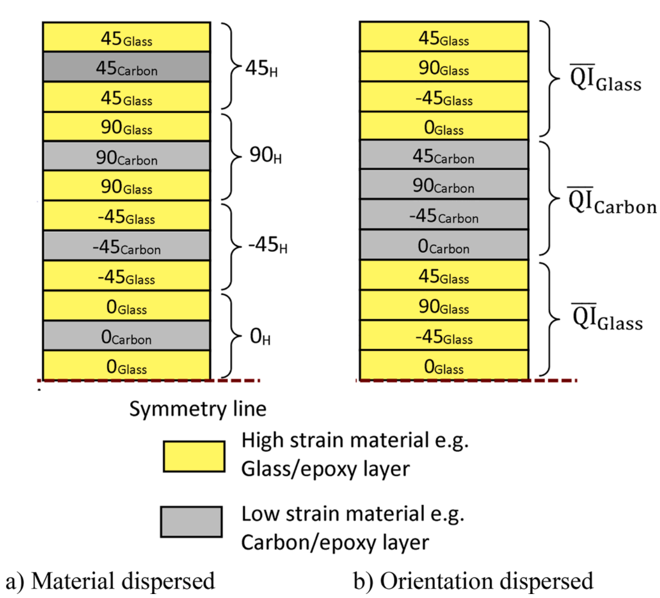

Fig. 4.9. Alternative quasi-isotropic hybrid configurations.

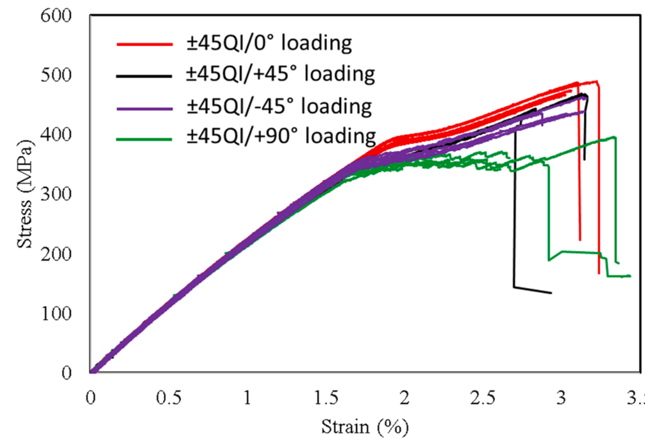

Fig. 4.10. Pseudo-ductile response of glass/carbon hybrid loaded in four fibre directions. Layup $[45_{S\text{-glass}}/90_{S\text{-glass}}/\text{-}45_{S\text{-glass}}/0_{S\text{-glass}}/0_{C\text{-}T300}/45_{C\text{-}T300}/90_{C\text{-}T300}/\text{-}45_{C\text{-}T300}]_s$ [139].

4.3.2. Pseudo-ductility in multi-directional laminates and loading modes other than tension

Modelling showed how pseudo-ductile behaviour could be achieved in multi-directional layups [136] and this has been demonstrated experimentally with quasi-isotropic laminates made from UD thin-ply hybrid sub-laminates with different carbon fibres [137]. An alternative concept with sublaminates formed by blocks of the same material with different ply orientations rather than blocks of different materials with the same orientation has also been proposed, as shown in Fig. 4.9, producing pseudo-ductile quasi-isotropic laminates of standard thickness S-glass and 0.029 mm high strength carbon plies [138]. This reduced the risk of free edge delamination and gave similar response in all the fibre directions in a slightly different layup, as shown in Fig. 4.10 [139]. Differences in the knee point strain were observed for different stacking sequences, and these were attributed to variations in the hybrid effect influenced by the stiffness of the adjacent plies as well as the carbon ply thickness. FE analysis suggests this is due to changes in stress concentrations affecting the interaction between fragmentation in different plies [140]. Loading at small off-axis angles also produces pseudo-ductile response, although the pseudo-ductile strain decreases [141]. Kohler et al. have also shown pseudo-ductility in quasi-isotropic hybrids of HR40/T800 carbon fibres, with 0.47 % pseudo-ductile strain and a strength of over 900 MPa [142]. Czél demonstrated pseudo-ductility in glass/carbon laminates with cross-ply glass and either cross-ply or spread-tow carbon fabric [143].

Fragmentation can also occur in compression, for example in unidirectional 0.03 mm ply M55 carbon / standard thickness S-glass laminates on the surface of specimens loaded in bending [144]. The carbon fibres break, forming a crack at an angle through the thickness, and then some relative movement between the fracture surfaces allows further loading and failure elsewhere, leading to a similar fragmentation behaviour and associated change in stiffness to that observed in tension. The visually observable fragmentation pattern and a schematic of the failure mechanism are shown in Fig. 4.11 [145]. Similar behaviour has also been obtained in direct compression tests, giving a significantly

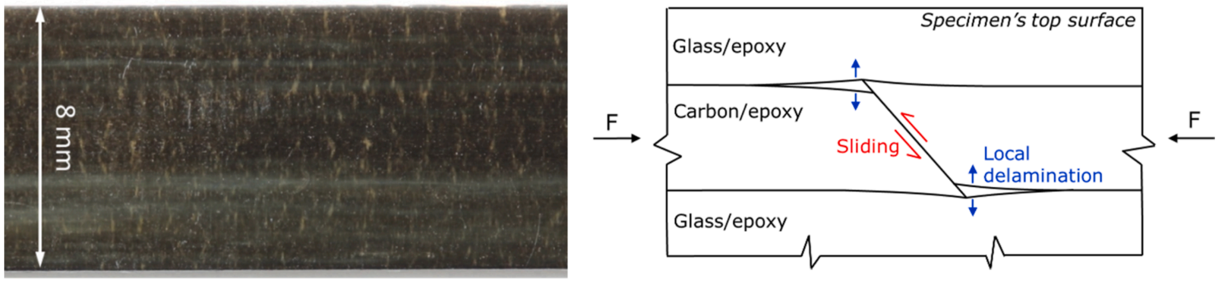

a) Top view of fragmentation pattern b) Side view schematic of micro-deformations

Fig. 4.11. Fragmentation of S-glass/ M55 carbon hybrid in compression [145].

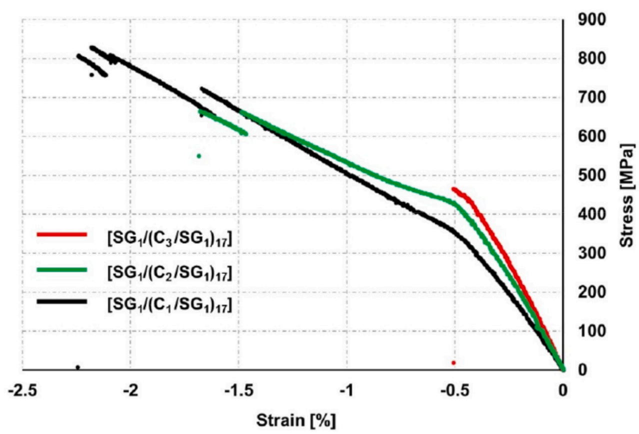

Fig. 4.12. Effect of ply thickness on pseudo-ductile response of UD S-glass/ M55 hybrid in compression [146].

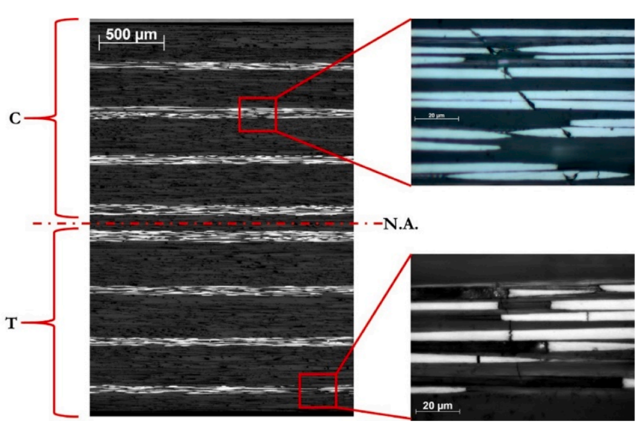

Fig. 4.13. Fragmentation cracks on compression (top) and tension side (bottom) of S-glass/M55 laminate in bending [147].

non-linear response as shown in Fig. 4.12, although with a reduction in slope after the knee point rather than a plateau [146]. The stress continues to rise more slowly after the knee point as fragmentation continues, but the carbon continues to carry some load, although the increasing load is taken mostly by the glass plies until delamination occurs, followed by complete failure. The strain at which delamination occurs decreases as the thickness of the carbon ply blocks increases, but the knee point strain does not change. When these laminates are loaded in bending, fragmentation first occurs on the compression side, then in tension followed by final failure in compression [147]. The different morphology of the fragmentations in compression (angled cracks) and tension (clusters of broken fibres close enough together to interact) is

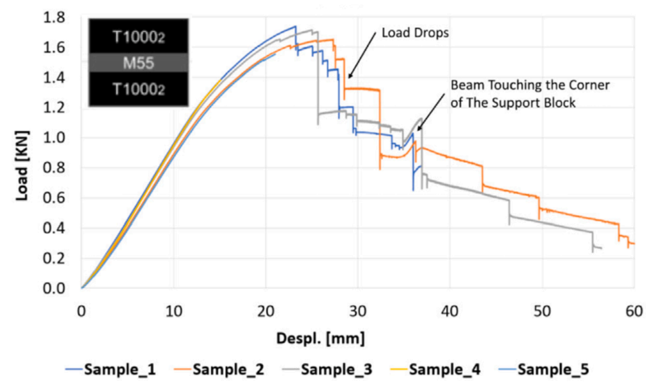

Fig. 4.14. Flexural response of asymmetric UD S-glass/pseudo-ductile carbon laminate [148].

illustrated in Fig. 4.13. The different behaviour in tension and compression highlights the challenge in optimising response for general applications.

Tests were carried out on S-glass/carbon hybrids under bending, with higher strain TR30 carbon fibres rather than high modulus M55 carbon fibres. A single block of two thin carbon plies between standard thickness glass plies was placed at the surface, with the specimen core made of glass. Fragmentation occurred in tension, but not in compression. Sudden failure then occurred in compression, with compressive strains as high as 2.5 % obtained in the carbon plies with no prior damage observed [144]. Analogous behaviour was found in hybrids with similar TC35 thin carbon plies throughout the thickness and layups $[SG/TC35_n/SG]_{4s}$ with n = 1, 2. Substantial non-linearity occurred due to fragmentation in tension. The final failure occurred in compression at strains of 2.66 % and 3.00 % for the 2 and 1 ply cases, which is more than double the expected compressive failure strain of the carbon, suggesting a strong hybrid effect in compression [147].

The different behaviour in compression with TR30 compared with M55 shows the importance of selecting appropriate fibres. Only the higher modulus carbon fibres tend to fail in compression by fibre failure, as required to produce pseudo-ductility, with most other fibres giving rise to catastrophic laminate failure due to microbuckling. Polymer fibres also have low compressive strength and might be suitable to hybridise with stronger fibres, although this does not appear to have been investigated yet.

Compressive failure in bending can be suppressed completely by putting a block of higher strain glass fibres on the compressive side of a pseudo-ductile laminate [148]. Fig. 4.14 shows the flexural response of an asymmetric laminate designed using a simple beam analysis. It has about 1.08 mm of S-glass on the compression side and then eleven repeats of a carbon hybrid sublaminate 0.16 mm thick of plies about 0.03 mm thick with layup $(T1000_2/M55/T1000_2)$, giving a total thickness of 2.96 mm. Substantial non-linearity was obtained initially due to fragmentation of the M55 plies, and large deflections. Load drops then occurred due to failure of T1000 plies followed by delamination, starting at the surface sublaminate which was under the highest tension and continuing progressively through the thickness, creating the load–deflection response in Fig. 4.14, with a large amount of energy absorbed. The reduced stiffness of the specimen meant that it bent double and could pass through the support rollers without completely failing. These results again show the potential to tailor the behaviour to the application, in this case to maximise pseudo-ductility and energy absorption under bending in one direction.

Fatigue response of pseudo-ductile hybrids has been shown to be good. Cyclic tension testing on unidirectional S-glass/TC35 carbon hybrids at 80 % of the knee point strain which showed no fibre failure on first loading sustained no damage after 100,000 cycles [149]. Specimens that were loaded statically until initiation of fragmentation and then fatigued showed gradual growth of damage until the carbon layers were fully delaminated after a few thousand cycles at 90 % of the knee point stress or a few tens of thousands of cycles at 70 %. Tests on glass/high modulus carbon and high modulus/high strength carbon/epoxy unidirectional fabric laminates for civil engineering applications have also shown good fatigue performance [129].

The good fatigue performance has also been shown to carry across into multi-directional laminates. Tension fatigue tests were carried out on two quasi-isotropic interlayer hybrids of Xstrand-glass/M46JB carbon and S-glass/T300 carbon, with the latter having a lower ratio of carbon to glass. Similar behaviour was found as for the unidirectional hybrids. The higher carbon content hybrid with the higher modulus fibres showed no stiffness reduction after 100,000 cycles at a stress level of 80 % of the knee point stress, but the lower carbon content hybrid showed a gradual reduction of up to about 10 % due to matrix cracking [150]. Even increasing the stress level to 90 % of the pseudo-yield stress gave only a gradual stiffness reduction up to about 10 % after 2000 cycles for the higher carbon content case, although the stiffness of the lower carbon hybrid reduced steadily, reaching a plateau of 50 % after 6000 cycles. These reductions were due to the appearance of fragmentation and delamination in addition to the matrix cracking in the low carbon case. Variables such as the ply thickness, the cyclic energy release rate and the interfacial fracture toughness were reported to control the fatigue induced damage, and can be selected to give the desired response. These results suggest that fatigue is not likely to be a serious limitation for well designed pseudo-ductile hybrids provided the cyclic loading is kept well below the fragmentation strain.

Tensile tests on S-glass / thin high-strength carbon hybrids at high loading rates have shown that fragmentation and pseudo-ductility still occur [151]. Pseudo-ductility is also maintained at −50 °C and + 80 °C [152]. Mousavi-Bafrouyi showed that pseudo-ductility of woven basalt / thin carbon hybrids loaded in bending tends to increase with increasing temperature [153].

Initial results under static indentation representative of impact [154] show different behaviour to conventional laminates, with carbon ply fibre fracture and delamination under the indenter and less damage to the inner layers, giving the ability to tailor the response and modify the failure mechanisms. Mousavi-Bafrouyi et al. investigated the effect of stacking sequence on the flexural and impact behaviour of woven basalt / thin carbon composites, showing pseudo-ductility when the carbon was placed away from the surface [155]. More research is needed to investigate impact response and residual strength after impact.

4.3.3. Other applications of fragmenting hybrid composites

The striped pattern visible on thin carbon/glass hybrids as shown in Fig. 4.2 can be used as a simple visual overload indicator, either forming the surface load bearing layer of the structure, or as a separate bonded-on sensor for composite or metallic structures [156]. It can also be incorporated into a smart self-warning repair patch [157]. By incorporating a pre-cut in the carbon layer, it can be used as a fatigue sensor.

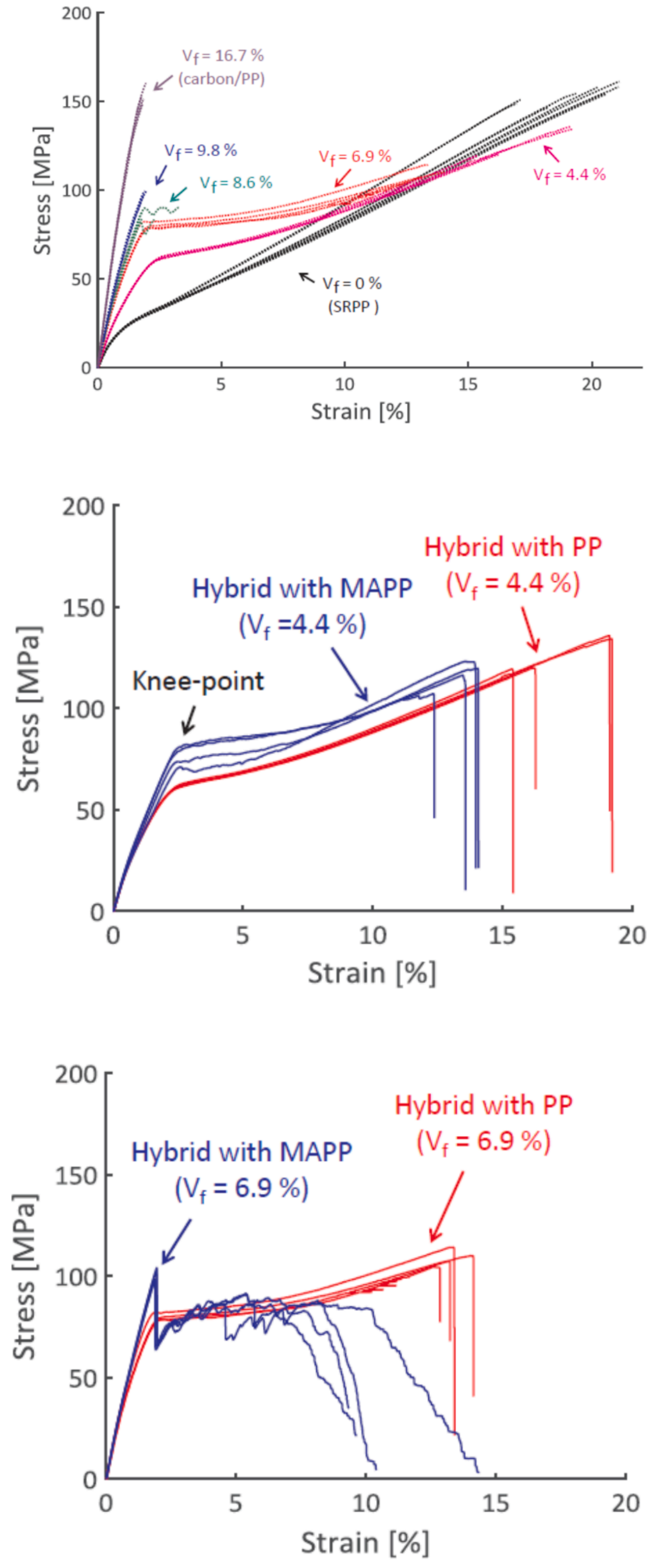

Fig. 4.15. Pseudo-ductile performance of carbon self-reinforced polypropylene of different volume fractions and treatment [169].

The clearly visible extent of delamination can be calibrated to estimate the number of fatigue cycles a structure has undergone [158]. Impact damage can also be detected that would otherwise not be visible by placing a hybrid sensing layer on the surface [159,160]. The simplicity, ease of manufacturing and implementation of carbon/glass hybrids as structural health monitoring sensors are advantageous compared to other mechanochromic systems based on dye-filled materials, modified polymers and structural colour materials, as reviewed in [159], offering great potential as user-friendly and cheap sensors that do not require power.

Hybrid specimens can also enable improved tensile testing. The glass plies on the surface of glass/carbon hybrids can completely eliminate the stress concentration where the specimen is gripped, producing consistent gauge section failures [144]. This gives higher experimental failure strain measurements than other test methods and allows some fundamental effects to be explored that could otherwise be obscured by variability and premature failure. Scaled hybrid specimens can be used to determine the size effect, whereby the tensile strain at failure decreases with increasing specimen volume [161]. Study of progressive ply fragmentation tests can be used to estimate the intrinsic variability of the material and deduce the Weibull modulus [161]. Hybrid specimens with cut plies can also be used to study the delamination behaviour at the interface, and to deduce the mode II traction-displacement relation for use in cohesive finite element analysis [162,163]. Since thin plies suppress delamination, and tab failures can be avoided, thin-ply hybrids allow some innovative methods of investigating the interaction of different stress components on failure. For example, thin carbon-fibre angle-plies sandwiched between glass have shown very limited effect of high in-plane shear stresses on fibre direction tensile failure [164]. Angle-plies have also been used to demonstrate the very limited interaction of large transverse compressive stresses on tensile failure of unidirectional plies [165].

4.4. Fragmentation in self-reinforced polymer and carbon fibre hybrids

Hine et al. studied hybrids of carbon fibre and self-reinforced polyamide 12 using different hybridisation methods, and observed pseudo-ductile behaviour in bending, although the tensile response was brittle [166]. Swolfs et al. investigated woven intralayer hybrids of carbon fibres and drawn polypropylene (PP) tapes [167], and obtained pseudo-ductility in bending tests. The importance of the interfacial bonding was highlighted, with maleic anhydride treated polypropylene (MAPP) producing higher strengths and moduli, but lower failure strains. In another paper various combinations of woven and unidirectional carbon and self-reinforced polypropylene (SRPP) were investigated [168]. Pseudo-ductility was obtained in tension with fragmentation of the carbon plies associated with load drops on the load–displacement response. Further work studied the brittle to ductile transition and showed how this could be controlled by suitable choice of stacking sequence and carbon fibre volume fraction, as presented in Fig. 4.15 [169]. Stress–strain responses were smooth, with strains of up to 15 % and significant increase in stiffness and yield stress compared with the baseline SRPP. Higher adhesion MAPP produced less desirable response with more load drops and lower ductile to brittle transition volume fraction. Mencattelli et al. showed that the response of carbon / SRPP hybrids could be further engineered by introducing laser cuts, leading to

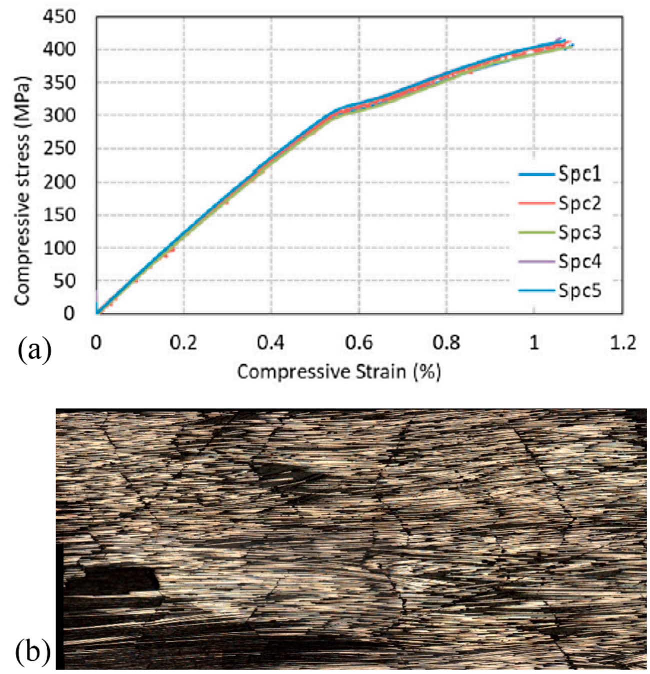

Fig. 4.17. Compressive behaviour of $[\pm 27_7/0]_S$ MR60/M55J carbon layup, a) Pseudo-ductile stress–strain response and b) compressive ply fragmentation in the central 0° plies [178].

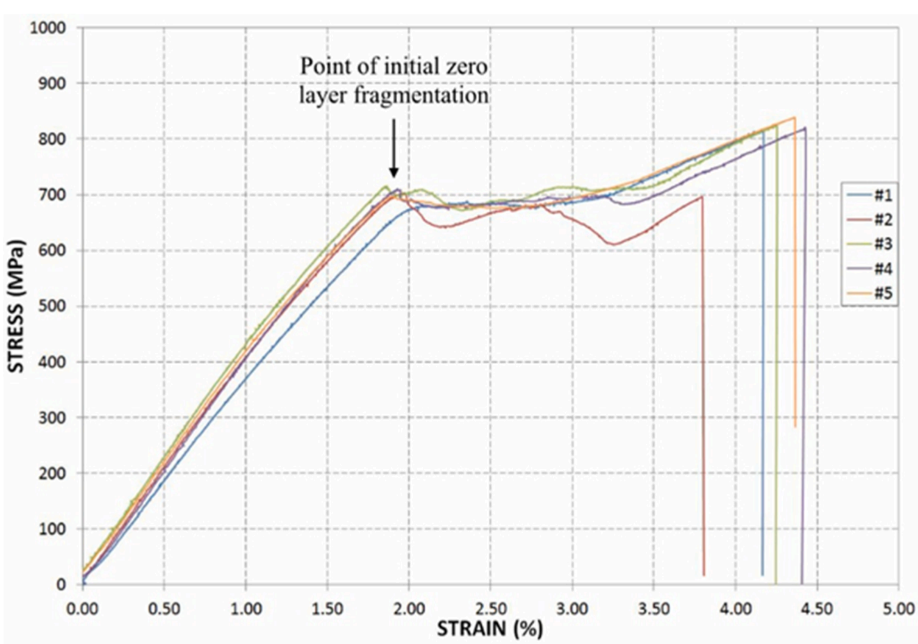

Fig. 4.16. Pseudo-ductile tensile response of $[\pm 26_5/0]_S$ laminate [172].

higher displacements, even more gradual failure, and greater energy dissipation [170]. Pseudo-ductility has also been successfully obtained with glass-fibre reinforced SRPP [171].

4.5. Combining fragmentation and reorientation in thin-ply composites

In Section 3 the concept of creating additional strain via reorientation of angle-plies was discussed. Introducing thin 0° plies into the layup allows fragmentation to occur in these plies in a similar way as in the thin-ply hybrids. In other words, the angle-plies behave like high-strain material sandwiching the 0 ° plies, similar to hybrids. Combining the two mechanisms of fragmentation and fibre rotation of the angle-plies gives a highly non-linear response, as shown for example in Fig. 4.16. This laminate of TR30 carbon/epoxy with a ply thickness of 0.03 mm and layup of $[\pm 26_5/0]_S$ gave a pseudo-ductile strain of 2.2 % [172], higher than would be achieved by either mechanism on its own. On reloading, these laminates do show some loss of initial modulus due to the fragmentation of the 0° plies, and so are pseudo-ductile rather than fully ductile [71]. Unpublished work found that gradual failure is maintained when loaded at angles of up to 6° to the 0° plies, although with reduced pseudo-ductile strain. High strain rate testing has demonstrated that pseudo-ductile behaviour can be retained, with modified response [151]. The effects of different temperatures and moisture on response have also been assessed [173]. Pseudo-ductility decreased at −50 °C but increased at 80 °C. Moisture had less effect on pseudo-ductility, but the strength was substantially reduced at 80 °C.

Different materials can be used for the 0° and angle-plies. For example layups $[\pm 25/0/\pm 25]$ and $[\pm 25_2/0]_S$ using thin ultra-high modulus YSH70A carbon for the 0° plies and MR60 intermediate modulus thin carbon for the angle-plies produces sub-laminates which are pseudo-ductile and only 0.15 mm and 0.25 mm thick respectively, with a sub-laminate modulus of about 130 GPa [174,175]. Multi-directional laminates of these pseudo-ductile sub-laminates can then be created, which also give a pseudo-ductile response [174]. A layup of $[(\pm 27_7/0)_S]_2$ MR60 angle-plies and M55J 0° plies gave a pseudo-ductile strain of 3.9 % [176]. Static indentation and impact tests were carried out, and subsequent tensile tests showed some pseudo-ductility was retained, although with reduced strains. Xiang et al. developed a model combining the effects of material non-linearity, fibre rotation and fragmentation that gave good predictions for the pseudo-ductile behaviour of angle-ply laminates with and without 0° plies [177].

Fragmentation of the 0° plies can also occur under compression, giving an analogous pseudo-ductile response to that in tension, although with lower strength and strain, as found for thin-ply hybrids. Layups of $[\pm 27_7/0]_S$ with MR60 angle-plies and M55J 0° plies tested in a sandwich beam showed the response in Fig. 4.17a, with a pseudo-ductile strain of 0.41 % [178]. Removing the outer layers revealed a pattern of angled cracks across the width of the carbon plies, as shown in Fig. 4.17b. Flexural loading was also investigated, showing the interaction between the different responses previously observed in tension and compression, leading to a more complex overall non-linear flexural response and delayed final failure in compression.

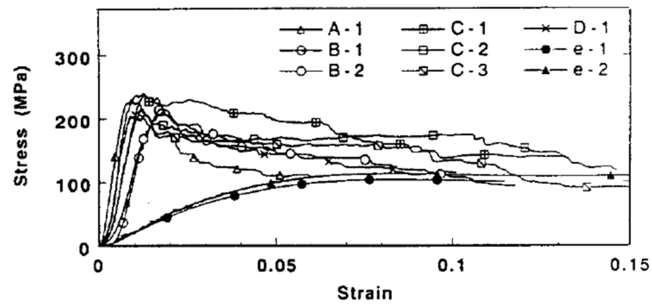

Fig. 4.19. Compressive response of 3D layer-to-layer carbon (A), layer-to layer S glass (B), 3D through-the-thickness carbon (C), through-the-thickness S-glass (D) and neat epoxy (e) [182].

Fatigue response has been shown to be good, similar to pseudo-ductile hybrids. Cyclic loading of $[\pm 25_7/0]_s$ carbon/epoxy laminates with intermediate modulus angle-plies and high modulus 0° plies showed no damage up until 10^6 cycles at 80 % of the pseudo-yield stress and up to 1000 cycles at 95 % [179]. Specimens pre-fractured by loading beyond the knee point also showed no significant damage when cycled at 80 % severity for 10^5 cycles, but delaminated slowly at higher loading. Laminates with all standard modulus carbon and layup $[\pm 25_6/0]_s$ showed similar behaviour, but with slightly lower performance.

A number of demonstrators have been manufactured and tested showing that the concept can be applied to real components including a skateboard [180] and a tubular tension member. The latter was 350 mm long and 50 mm diameter, made of TR30 carbon thin plies with layup $[\pm 26_6/0]_S$ and successfully carried nearly 90 kN with pseudo-ductile failure, Fig. 4.18 (unpublished work).

4.6. Fragmentation and reorientation in 3D woven and braided architectures

3D woven composites can show non-linear response, with localised failures constrained by the 3D fibre architecture, although performance is lower than in laminated composites due to the lower fibre volume fraction and non-straight fibres. For example Cox et al. showed considerably higher failure strains in tension than those of the carbon fibres in layer-to-layer and through-the-thickness interlock weave architectures

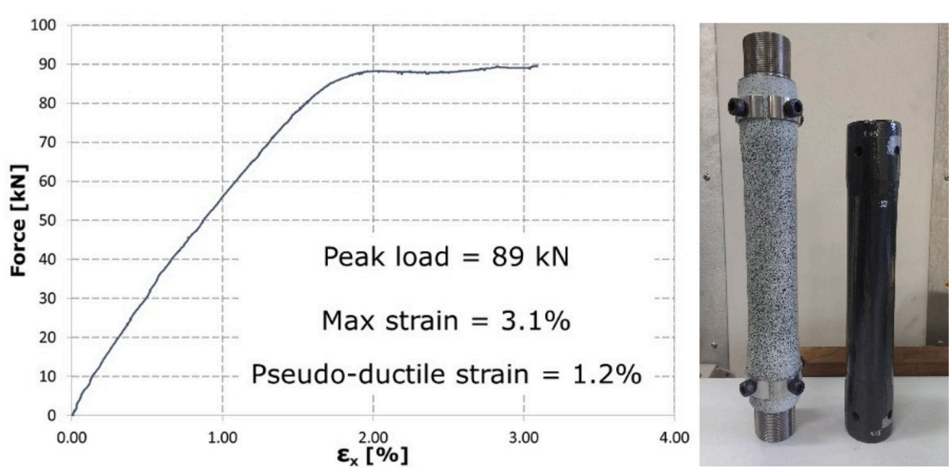

Fig. 4.18. Pseudo-ductile response of a tubular tension member.

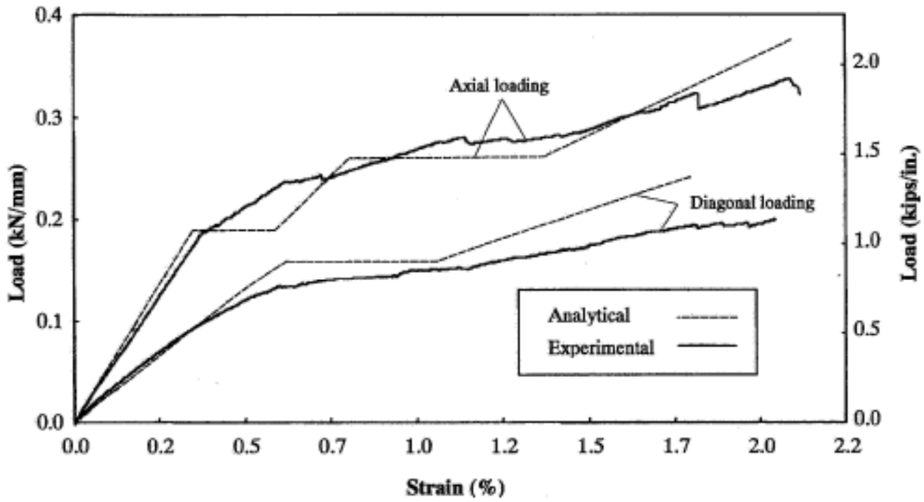

Fig. 4.20. Pseudo-ductile response of triaxially braided hybrid fabrics [184].

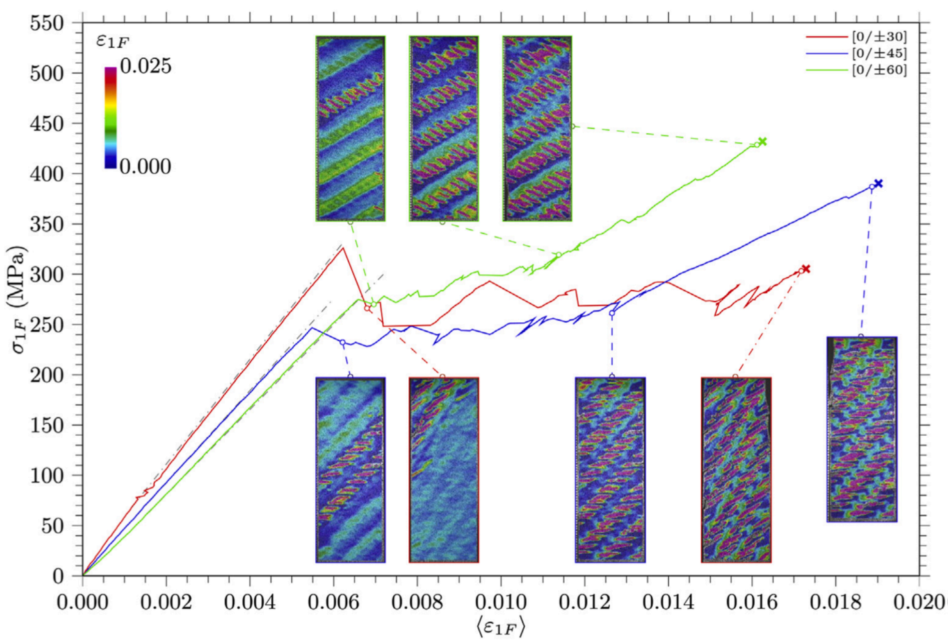

Fig. 4.21. Pseudo-ductility in triaxially braided composites loaded in braided fibre directions [185].

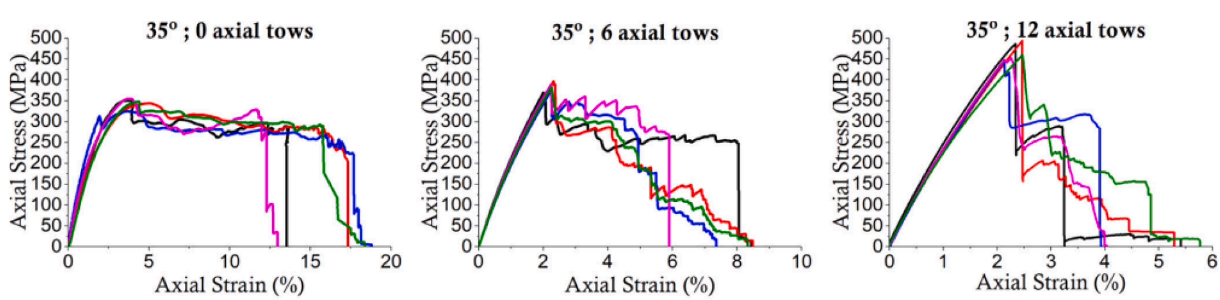

Fig. 4.22. Effect of axial tows on pseudo-ductility of ± 35° braided composites [186].

as a result of tow straightening and discrete tow ruptures that were contained [181]. Highly ductile behaviour was obtained in compression for both carbon and glass fibres, with strains occasionally exceeding 15 %, Fig. 4.19 [182]. More recently Das et al. modelled response of 3D non-woven composites in compression, simulating the multiple constrained kink bands giving rise to the non-linearity [183].

Grace et al. created triaxially braided fabrics for reinforcing concrete structures [184]. Axial tows consisted of low extension ultra-high modulus carbon, medium extension high modulus carbon and high extension E glass fibres. Tows at 45° consisted just of high modulus

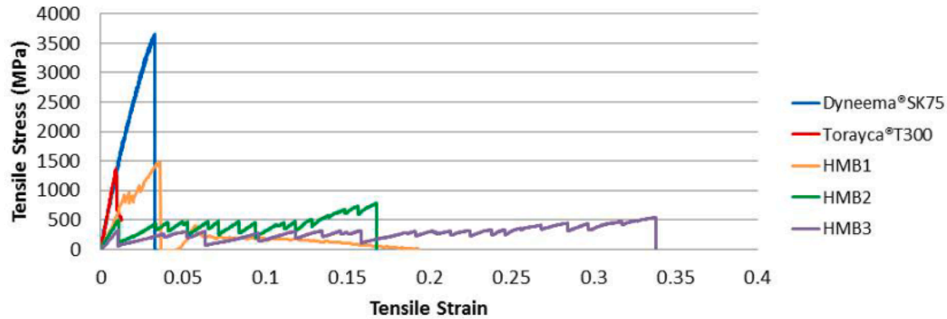

Fig. 4.23. Stress–strain response of dry microbraids compared with baseline fibres with braiding angles of 14° (HMB1), 33° (HMB2) and 39° (HMB3) [189].

carbon and glass. The fabrics showed considerable non-linearity when loaded in both axial and 45° directions, as shown in Fig. 4.20, and this behaviour carried across into the response of reinforced concrete beams.

Wehrkamp-Richter et al. investigated triaxially braided composites of HTS40 / RTM6 carbon epoxy with [0/±30], [0/±45] and [0/±60] fibre orientations [185]. Flattened braided specimens showed considerable pseudo-ductility when loaded in one of the braided fibre directions, caused by transverse cracking, alignment of the angle-plies, debonding and pull-out of the tows. The [0/±30] layup showed load drops at first failure, but the [0/±45] and [0/±60] cases exhibited a smoother transition with a long plateau region, as shown in Fig. 4.21. Meso-scale modelling was also presented. Potluri et al. showed pseudo-ductility in braided high strength carbon composites with braiding angles of 35, 45 and 55°. Best pseudo-ductile performance was obtained with the lowest braiding angle and no 0° fibres, with higher stresses but lower strains obtained with the inclusion of 0° fibres, as shown in Fig. 4.22 [186].

Another architecture with the potential to offer a lower-cost ductility solution in comparison to thin-ply prepreg-based laminates is dry fibre micro-wrapped hybrid tows. Unidirectional fabric laminates consisting of high modulus fibres wrapped with high strain-to-failure fibres exhibited pseudo-ductility through progressive fibre fragmentation and pull-out with up to 1.3 % pseudo-ductile strain [187].

Del Rosso et al. made hybrid dry microbraids by braiding Dyneema™ fibres over a unidirectional core of T300 carbon fibres at various angles [188,189]. Very high strains were achieved with load drops as the carbon fibres progressively failed and the load was transferred via friction on to the Dyneema™ fibres. Stresses of up to 500 MPa and strains up to 30 % were measured depending on the braiding angle, Fig. 4.23.

5. Ductility and pseudo-ductility in discontinuous composites

5.1. Introduction

It is widely accepted [190] that a discontinuous-reinforcement architecture (e.g. based on discontinuous fibres or platelets) can provide mechanisms for ductility or pseudo-ductility in composites. These mechanisms typically involve slip at the interface between the reinforcing elements (i.e. fibres or platelets) and the matrix, and/or additional matrix deformation near the ends of the reinforcing elements through plasticity and/or damage.

Nature is a main source of inspiration to use discontinuous-

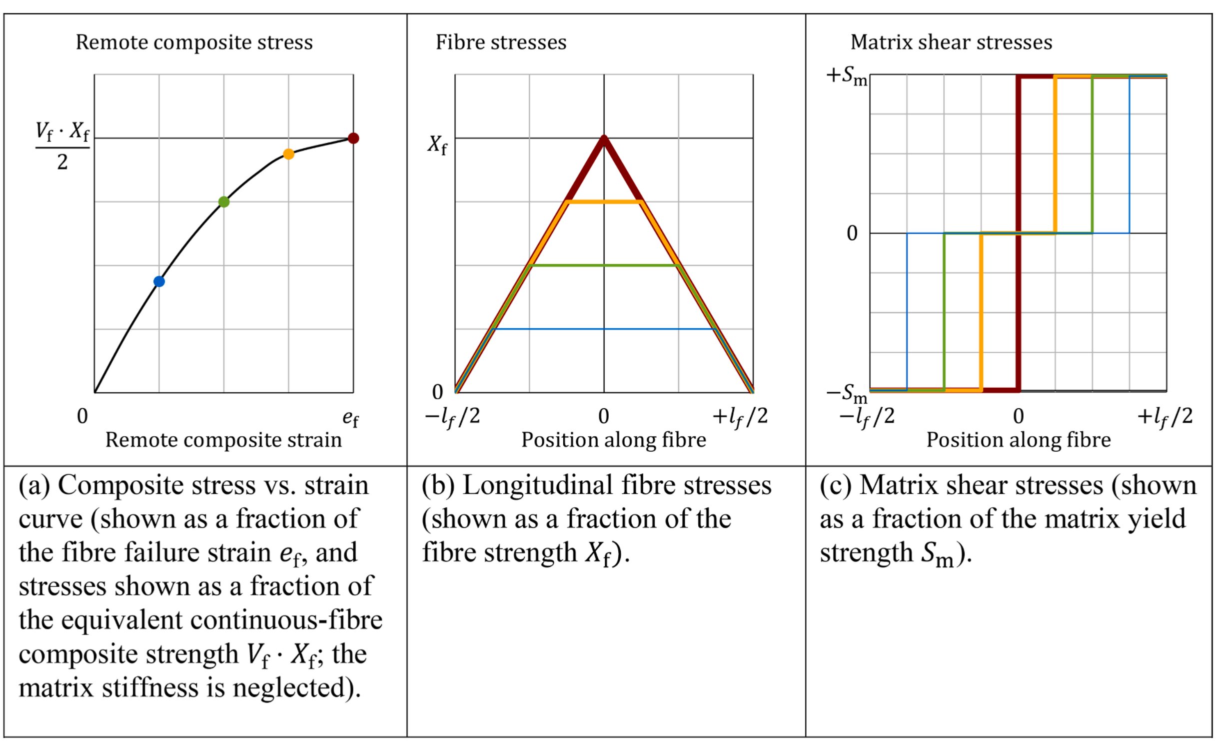

Fig. 5.1. Tensile response of an aligned discontinuous composite with critical fibre length, $l_f = l_c$, according to a unit-cell shear-lag model assuming a perfectly-plastic matrix. Each point highlighted in the subfigure (a) corresponds to a stress profile in subfigures (b) and (c).

reinforcement architectures in synthetic composites [190]: most biological composites with a structural function (e.g. nacre, bone, tooth enamel) feature a discontinuous architecture, which is key to the combination of high stiffness with damage tolerance typically observed in natural composites. This has motivated the development of several synthetic fibre-reinforced discontinuous composites with improved damage tolerant features, e.g. high impact resistance [191], high fracture toughness [190,192], and a non-linear stress–strain response under flexure [193,194] or under tension; this section will focus on the latter, since a non-linear response is required to obtain pseudo-ductile strains as defined in Section 1, and tensile loading is intrinsically more brittle than flexure.

When manufacturing discontinuous composites for high-performance applications, it is key to achieve a dense packing of the reinforcing elements (since they are the main load-carrying element in the composite), which requires very good alignment [195,196]. Such high alignment has the additional advantage of maximising the stiffness and strength in the reinforcement direction. Therefore, this section will focus on aligned discontinuous composites (and their laminates), with discontinuities either at the micro- (i.e. fibre) or meso- (i.e. ply) scales.

Section 5.2 will introduce the main deformation, damage and failure mechanisms in discontinuous composites, and how they can be related to ductility or pseudo-ductility. Sections 5.3 and 5.4 will review composites with pseudo-ductility induced by discontinuities at the ply or fibre level, respectively; Section 5.5 will focus on hybrid discontinuous fibre-composites with pseudo-ductility governed by fibre fragmentation.

5.2. Mechanisms for ductility or pseudo-ductility in discontinuous composites

The most classical model for failure of discontinuous composites is Kelly and Tyson's yield theory [197]. This proposes that, in an aligned short-fibre composite with a perfectly-plastic matrix (which is a reasonable approximation for polymeric matrices, as they lack strain hardening under shear [198,199]), stresses are transferred to the fibres through shear of the matrix, in a shear-lag process; this leads to two fronts of matrix yielding initiating at the fibre-ends and propagating stably along the length of the fibre, linearly building up longitudinal stresses in the fibre (as schematically represented in Fig. 5.1), until one of the two failure mechanisms occurs:

(i) The two matrix yielding fronts meet at the central section of the fibre, after which the perfectly plastic matrix will not be able to transfer any additional load to the fibre and will continue to plastically flow until the fibre pulls out and the composite fails. This failure mechanism should dominate composites with relatively short fibres, and lead to a ductile composite response;

(ii) The longitudinal tensile stresses in the central region of the fibre reach the fibre tensile strength, at which point the fibre fails in tension. This failure mechanism should dominate composites with relatively long fibres, and lead to a brittle composite response.

The transition between these two failure mechanisms defines the critical fibre length l_c (for a fibre radius r_f), which is governed by the matrix yield stress in shear S_m and fibre tensile strength X_f:

$$l_c = \frac{X_f}{S_m} \cdot r_f. \tag{5.1}$$

A key consequence of Kelly-Tyson's model is that the critical aspect-ratio $\alpha_c = l_c / r_f$ of a discontinuous composite is independent of the absolute size of the reinforcement, and depends only on the ratio between the strength of the fibre and the matrix; modelling work (validated by experiments) in Section 5.3 will demonstrate this is not strictly valid, especially for large reinforcing elements.

Kelly-Tyson's model [197] has been proposed several decades ago, and since then many models have been developed to capture the response of discontinuous composites more accurately (as will be described in Sections 5.3-5.5). Nevertheless, Kelly-Tyson's critical fibre length concept is still the most widely used [200–203] to design discontinuous composites and to predict and explain their response, both with ductile and brittle polymer matrices, and with reinforcing elements at several length-scales. Nevertheless, it is now acknowledged that failure of discontinuous composites is much more complex and governed by several different mechanisms and features which are not accounted for in Kelly-Tyson's model:

- Reinforcement (e.g. fibre) failure: this typically leads to a brittle composite response, unless the strength distribution of the reinforcing elements is extremely wide. A pseudo-ductile response can be achieved [204] by hybridising fibre types (as already reviewed for continuous-fibre composites in Section 4), which will be explored in Section 5.5;
- Progressive shear yielding of the matrix / interface (this is considered by Kelly-Tyson's model, and typically leads to some non-linearity in the stress–strain curve, although ductility can be significantly hindered by variability in the microstructure (e.g. random location of fibre-ends, as will be explained in Section 5.4) [205];
- Progressive interfacial debonding (i.e. shear-dominated crack initiation): this is a similar mechanism to Kelly-Tyson's matrix yielding, but governed by the mode-II initiation fracture toughness of the matrix/interface rather than by the matrix shear yield stress. This mechanism may lead to some pseudo-ductile behaviour, depending on the balance between the toughness of the interface and the dimensions of the reinforcing element [206] (as will be explained in Sections 5.3 and 5.4);
- Sudden transverse matrix cracking or sudden interfacial debonding: this is initiated by stress concentrations at the fibre ends in composites with a brittle matrix and/or brittle interface, and it typically leads to a very brittle composite response [202] (so it will not be discussed in this paper);
- Sudden macro-scale fracture propagating from a cluster of micro-scale damage: composites with significant microscale variability (e.g. with stochastic fibre strength distributions, random interfibre distance and fibre packing, stochastic matrix properties, random position of fibre ends) may fail due to unstable (and, therefore, brittle) crack growth from small clusters of microscopic damage, governed by the fracture toughness of the composite [205,207–209] (as will be discussed in Section 5.4).

5.3. Pseudo-ductile composites with slip due to ply-level discontinuities

Composites with ply-level discontinuities can be manufactured by introducing cuts across the fibres in unidirectional prepreg-plies to form the ends of the discontinuous reinforcing elements and laying up the plies accordingly to the desired geometric arrangement of the reinforcing elements. The cuts can be introduced with manual cutters [210], automated ply cutters [211,212], laser micro-milling machines [192,213], or through automated tape placement [214]. It is usually beneficial to use a lay-up alignment system [192] if the relative position of the discontinuities in different plies is to be controlled, as small shifts between the desired position of the plies may lead to a reduction in performance [213].

Composites with perfectly-staggered, ply-level discontinuities (as shown in Fig. 5.2a) are analogous to "Brick-and-Mortar" (BaM) composites, where the "bricks" are the composite discontinuous-ply units, and the "mortar" is the interface between plies (which can physically represent a resin-rich-region, an interleave, or simple interface). BaM composites constitute the simplest model system for discontinuous composites: they have a (nominally) regular microstructure and (nearly) deterministic micromechanical properties, which represent significant

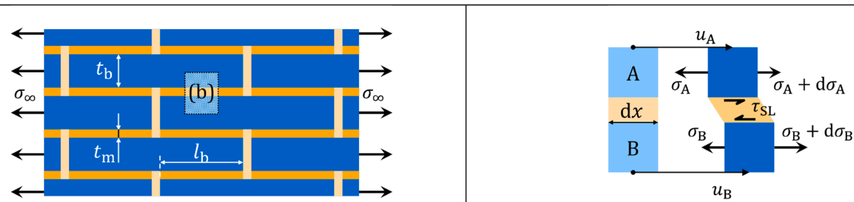

(a) Geometry of a perfectly-staggered brick-and-mortar composite under longitudinal tension.

(b) Shear-lag analysis of the region highlighted in subfigure (a).

Fig. 5.2. Schematic representation of a brick-and-mortar composite, where the bricks are shown in blue, and the mortar is shown in orange [206]. (For interpretation of the references to colour in this figure legend, the reader is referred to the web version of this article.)

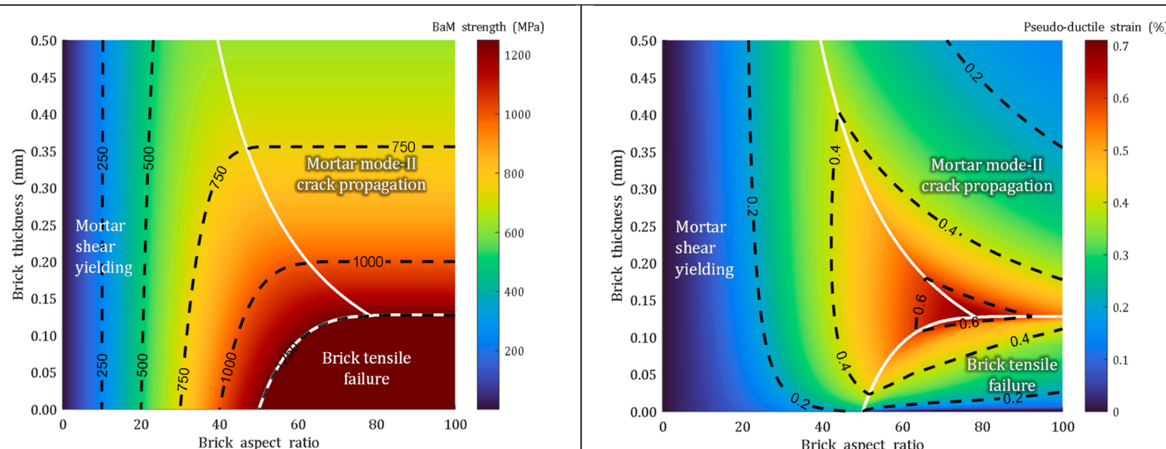

(a) Strength map.

(b) Pseudo-ductile strain map. For the composites failing through mode-II crack propagation in the mortar, the failure strain is taken at the onset of the stress plateau, to account for the localisation of strains which is likely to occur (due to the lack of intrinsic strain-hardening mechanisms).

Fig. 5.3. Strength, pseudo-ductile strain, and failure modes of a BaM composite, as predicted by Pimenta and Robinson's non-linear shear lag model [206]. Black dashed lines represent combinations of brick aspect ratio and thickness which result in the same composite strength (a) or pseudo-ductile strain (b), and white lines represent transitions between failure modes.

advantages over composites with discontinuities at the fibre level. This makes BaM composites particularly well suited for analytical modelling, which is usually done through shear-lag approaches [206,215] (as illustrated in Fig. 5.2b).

Most shear-lag models for BaM composites consider a perfectly-plastic (analogous to Kelly-Tyson's [197] Eq. (5.1) mortar. However, Pimenta and Robinson [206] developed a shear-lag model considering a generic shear response of the mortar, which accounted for a non-linear stress–strain relationship and finite fracture toughness of the mortar for the first time. This model demonstrated that the response of a BaM composite is governed not only by the brick aspect ratio (as suggested from Eq. (5.1), but also by the absolute brick thickness, as illustrated in Fig. 5.3 for a specific material (representative of a standard carbon/epoxy composite); the strength of BaM composites with thick bricks and large aspect ratio is bounded by the propagation of mode-II cracks in the mortar, governed by fracture mechanics (i.e. fracture toughness) rather than plasticity (i.e. yield strength).

This non-linear shear lag model [206] has been used to design BaM specimens with UD ply blocks as the bricks, and the interlaminar region as the mortar [210,214,216]. These experiments successfully demonstrated a non-linear response governed by fracture mechanics (Fig. 5.4), using different bricks materials and different methods to create the discontinuous microstructure. The effect on pseudo-ductility of platelet overlap length, platelet staggering; pattern, platelet thickness and interlaminar fracture toughness have also been investigated experimentally and by computational simulations [217]; this showed that, for a given platelet thickness, intermediate levels of toughness maximise both pseudo-ductility and strength, and that staggering the position of platelet-ends in a less regular manner would lead to a small increase in strength and reduction of pseudo-ductility.

This non-linear response provides a warning before failure (which can be used to increase the actual design limit of these materials), while maintaining the high modulus of the UD prepreg. By using thermoplastic interlayers it is also possible to make delamination damage repairable by the application of heat [119].

A key problem with BaM composites is that, once a mode-II crack is fully initiated, there is no strain-hardening mechanism intrinsically built in the architecture (unless there is a very significant R-curve behaviour at the scale of the overlap length), which leads to localisation of damage and, consequently, limits pseudo-ductility [206]. This can be overcome through hybrid interleaving between the bricks, using a tougher mortar insert at the centre of their overlaps (shown in Fig. 5.5) [218]. FE simulations predicted an intermediate stress plateau corresponding to crack propagation in the brittle mortar, followed by strain-hardening up to the

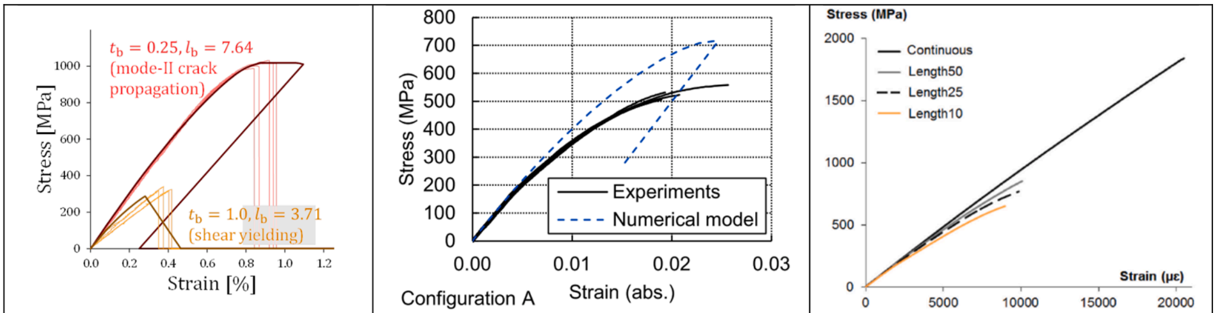

(a) Carbon/epoxy bricks, manufactured manually by Czél et al. [210]. Each hue (red and yellow) represents a different brick thickness and overlap length; lighter lines represent experimental results, and darker lines represent model predictions.	(b) Carbon/PEEK bricks, manufactured manually by Bachmann et al. (for brick thickness $t_b = 0.56$, overlap length $l_b = 14.3$) [216].	(c) Carbon/epoxy bricks, manufactured by automated tape placement by Rodríguez-García and Guzman de Villoria (for three distinct brick lengths (i.e. $2 \times l_b$), brick thickness $t_b = 0.184$) [214].

Fig. 5.4. Experimental tensile stress–strain curves of BaM composites, showcasing a non-linear response due to mode-II crack initiation between the bricks. All dimensions in mm.

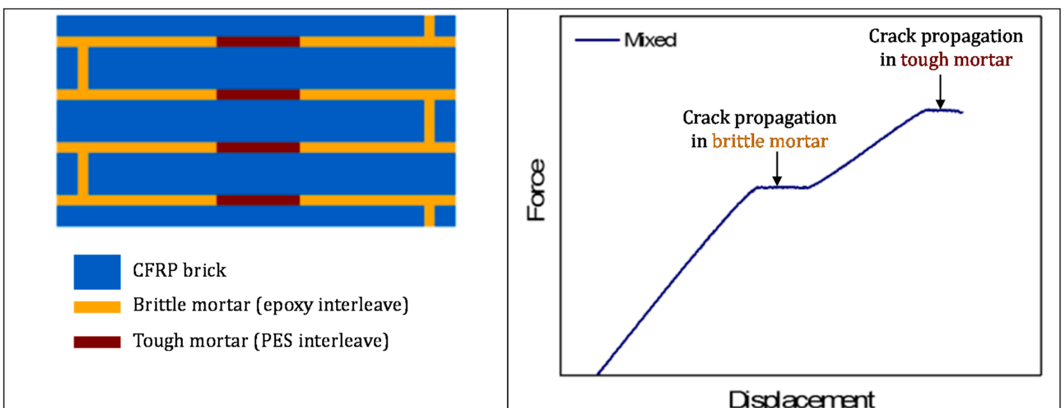

(a) Architecture.	(b) Predicted tensile response.

Fig. 5.5. BaM composite with hybrid interleaving, using a tougher mortar insert to provide a strain-hardening response [218].

stress corresponding to crack propagation in the tougher insert.

While a perfectly-staggered and two-dimensional BaM architecture (as shown in Fig. 5.2a) is a useful model system, real-life applications will necessarily have a more complex staggering of the bricks, with stochastic asymmetries in the overlaps between bricks, both in the length-wise and depth-wise directions. Nevertheless, FE simulations by Kravchenko et al. [200] demonstrated that it is still possible to generate some pseudo-ductility despite these asymmetries; the benefit of large brick aspect-ratios in the strength of BaM composites was demonstrated not only by an increase of average strength, but also by a reduction of the variability due to stochastic asymmetries in brick staggering.

BaM architectures have been extended to two hierarchical levels [213,219], where large-scale bricks are themselves brick-and-mortar composites. Experimental results demonstrated that, compared to non-hierarchical counterparts, hierarchical BaM microstructures dissipate more energy stably before failure, present a more non-linear response, delay damage localisation further, and are less sensitive to microstructural imperfections [213]. Moreover, by relaxing self-similar constraints and exploiting synergies between the scales [219], it was possible to design non-self-similar hierarchical BaM microstructures which exhibit a tailorable non-linear response, stable damage diffusion throughout the entire specimen, permanent deformation after damage initiation, and a stable stress plateau even under cyclic loading.

The concept of generating a non-linear response in composites through controlled mode-II crack initiating from ply-level discontinuities has been demonstrated in multi-directional laminates [220]. The possibility of exploring friction (instead of adhesion) between discontinuous reinforcing elements with a bow-tie shape (designed to promote interlocking during pull-out) has also been explored [221]. In addition, ply-level discontinuities introduced at the low-strain ply of interply hybrid composites (reviewed in Section 4.3.1) [133,222,223] provide specific initiation points for mode-II delaminations, which can increase pseudo-ductile strains further; moreover, introducing ply-level discontinuities in the low-strain ply rather than relying on its fragmentation can expand the design space of interply hybrids, by enabling the use of thicker low strain layers without risking sudden load drops at the onset of fragmentation.

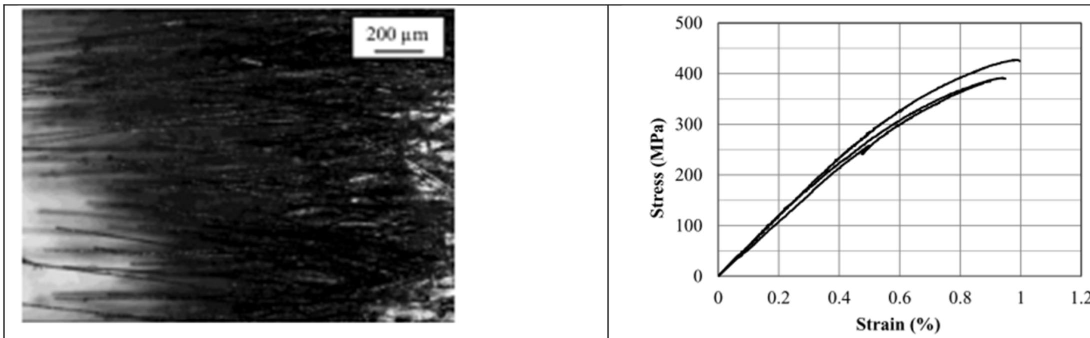

(a) Extensive fibre pull-out on the fracture surface.

(b) Non-linear stress-strain curve under tension.

Fig. 5.6. Carbon/PP ADCs with non-linear response due to slip at the fibre–matrix interface [231].

5.4. Pseudo-ductile composites with slip due to fibre-level discontinuities

While composites with fibre-level discontinuities have been used in industrial applications (e.g. in injection moulded components) for decades, aligning the fibres has been historically a key challenge to achieving high fibre content and high performance. A wide range of processes have been developed to align discontinuous fibres in composites, as reviewed by Such et al. [195]; most are based on dispersing the fibres in a fluid carrier that re-orients them through convergent flow, centrifugal forces, or a change in momentum.

Early work on Aligned Discontinuous Composites (ADCs) has produced composites with a non-linear stress–strain curve, either with thermoplastic or thermosetting matrices, using carbon fibre lengths around 1 mm (which is the minimum fibre length for which a good fibre alignment has been observed by Sanadi and Piggott) [224]; however, the fibre content was very low (20 % in volume), leading to poor strength (around 100 MPa) and limited failure strain (around 1.2 %). Further experimental research by Nishikawa et al. [201] using injection moulding to produce aligned carbon fibre/PP ADCs has slightly improved strength, although this was still very much limited by a low fibre content.

The development of alignment processes has seen tremendous advances in the last decade, with state-of-the-art processes reported to produce ADCs with nearly 60 % fibre volume fraction and over 90 % of the fibres aligned within 10°: HiPerDiF (High Performance Discontinuous Fibre technology, invented at the University of Bristol [225,226]), TuFF (Tailored Universal Feedstock for Forming, invented at the University of Delaware [227,228]), and a centrifugal hydrodynamic alignment process, developed at the University of Nottingham [196,229]. These processes led to a breakthrough in mechanical properties, producing ADCs with Young's modulus and tensile strength reaching those of the continuous-fibre counterparts [203,229,230]; however, this was achieved using fibres one order of magnitude longer than Kelly-Tyson's critical value, so the stress–strain curves were linear and no ductility or pseudo-ductility was observed in those cases.

To produce ADCs with pseudo-ductile response, the HiPerDiF process was used to align 3 mm long carbon fibres embedded in a PP matrix, that gives a poor interfacial adhesion [231]; the fibre length was approximately the same as the Kelly-Tyson critical fibre length (as estimated by Eq. (5.1). The measured stress–strain curve showed significant non-linearity, with a progressive reduction of the tangent modulus, and the fracture surface featured extensive pull-out (as shown in Fig. 5.6); therefore, this is the most convincing demonstration of ductility or pseudo-ductility in a composite through slip introduced at the fibre-level. Nevertheless, the failure stress (400 MPa) and strain (below 1 %) were modest compared to other HiPerDiF results, partially due to the introduction of fibre misalignments during the compaction process, and partially due to a low fibre content (36 % in volume).

A similar non-linear behaviour, has been observed with natural fibre composites, produced with the HiPerDiF method [232], particularly when reducing the length of caraua fibres from 6 to 2 mm, and therefore approaching the Kelly-Tyson critical fibre length, or changing the matrix type from Epoxy to PP.

Despite these advances, the strength and ductility/pseudo-ductility

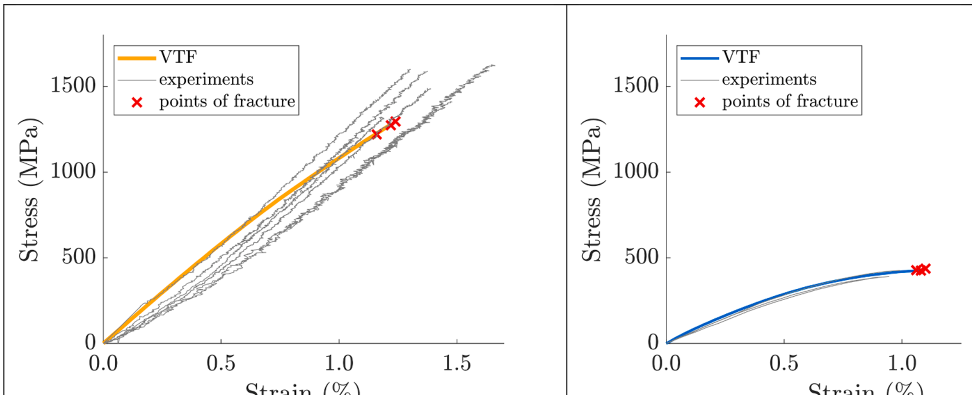

(a) Linear-elastic brittle behaviour in CF/epoxy specimens, with fibres much longer than Kelly-Tyson's critical length.

(b) Non-linear behaviour in CF/epoxy specimens, with a fibre length near Kelly-Tyson's critical value.

Fig. 5.7. Stress–strain response of ADCs: experimental results [203,231] vs. predictions from a semi-analytical virtual testing framework (VTF) [208].

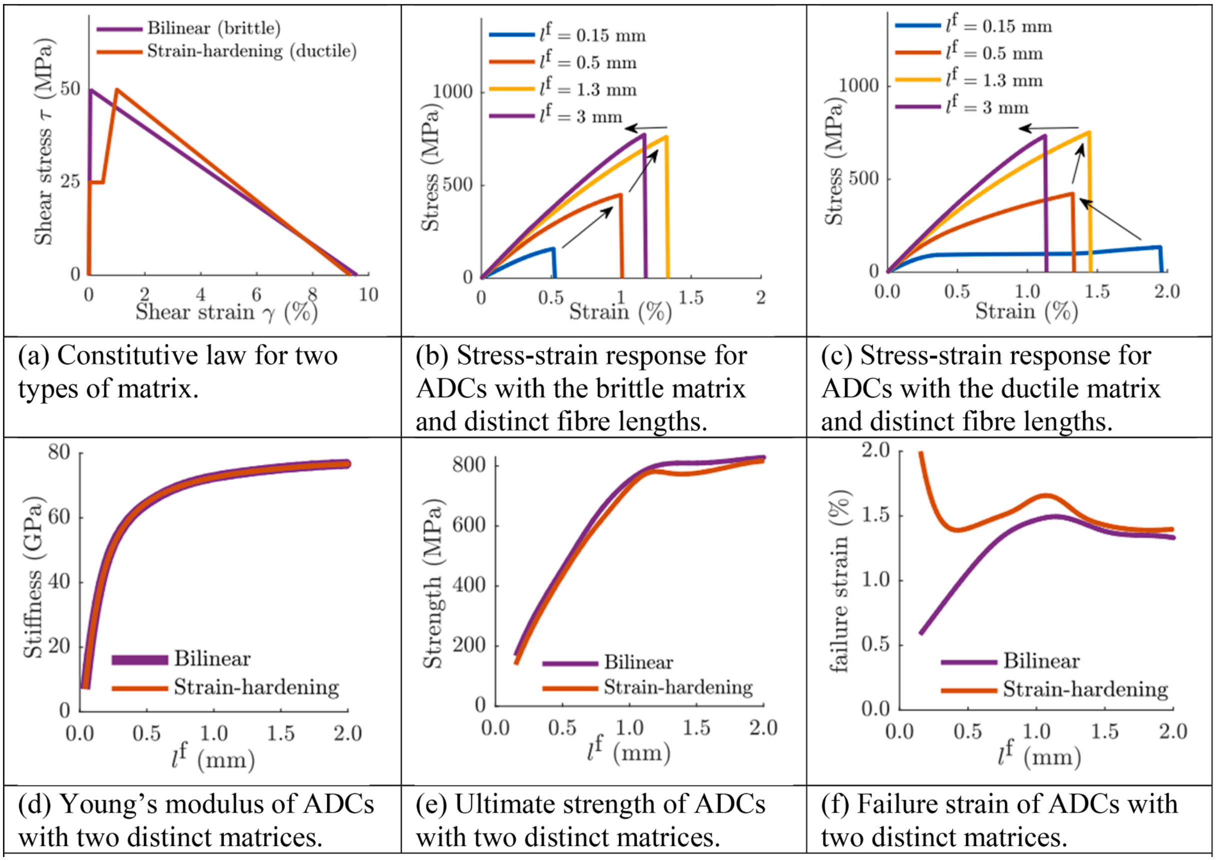

(a) Constitutive law for two types of matrix.

(b) Stress-strain response for ADCs with the brittle matrix and distinct fibre lengths.

(c) Stress-strain response for ADCs with the ductile matrix and distinct fibre lengths.

(d) Young's modulus of ADCs with two distinct matrices.

(e) Ultimate strength of ADCs with two distinct matrices.

(f) Failure strain of ADCs with two distinct matrices.

Fig. 5.8. Effect of fibre length and type of matrix on the predicted response of ADCs (for $V_f = 36\%$) [205].

measured experimentally for ADCs [231] is still considerably lower than that predicted by Kelly-Tyson's model (shown in Fig. 5.1), with pseudo-ductile strains below 0.4 %. Further development of FE simulations of small Representative Volume Elements (RVEs, representing less than 50 individual fibres explicitly) also suggested that it is possible to combine high strength and ductility for intermediate fibre lengths [233,234], although this has not been confirmed experimentally; a possible explanation is that models focused on such small scales cannot capture the intrinsic variability and failure processes of actual ADCs.

To bridge the gap between model predictions and experimental results and to provide a design tool for ADCs, a semi-analytical virtual testing framework has been proposed to simulate the material behaviour across the required length-scales (from the fibre–fibre interaction up to the full specimen) [205,208,209,235]. This framework considers the finite shear strength and finite mode-II fracture toughness of the matrix (and/or interface) through a shear-lag model [206], and fibre strengths governed by a Weibull distribution; it also considers several critical sources of variability (most importantly in the position of fibre ends, and also in inter-fibre distance, matrix strength, and fibre stiffness), which significantly impact the ultimate strength and failure strain [208]. Crucially, final failure is predicted by a homogenised non-linear fracture mechanics criterion (modelling the formation of critical clusters of damage from which fracture may propagate unstably), which captures the behaviour of specimens with linear and non-linear response, as observed experimentally (Fig. 5.7).

The predictions from this virtual testing framework [205] suggest that, for a carbon fibre (CF) ADC with brittle matrix (e.g. epoxy), the ultimate strength, failure strain, and pseudo-ductile strain could all be

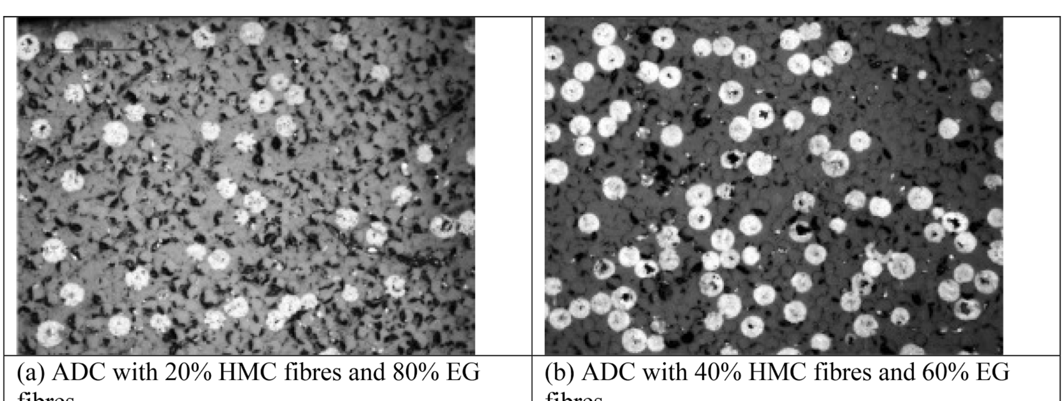

(a) ADC with 20% HMC fibres and 80% EG fibres.

(b) ADC with 40% HMC fibres and 60% EG fibres.

Fig. 5.9. Cross-section microstructure of intermingled ADCs with High-Modulus-Carbon (HMC) fibres (shown in white) hybridised with E-Glass (EG) fibres, produced by the HiPerDiF method [204].

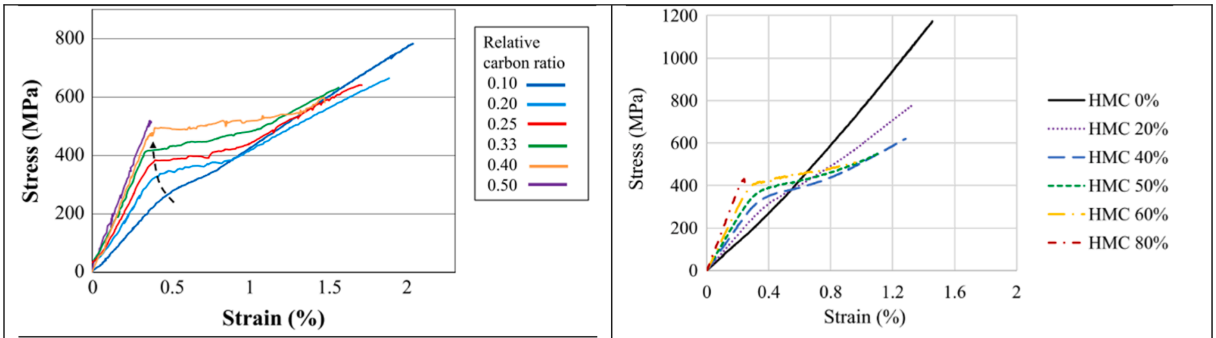

(a) HMC/EG hybrids [204]

(b) HMC/HSC hybrids [134].

Fig. 5.10. Pseudo-ductile response of intermingled hybrid ADCs (with epoxy matrix), using High-Modulus-Carbon (HMC), High-Strength-Carbon (HSC), and E-Glass (EG) fibres (3 mm long).

maximised for fibres 1.0–1.5 mm long (Fig. 5.8); however, achieving a good alignment of such short fibres has proven difficult [231]. Replacing the brittle epoxy matrix with a ductile and strain-hardening one could potentially increase the ductility of ADCs with fibres less than approximately 1 mm long, however, using such short fibres leads to a significantly reduced strength (as shown in Fig. 5.8f) [205].

An alternative to aligning short fibres to create ADCs is to introduce fibre ends in composite prepregs or tapes in-situ, e.g. through stretch-breaking [195]; however, this creates discontinuous fibres much longer than Kelly-Tyson's critical length, and therefore cannot promote pseudo-ductility (although it can improve the composite's formability). This limitation could be overcome by modulating the strength and diameter of carbon fibres along their length using laser irradiation [236]: this could effectively generate fibre-breaks in-situ at the required length scales, and also promote mechanical interlocking during slip at the interface due to wedging as a result of the varying diameters, which could potentially stabilise the failure process.

5.5. Pseudo-ductile composites with fragmentation of short fibres

As mentioned in Section 4, hybridising Low Strain (LS) with High Strain (HS) fibres is an effective approach to introduce non-linearity in the response of composites. However, with continuous-fibre composites, the level of intermingling is limited (typically to interply hybrids, where the different fibre types are segmented in different plies, as reviewed in Section 4.3.1), which constrains the selection of suitable LS and HS materials, and prevents the full exploitation of hybrid effects [84]. On the contrary, discontinuous fibre architectures can maximise intermingling of fibre types (as shown in Fig. 5.9) and, therefore, open scope for hybrid composites with a wider range of fibres and more tailorable mechanical properties.

Aligned discontinuous composites with hybrid fibre types were first produced by Parratt and Potter and Richter in the 1970s [237,238], using flow-based alignment processes as mentioned in Section 5.4. Tensile testing of ADCs reinforced with 25 % or 40 % of High Modulus Carbon (HMC) fibres intermingled with 75 % or 60 % of E-Glass (EG) fibres showed a non-linear and pseudo-ductile stress–strain curve, similar to those reported for interply hybrids in Section 4 (i.e. comprising an elastic region, a stress plateau corresponding to fragmentation of the HMC fibres, and a strain-hardening region from the end of fragmentation to the failure of the EG fibres) [237].

More recently, several hybrid ADCs have been manufactured with the HiPerDiF process [204]; this is achieved by dispersing the different fibre types together in a water suspension, and using the same water-based alignment process as used for mono-fibre composites (described in Section 5.4). Most of the work [204,209,239,134] has focused on hybridising HMC with EG or with High Strength Carbon (HSC) fibres; this successfully produced pseudo-ductile responses for hybrid ADCs with well-designed ratios between the LS HMC fibres and the HS EG and HSC fibres, with a tailorable trade-off between the Young's modulus and pseudo-ductility, as shown in Fig. 5.10. Hybridising HSC and EG fibres did not produce a pseudo-ductile response, due to the relatively similar failure strains of the two fibre types (which led to catastrophic failure of the EG fibres before fragmentation of the HSC fibres could develop);

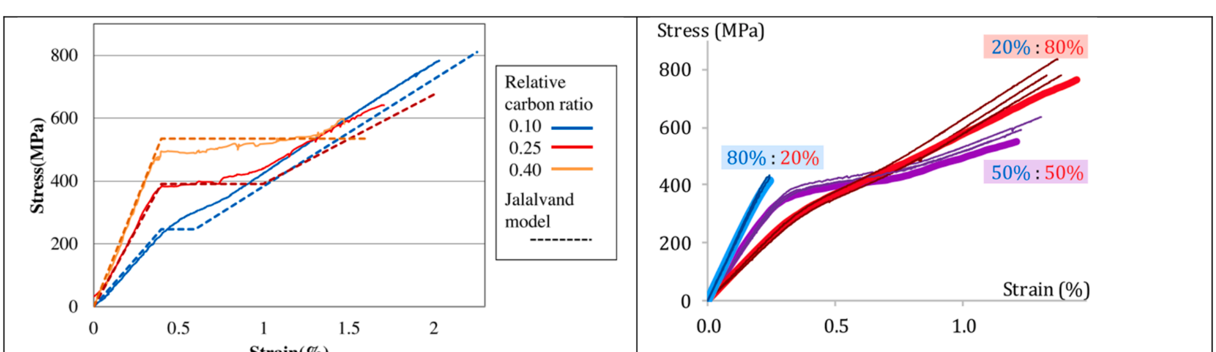

(a) Using a model for interply hybrids [204]. Full lines represent experimental results, dashed lines represent model predictions.

(b) Using a model for fibre-level hybrids [244]. Thin lines represent experimental results, thick lines represent model predictions. The labels show the volume proportions of the two fibre types (HMC:EG).

Fig. 5.11. Response of HMC/EG hybrid composites: experimental results [204] vs. model predictions [107,208,235] for distinct ratios between the fibre types.

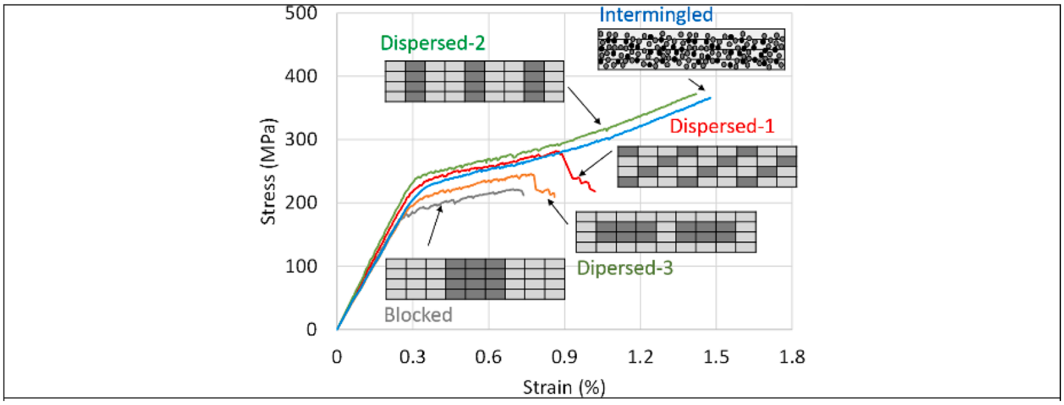

Fig. 5.12. Effect of clustering the LS fibres on the response of hybrid ADCs, as measured experimentally [209] (adapted).

however, it did produce a clear hybrid effect (i.e. an enhancement in the apparent HSC failure strain, visible as a shift of the strain at which the knee point occurs in the stress–strain curves, due to the utilisation of the full strength distribution of the fibres, as described in Section 4.2) [134,204,240].

For large fibre aspect-ratios (as used experimentally, with $1\text{mm} \leq l_f \leq 3\text{mm}$), the effect of the discontinuous nature of the fibres on the Young's modulus, ultimate strength and failure strain is small [235,241]. Therefore, the response of hybrid ADCs is relatively similar to that of interply hybrids with similar fibre types and ratio (apart from ADCs not being susceptible to delamination, due to the high level of intermingling). Nevertheless, the onset and end of fragmentation of the LS fibres is smoother for hybrid ADCs than for interply hybrids, and the fragmentation region has a distinct positive slope [204,134] (rather than being a stress plateau, as occurs for interply hybrids). These differences are due to the large number of fractures and the variability in the strength distribution of individual LS fibres, which creates a range of stresses over which fragmentation occurs [208,235] (while, for interply hybrids, the strength of a LS ply is closer to a deterministic value).

Another difference between the response of interply continuous-fibre and intermingled ADC hybrids is a negative hybrid effect on the Young's modulus of the latter, which makes a hybrid ADC slightly softer than predicted by the conventional "in-parallel" rule-of-mixtures (and this difference increases with increasing levels of intermingling). This negative hybrid effect on the modulus is due to two effects: firstly, in the intermingled fibre arrangement the different fibre types are no longer working exclusively "in parallel", but also partially "in-series" (in which case the rule-of-mixtures results in a modulus dominated by the softer material); secondly, linear-elastic shear-lag modelling shows that the stress transfer between dissimilar neighbouring fibres is less efficient than that between fibres with the same diameter and modulus [241,242].

Given the similarity between the response of ADC and continuous-fibre hybrids, analytical models developed for the latter [107] can be used to predict the response of the former with reasonable accuracy (apart from the small negative hybrid effect on stiffness and the effect of variable LS fibre strength, as discussed in the previous paragraph), as illustrated in Fig. 5.11a [204,134]. However, to capture hybrid effects, the progressive fragmentation of the LS fibres, and final failure due to formation of critical clusters of damage at the fibre scale, the virtual testing framework for ADCs described in Section 5.4 has been extended to account for hybrid fibre types [235,241], with results illustrated in Fig. 5.11b. This framework can be used to optimise the material design of hybrid ADCs for a wide range of scenarios [243].

Although a key advantage of ADCs over interply hybrids is maximising fibre intermingling, HiPerDiF can also be used to manipulate the arrangement of different fibre types [209]; this showed that promoting clustering of the LS fibres reduces the strength, the failure strain, and the pseudo-ductile strain of a hybrid ADC, due to premature failure propagating unstably from the LS-fibre clusters, as illustrated in Fig. 5.12. Results from the semi-analytical virtual testing framework suggest that isolating individual LS fibres in a hybrid could lead to significant improvements of ultimate strength and strain, as well as pseudo-yield strength and pseudo-ductile strain [209]; this potential is still to be realised experimentally. Moreover, using ADCs can expand the design space of pseudo-ductile hybrids even in interply configurations; this has been experimentally demonstrated for SRPP hybridised with carbon-fibre plies, which presented stable pseudo-ductility over a wider range of carbon ratios using ADC carbon plies rather than continuous ones [245].

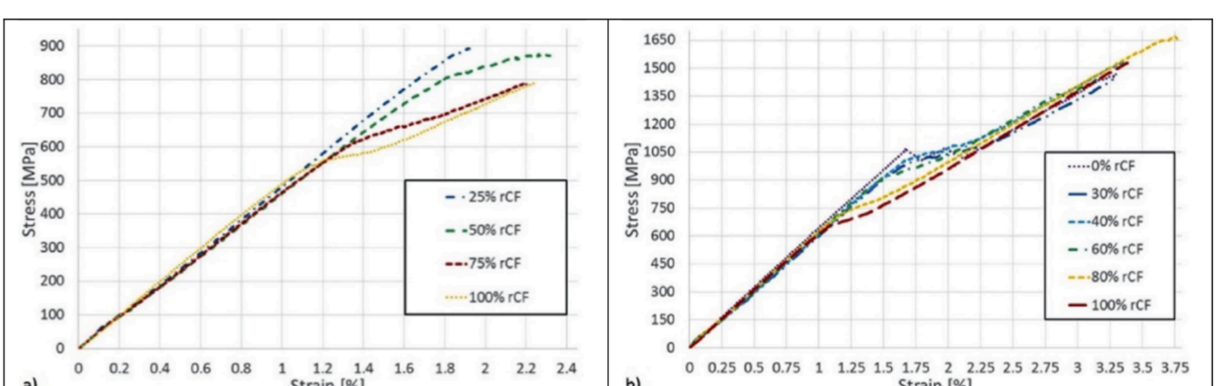

Fig. 5.13. Response of hybrid composites with intermingled discontinuous recycled and virgin carbon fibres interply with continuous E- (in subfigure a) and S- (in subfigure b) glass-fibre layers [246].

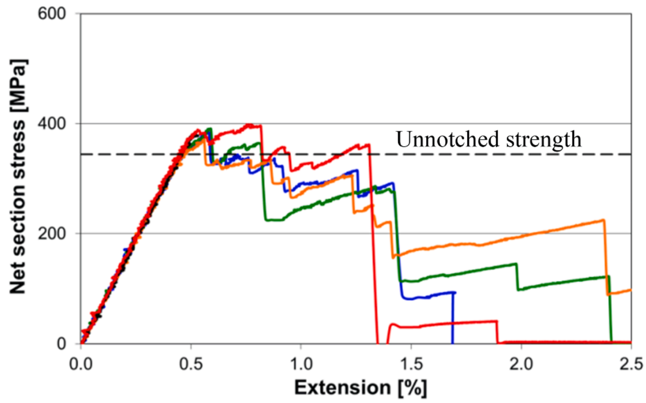

Fig. 6.1. Open-hole tension of QI hybrid carbon/epoxy specimens [137].

The fibre-type arrangement in hybrid composites can be further tailored to produce hierarchical pseudo-ductile hybrid composites, hybridising HS continuous-fibre plies (with S-Glass fibres) with ADC hybrid intermingled layers (which themselves hybridise HSC or EG fibres with HMC fibres) [134]. These hierarchical hybrid composites can be tailored to produce stress–strain curves with two distinct knee points: the first corresponding to fibre-level fragmentation of the LS HMC fibres in the ADC hybrid layer, and the second corresponding to ply-level fragmentation of the entire ADC hybrid layer (i.e. due to failure of the EG or HSC fibres). This combination further increases the design space of pseudo-ductile hybrid composites, and it has been observed to increase pseudo-ductile strains compared to those in non-hierarchical hybrid ADCs (by promoting dispersed delaminations propagating from the ply-level failures of the hybrid ADC layer, in well-designed configurations).

Hybrid ADCs also offer the possibility to exploit recycled carbon fibres (rCFs) to create a pseudo-ductile response governed by fibre fragmentation in hybrid combinations that would not be feasible with virgin carbon fibres (vCFs) only; this pseudo-ductile response is enabled by a decrease of the strength of recycled fibres, due to damage that occurs in some fibre-reclamation processes. Examples of hybrid composites featuring a non-linear response due to fibre fragmentation include intermingled rCF/vCF interply with E- or S-glass layers (illustrated in Fig. 5.13) [246], intermingled rCFs with different fibre lengths interply with EG layers [247], and flax/rCF intermingled composites [248].

The pseudo-ductile response of hybrid ADCs has been demonstrated not only in UD composites as described previously in this section, but also with quasi-isotropic lay-ups [239], using HMC fibres hybridised with either HSC or EG. Although this led to a small reduction in pseudo-ductile strains, the stress–strain curves of the quasi-isotropic ADC laminates were distinctively non-linear, with a clear knee point corresponding to the onset of fragmentation of the HMC fibres in the 0° ADC plies, followed by a strain-hardening region.

6. Notched response of ductile and pseudo-ductile composites

One of the main reasons for introducing ductility and pseudo-ductility into composites is to allow the associated non-linearity to redistribute load at stress concentrations in a similar way to stress redistribution due to plasticity in ductile metals.

The effect of pseudo-ductility due to fragmentation in hybrid composites has been shown to be effective in reducing notch sensitivity, as expected. This has been investigated by modelling, which showed that the ratio of pseudo-ductile strain to failure initiation strain is a key parameter [249]. Notched quasi-isotropic pseudo-ductile laminates were made from hybrid carbon sub-laminates with layup $[45/90/-45/0]_s$ where each "ply" consisted of a hybrid sublaminate with layers of XN-80 ultra-high modulus fibres between T1000 intermediate modulus layers each about 0.06 mm thick with the same orientation and a total thickness of 0.192 mm. Specimens 16 mm wide were tested with and without 3.2 mm holes and sharp notches of the same width [137]. Fig. 6.1 shows the response, indicating that the failure stress of the specimens at the ligaments (net section stress) has actually exceeded the un-notched strength of the laminate. Although the initial response appears quite linear, fragmentation is occurring at the notch quite early on, but the load is redistributed and complete failure does not occur. In addition, after the net section strength has been reached, specimens did not immediately fail catastrophically. The pseudo-ductility is not sufficient to maintain the full stress beyond this point but there is still some residual load carrying capacity, gradually reducing with further increase of the overall strain. A similar notch-insensitive response was obtained with sharp notches [137]. Multi-directional glass/carbon hybrids have also been investigated. Sub-laminates of quasi-isotropic thin T300 carbon plies between standard thickness S-glass with layup $[60_G/-60_G/0_G/0_C/60_C/-60_C]_S$ were tested and shown to be insensitive to sharp notches or open holes [250]. Similar reduced notch sensitivity was also shown for Xstrand-glass/M46JB carbon hybrids with 0/±60 and 0/±30 layups.

Notched pseudo-ductile hybrids have been shown to have good fatigue performance. Tension fatigue tests have been carried out on open

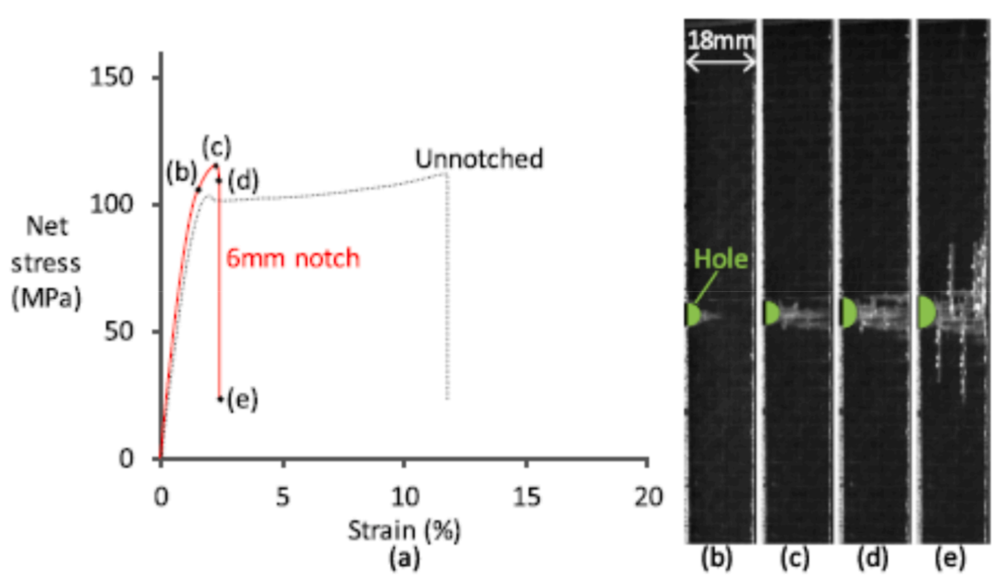

Fig. 6.2. Notch insensitivity of 9% volume fraction UD carbon/SRPP hybrid [254].

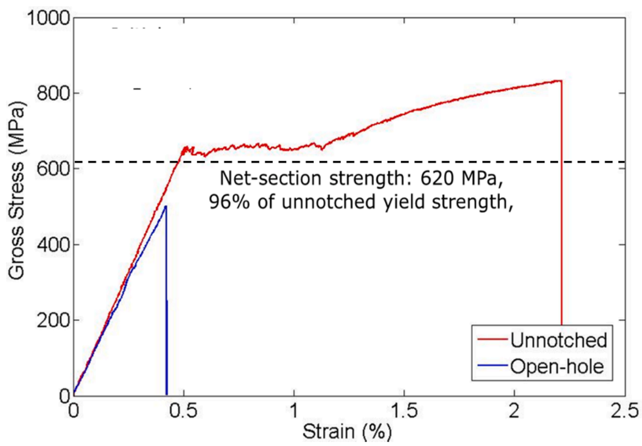

Fig. 6.3. Open-hole tension response of $[\pm25_2/0]_{s4}$ IM-HM carbon/epoxy laminates [175].

hole quasi-isotropic Xstrand-glass/M46JB carbon and S-glass/T300 carbon interlayer hybrids, with the latter having a lower proportion of carbon plies [150]. There was no stiffness reduction after 100,000 cycles at a stress level of 50 % of the knee point stress for the unnotched Xstrand/M46JB hybrid with the higher carbon content, and only a gradual reduction in stiffness of up to about 10 % for the S-glass/T300 hybrid. At higher cyclic loads there was some damage, but the composites were still able to withstand thousands of fatigue cycles. At 70 % of the pseudo-yield stress there was a reduction in stiffness of about 5 % for Xstrand/M46JB after about 2000 cycles, but 40 % at 30,000 cycles for S-glass/T300.

Sapozhnikov et al. demonstrated notch insensitivity in open hole tension tests on quasi-isotropic Dialead™ high modulus / T800 intermediate modulus carbon hybrids with standard ply thicknesses using a tough epoxy resin [251]. Danzi et al. carried out double edge notch tension tests on cross-ply T800 intermediate modulus / HR40 high modulus carbon hybrids using specimens with different notch to width ratios to establish the translaminar fracture toughness and R-curve [115]. Specimens with two 0.023 mm HR40 plies sandwiched between three 0.053 mm T800 plies each side showed less effect of notch size on strength than baseline laminates with alternating single 0 and 90 plies. The double ply specimens also showed much higher translaminar fracture toughness, although this was attributed mainly to the thicker ply blocks.

Pseudo-ductility and notch insensitivity has also been demonstrated in quasi-isotropic composites with some of the plies cut perpendicular to the fibre direction or cut perpendicular to the loading direction [220].

Gradual failure has been found in bearing and bearing-bypass tests [252] and in compact tension tests on similar glass/carbon laminates [253].

Nijs et al. demonstrated notch insensitivity in UD carbon fibre / SRPP hybrids [254]. With optimised manufacturing similar open hole net section strength could be achieved as the un-notched strength, with some pseudo-ductility in the notched specimens, Fig. 6.2. There is still a sudden load drop for this case with 9 % carbon fibre volume fraction, but with only 6.2 % carbon, pseudo-ductility was maintained beyond the peak stress, with fragmentation spreading over the whole length of the specimen.

Table 1
Summary of properties of different examples of pseudo-ductile composites. UD tension unless otherwise noted.

Approach	Example	Ref.	Figure	Initial modulus (GPa)	Yield / pseudo-yield stress (MPa)	Strength (MPa)	Pseudo-ductile strain (%)	Comments	Symbol in Figs. 7.1, 7.2
Polymer fibres	SRPP	13	2.2	4	35	130	15	Recyclable	■ (green)
Cellulose fibres	Cordenka/PHB	35	2.9	15	100	250	10	Recoverable stiffness - ductile	■ (blue)
Steel fibres	Stainless steel/ epoxy	50	2.15	82	174	312	19	High density	■ (black)
Reorienting angle-plies	±45° thin carbon/ epoxy	66	3.2	9	64	400	14	Recoverable stiffness - ductile	◆ (black)
	±25° thin carbon/ epoxy	66	3.4	39	454	927	1.2		◆ (green)
Wavy plies	Carbon/epoxy	77	3.7	48	~100	250	0.5	In compression	◆ (blue)
Fragmenting continuous fibre hybrids	Glass/thin carbon/ epoxy	105	4.4	53	1129	1300	1.2		● (orange)
	HM/IM thin carbon/epoxy	114	4.6	245	990	1300	0.9		● (red)
	SRPP/carbon	169	4.15	6	80	100	12		● (purple)
Combined fragmentation/angle-ply reorientation	$[\pm26_5/0]_S$ thin carbon/epoxy	172	4.16	40	692	801	2.2		● (dark red)
3D woven	Carbon, through-thickness angle interlock	182	4.19	38	240	240	12	In compression	● (blue)
Braiding	±35 carbon	186	4.22	22	300	344	12		● (green)
Microbraiding	±39 Dyneema, carbon core	189	4.23	13	500	750	15	Large load drops	● (black)
Discontinuous plies	Carbon/epoxy	210	5.4a	149	~800	1010	0.23	Non-linear - no sharp knee point	▲ (blue/red)
	Carbon/PEEK	216	5.4b	42	~200	530	1.2		▲ (black)
Discontinuous fibres	Carbon/PP	231	5.6b	57	~300	401	0.24		▲ (blue)
Fragmenting short fibre hybrids	HM carbon/glass	204	5.10a	134	441	542	0.88		▲ (green)
Typical values for conventional materials	UD IM carbon/ epoxy	–	–	160	2800	2800	0		×
	6061-T6 Al alloy	–	–	69	275	310	11.6		✱

McBride et al. investigated the notched behaviour of hybrid unidirectional composites made from layers of glass and steel fibres with an epoxy matrix [55]. The all-steel fibre composites showed a ductile behaviour with little reduction in net-section tensile strength with a hole. Glass-fibre composites showed some reduction in open-hole strength compared to unnotched specimens, but glass-steel specimens showed less reduction, demonstrating the benefits of hybridising glass fibre composites with steel fibres.

Regarding other architectures, Vieille and Taleb showed that ductility and damage in angle-ply laminates reduces hole sensitivity in [±45] laminates of woven carbon/epoxy and PPS at both room temperature and 120° C [72]. Cox et al. showed that 3D woven composite plates with a circular hole showed little notch sensitivity [181].

Pseudo-ductility also greatly reduces notch sensitivity in thin-ply angle-ply laminates with fragmenting 0° plies. FE modelling has shown that a notch-insensitive response should be obtained provided the ratio of pseudo-ductile strain to pseudo-yield strain (i.e. strain at the knee point) is sufficiently high [255]. Fig. 6.3 shows the response of a $[\pm 25_2/0]_{s4}$ laminate with intermediate modulus angle-plies and high modulus 0° plies. The unnotched behaviour is compared with that of a 16 mm wide specimen with a 3.2 mm hole, showing that the net-section open hole strength is similar to the unnotched pseudo-yield stress [175]. Gradual failure with load redistribution has also been demonstrated in bolt bearing tests on angle-ply laminates with 0° plies [256].

7. Summary and perspectives

This review has considered the mechanisms by which high performance ductile or pseudo-ductile composites can be created, including via ductile fibres, fibre reorientation, fragmentation, and slip between discontinuous layers and fibres. A summary of the main different approaches and typical properties achieved is given in Table 1.

Ductile polymer fibres exist, as discussed in Section 2.2, but there is a trade-off between high stiffness and strength on the one hand and high strain and ductility on the other. Fibres such as PP can produce truly ductile composites, but only modest performance. Similarly natural and man-made cellulose-based fibres (Section 2.3) can exhibit a non-linear response, with Cordenka™ being one of the most promising. However stiffness and strength are still modest compared with conventional fibres such as carbon and glass. Composites made of polymer fibres such as aramid or PBO, although brittle in tension, exhibit highly non-linear behaviour in compression. Although their strength is low, they can carry considerable load in bending, with high pseudo-ductility. They may also be interesting to hybridise with other fibres. Some high performance carbon nanotube based fibres have been reported (Section 2.4), with high stiffness, strength, failure strain and true ductility. There is considerable scope to further develop and optimise these fibres and to use them to create high performance composites. Ductile composites can be produced with steel fibres, providing high initial stiffness, but strengths are modest when using fibres possessing high failure strains, and they may not be suitable for weight sensitive applications (Section 2.5).

Fibre reorientation in angle-plies (Section 3.2) can produce high strains with brittle fibres such as carbon, provided matrix cracking and delamination is avoided by using thin plies or tough resins. Much of the deformation can be reversible, making these composites truly ductile. Large angles can produce pseudo-ductile strains of as much as 14 %, but with low moduli and only modest strength. The angle can be chosen to obtain the desired trade-off between strength and modulus on the one hand, and pseudo-ductile strain on the other, with studies suggesting 25-30° provides a good balance. The key issue here is to avoid delamination, which has been successfully demonstrated using thin plies. There is also scope to investigate tougher matrices, which may allow similar performance with standard ply thicknesses. Some concepts with wavy fibres have been shown to generate additional strain, especially in tension (Section 3.3). Some concepts exploiting extra length can also be extended to the structural level to produce components with high strains and energy absorption (Section 3.4).

Progressive ply fracture can be achieved in conventional composites under certain conditions, producing gradual failure (Section 4.2). For example, in composites loaded in bending, and for materials where failure initiates in tension rather than catastrophically in compression, progressive fracture and delamination from the surface can occur. Since there is damage, there is a loss of modulus, and so this behaviour is pseudo-ductile rather than ductile. Broadening the distribution of fibre strengths tends to give more gradual failure, and merits further research. Work to date has been more concerned with reducing variability without recognising that there may be benefits in increasing it. Hybridising with fibres of different stiffnesses and failure strains is an excellent way to achieve this. Much work has been done with hybridised rebars, although there are usually load drops as the different fibre types fail, which may be acceptable for this application, but in other cases is less desirable.

To get a truly pseudo-ductile response without load drops, pull-out of failed fibres or delamination of fractured plies must be avoided. Preventing or postponing localised failure can be done by intimate mixing of different fibres, and whilst it is very difficult to achieve the necessary arrangements with continuous fibre fibre tows, the strategy has been deployed successfully with short fibres (Section 5.5). Improved techniques to mix different continuous fibres merit further consideration. Alternatively, with thin plies, there is insufficient energy to drive delamination and a pattern of progressive fragmentations can be created, producing a plateau on the stress–strain curve and significant pseudo-ductile strain, as discussed in Section 4.3. The relative volume fraction of the different fibres needs to be carefully chosen to avoid catastrophic failure when the low strain fibres break. Analysis methods have been developed, and damage mode maps proposed, to design pseudo-ductile laminates that fail without catastrophic delamination or complete fibre breakage, and to achieve the best balance between pseudo-yield stress and pseudo-ductile strain. There is a strong trade-off between pseudo-ductile strain and strength, but a synergistic relationship with modulus. Hybridising with higher modulus, lower strain fibres creates pseudo-ductility whilst at the same time increasing the composite modulus. Various combinations of fibres can be hybridised, with glass/carbon and high modulus/high strength carbon receiving most attention. The broad selection of available fibres opens up the design space to create materials optimised for particular applications. A hybrid effect with higher failure strains can also be achieved in very thin plies due to constraint on forming critical clusters of broken fibres, enabling greater advantage to be taken of the basic strength of the fibres.

The fragmentation observed in thin-ply hybrid composites carries over to produce pseudo-ductile response in multidirectional laminates. Here an additional challenge arises in avoiding delamination between plies that may arise at discontinuities such as free edges, and again the use of thin plies is beneficial. Ply fragmentation can also occur in compression with high modulus fibres, producing a non-linear response with a change in the slope of the stress–strain curve, although the flat plateau seen in tension does not arise as the broken fibres can still carry some load in compression. Again, thin plies are needed to avoid catastrophic delamination after fibre failure. Pseudo-ductile behaviour is different in tension and compression, and only certain types of fibres fragment in compression, so careful selection and tailoring is required to obtain optimal performance under general loading. More combinations of different fibres should be investigated, including hybrids with polymer fibres for potential pseudo-ductility in compression.

Pseudo-ductile behaviour of thin-ply hybrids can be achieved in bending, and the challenge here is to optimise the layup to take advantage of the different responses in tension and compression. Different materials can also be used on the two sides when the bending is predominantly in one direction. Thin-ply hybrids have been shown to have good fatigue performance if the strain is kept below 80 % of the knee point. If this value is exceeded, delamination is likely to occur, but may propagate quite slowly depending on the configuration and load amplitude. Pseudo-ductility can be maintained over a range of temperatures and at high strain rate.

Pseudo-ductility and high strains can be achieved by adding carbon fibres to SRPP, although the strength and stiffness are limited by the modest amounts of carbon that can be added without reverting to brittle failure (Section 4.4). Hybridising with fibres other than carbon would be interesting. For example, it may be possible to introduce a larger proportion of lower modulus fibres without creating brittle failure. Further optimisation of the adhesion may also be beneficial.

Fragmentation and fibre reorientation can be combined (Section 4.5) for example by replacing the glass in a glass/carbon hybrid with carbon angle-plies, which have a higher failure strain and lower modulus than 0° plies. Pseudo-ductile strains of over 2 % and failure strains of over 4 % have been achieved in an all-carbon laminate as a result of combining the mechanisms. However, pseudo-ductility is reduced at high strain rates and low temperature. These laminates can also fragment and exhibit pseudo-ductility in compression with high modulus 0° fibres. Fatigue behaviour has also been investigated, with similar good behaviour as with hybrids. There is considerable scope to investigate different combinations of materials to optimise performance. Braided and 3D woven architectures have been shown to be capable of demonstrating pseudo-ductility, with similar fragmentation and fibre reorientation mechanisms, although often with less smooth stress–strain responses (Section 4.6). Most of these materials were not developed specifically to increase pseudo-ductility, and there are opportunities to tailor the architectures to reduce the undesirable load drops.

Discontinuous composites provide an additional mechanism for generating extra strain by slip between ply fragments (Section 5.3) or fibres (Section 5.4), producing a non-linear response that gives a warning before failure. However, the extra strain that can be obtained is limited due to the very high stresses arising at the discontinuities, and failure strains and strengths are always lower than those of continuous-fibre composites; moreover, the discontinuities at the ply- or fibre-ends are potential triggers for damage initiation under cyclic loading, which need further investigation. Discontinuous fibre composites allow intimate mixing of different fibres, which is very difficult to achieve with continuous fibres. Aligned fibre hybrid composites have demonstrated the largest potential for pseudo-ductility and other performance targets in discontinuous materials (Section 5.5). The design space can be greatly increased by combining different lengths as well as different types of fibres to optimise performance. A range of pseudo-ductile responses have been demonstrated in tension, and more work is needed to look at other loading modes, especially compression and fatigue. Aligned discontinuous fibre composites provide a route to make use of recycled fibres, which are usually in a discontinuous, randomly-oriented form. This approach enables the creation of a high value product, contributing to the sustainability of composites. Recycled and virgin fibres can be combined to optimise mechanical properties. These discontinuous fibre composites can also show a ductile response during component manufacturing, allowing more complex geometries to be formed with less defects. The understanding gained on the mechanics of brick and mortar composites has also been a stepping stone towards the development of models for randomly-oriented discontinuous composites.

There is scope to incorporate the mechanisms in discontinuous fibres as discussed in Section 5 into continuous composites, by designing them to fragment into discontinuous composites, under load, leading to the non-linear, pseudo ductile responses seen in aligned discontinuous composites (ADC). The challenge is to isolate the fibre breaks to prevent localisation that would lead to premature failure. The approach is analogous to that in thin-ply hybrid composites such as glass/carbon, where the glass supports the multiple fragmentation of the carbon plies (Section 4). A similar approach could be achieved, in future, using fibre scale hybridisation, developing the models explored for glass/carbon hybridisation in ADCs [208].

Alternatively, nanostructured interphases could provide a means to increase fragmentation, by minimising stress concentrations associated with fibre breaks at the same time as limiting debonding. Initial work, mentioned in Section 4.2, suggests that the interphase approach is worth further exploration. Specifically, a nanonacre interface increased the number of fibre breaks before failure significantly, and increased absolute composite strength in tension as a result [89]. Logically, with further fragmentation, non-linearity would be expected to develop.

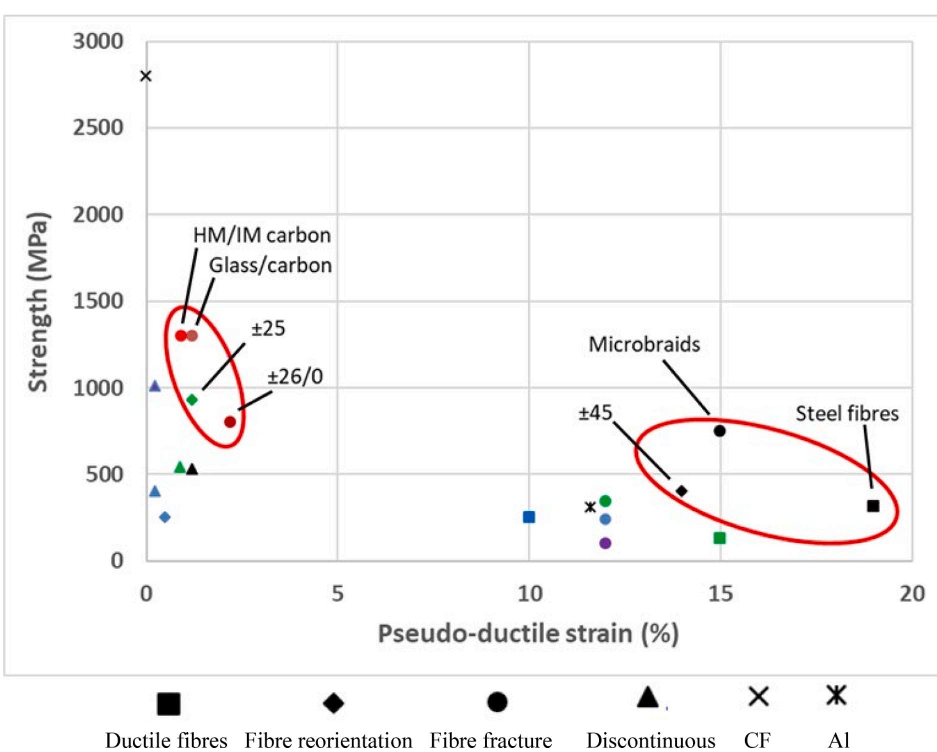

Fig. 7.1. Trade-off between strength and ductility (see Table 1 for full key).

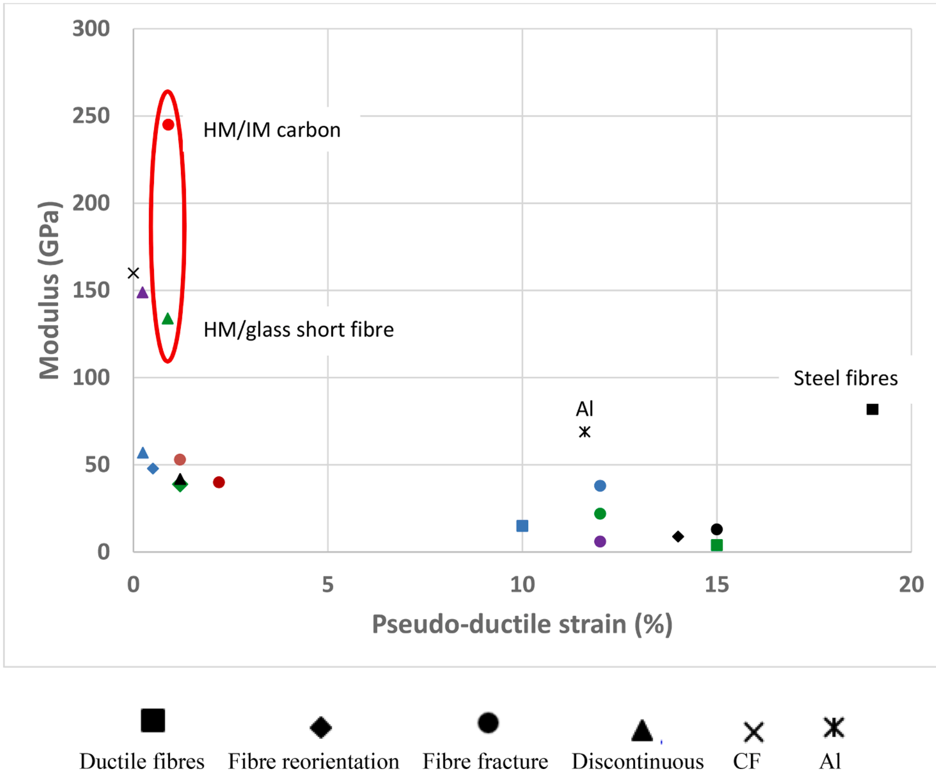

Fig. 7.2. Trade-off between modulus and ductility (see Table 1 for full key).

The research on discontinuous composites summarised in Section 5 highlighted the importance of the exact microstructure (e.g. the relative staggering of fibre- or ply-ends [199,207,212,216], or the relative position of different fibres in hybrid composites [208]) on the magnitude of pseudo-ductility generated. Although further research is needed, the work reported seems to suggest that pseudo-ductility could be maximised by precisely placing the fibres, e.g. by controlling the staggering of fibre- or ply-ends and the intermingling of hybrid fibres. This could motivate the development of manufacturing methods able to generate structured and controlled assemblies of fibres, and also further analytical/numerical studies to explore optimal geometries of those assemblies.

Several studies have confirmed that pseudo-ductile hybrid composites show greatly reduced sensitivity to notches due to the ability for local damage to redistribute load around the stress concentrations, as discussed in Section 6. Similar effects can be expected in compression and with other pseudo-ductile architectures and should be investigated. Lack of sensitivity to stress concentrations is very important given that notched strength is a major driver of composite structural design, especially in compression. Less work has been done on impact response, and compression after impact, and these aspects should be a key priority for further research. Impact damage can have a similar effect of redistributing load as a notch, so pseudo-ductility may be beneficial. However, delamination is crucially important, and has not yet been investigated in detail. The ability to tailor behaviour by hybridising different fibres offers considerable scope to optimise performance, and a wider range of fibres and combinations should be investigated.

Fig. 7.1 plots the strengths and pseudo-ductile strains of the examples from Table 1. The different symbol shapes correspond to the approaches in Sections 2 to 5, with the colour key given in the table. Conventional UD carbon/epoxy and an aluminium alloy are also included for comparison. The figure shows the trade-off and the difficulty in simultaneously achieving high values of both properties. Composites such as carbon fibre/epoxy are very strong, but brittle. All the approaches to introducing ductility involve a reduction in strength. A

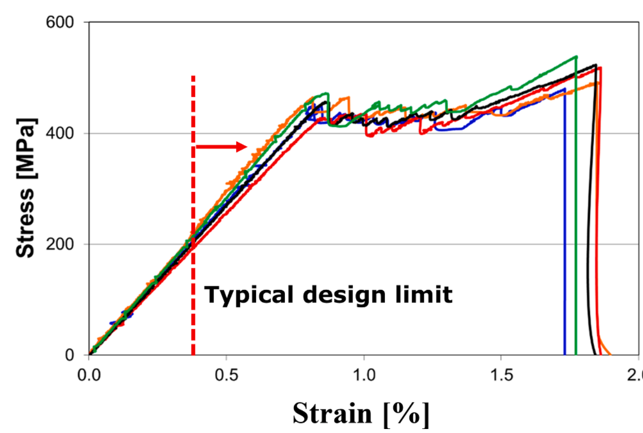

Fig. 7.3. Typical pseudo-ductile stress–strain response showing potential to increase design strain.

group of four points circled in red on the left show promising responses, with some pseudo-ductility whilst retaining reasonable strength. On the other hand approaches producing high ductility generally have low strengths. The three points circled in red on the right have better combinations of properties, but all have some disadvantages. The micro-braided composites show a series of load drops rather than a smooth stress–strain response; reorienting thin angle plies have low initial modulus; and steel fibre composites have high density.

The wavy-ply sandwich concept (Fig. 3.10) was not included in Table 1 or Fig. 7.1, because the low initial modulus followed by a very pronounced strain hardening renders the calculation of the pseudo-ductile strains problematic; nevertheless, this concept demonstrates that it is possible to combine large failure strains up to 9 % with very high strength of 1570 MPa and high energy absorption of over 9 kJ/kg.

Fig. 7.2 shows a similar trade-off between modulus and pseudo-ductile strain. Most of the materials have moduli less than aluminium alloy. The comparison would be more favourable plotted in terms of specific moduli, but not all values for density were given in the papers. The two materials circled on the left stand out as having high stiffness combined with some pseudo-ductility. These are both hybrids including high modulus carbon fibre, demonstrating how it is possible to create more gradual failure by fragmentation and simultaneously increase the modulus over the baseline material. The high modulus/intermediate modulus carbon hybrid also featured in the ringed group on the left of Fig. 7.1, and the high modulus/glass short fibre composite was not far below.

Overall, the examples circled on the left of Fig. 7.1 appear to be the best in introducing more gradual failure without too much sacrifice of other properties. Three of these examples involve ply fragmentation, one is based on ply reorientation and one combines the two mechanisms, thereby producing the highest pseudo-ductile strain of the group. Fragmentation appears to be the most promising approach for creating pseudo-ductility, especially when combined with angle plies, and can also produce pseudo-ductility in compression, as shown in Fig. 4.10. The approach is capable of translating into structural performance, as shown in Fig. 4.16. Hybridising with high modulus carbon enables a good modulus to be obtained as well. Further research should be carried out to optimise the choice of fibres for a wider range of loading cases and to investigate behaviour in notched compression and compression after impact.

Since pseudo-ductility is associated with a reduction in ultimate strength, research into truly ductile fibres, for example based on high stiffness and strength nanomaterials with high aspect ratio should be a priority. However, composite design strains are much lower than the ultimate failure strains of the fibres, due to the effects of notches and impact damage. If these concerns can be alleviated through the introduction of pseudo-ductility, it may be possible to increase design strains. Fig. 7.3 shows the tensile response of a quasi-isotropic thin-ply T1000/M55 laminate with an average knee point strain of 0.82 %. Typical design strains are less than half of this, and so there should be scope to use higher strains whilst still keeping well below the point of onset of damage. Further work is needed to see to what extent this ambition can be achieved.

A key benefit of pseudo-ductile laminates is the additional strain beyond the knee point (or onset of non-linearity) that can allow excessive deformations to be safely handled. The damage and reduction of stiffness means that the effect of such occurrences can be detected. Warning that strain limits have been exceeded whilst still maintaining load carrying capacity allows continued operation until repairs can be made. With glass/carbon hybrids the fragmentation produces a striped pattern which can be observed visually, without any special equipment, offering a very simple non-destructive test for unpainted structures. For painted areas excessive strains can still be detected by conventional approaches such as ultrasonic scanning. There are many potential applications to be explored, either for load bearing surface layers or for bonded-on sensors. High energy absorption is another benefit of some of the pseudo-ductile configurations that have been investigated, and should be researched further.

Such materials can lead to composite structures that avoid catastrophic failure and have increased damage tolerance with additional margins to safely handle overloads. This more forgiving behavior offers huge opportunities for widening the areas where composites are used, and more work is needed to explore potential new applications. Areas of further research have been identified above that could further contribute to generating ductility or pseudo-ductility, and to creating high performance polymer matrix composite structures that fail gracefully.

CRediT authorship contribution statement

M.R. Wisnom: Writing – review & editing, Writing – original draft, Supervision, Investigation, Funding acquisition. **S. Pimenta:** Writing – review & editing, Writing – original draft, Supervision, Investigation. **M.S.P. Shaffer:** Writing – review & editing, Writing – original draft, Supervision, Investigation, Funding acquisition. **P. Robinson:** Writing – review & editing, Supervision, Investigation, Funding acquisition. **K.D. Potter:** Writing – review & editing, Supervision, Investigation, Funding acquisition. **I. Hamerton:** Writing – review & editing, Supervision, Investigation. **G. Czél:** Writing – review & editing, Investigation. **M. Jalalvand:** Writing – review & editing, Investigation. **M. Fotouhi:** Writing – review & editing, Investigation. **D.B. Anthony:** Writing – review & editing, Investigation. **H. Yu:** Writing – review & editing, Investigation. **M.L. Longana:** Writing – review & editing, Investigation. **X. Wu:** Writing – review & editing, Investigation. **A. Bismarck:** Writing – review & editing, Writing – original draft, Supervision, Investigation, Funding acquisition.

Declaration of competing interest

The authors declare that they have no known competing financial interests or personal relationships that could have appeared to influence the work reported in this paper.

Data availability

No data was used for the research described in the article.

Acknowledgement

Funding from the UK Engineering and Physical Sciences Research Council (EPSRC) under the Programme Grant EP/I02946X/1 on High Performance Ductile Composite Technology is gratefully acknowledged. Gergely Czél is grateful for the support from the National Research, Development and Innovation Office (NRDI, Hungary) through grant OTKA FK 131882, the János Bolyai Research Scholarship of the Hungarian Academy of Sciences and from the ÚNKP-23-5-BME-433 New National Excellence Program of the Ministry for Culture and Innovation allocated from the source of the National Research, Development and Innovation Fund.

References

[1] Bank LC. Progressive failure and ductility of FRP composites for construction: review. J Compos Constr 2013;17(3):406–19. https://doi.org/10.1061/(asce)cc.1943-5614.0000355.

[2] Loos J, Schimanski T, Hofman J, Peijs T, Lemstra PJ. Morphological investigations of polypropylene single-fibre reinforced polypropylene model composites. Polymer 2001;42(8):3827–34. https://doi.org/10.1016/s0032-3861(00)00660-1.

[3] Romhany G, Barany T, Czigany T, Karger-Kocsis J. Fracture and failure behavior of fabric-reinforced all-poly (propylene) composite (Curv®). Polym Adv Technol 2007;18(2):90–6. https://doi.org/10.1002/pat.806.

[4] Hine P, Ward M, Teckoe J. The hot compaction of woven polypropylene tapes. J Mater Sci 1998;33:2725–33. https://doi.org/10.1023/A:1017540530295.

[5] Ward I, Hine P. The science and technology of hot compaction. Polymer 2004;45(5):1413–27. https://doi.org/10.1016/j.polymer.2003.11.050.

[6] Babu NK, Mensah RA, Shanmugam V, Rashedi A, Athimoolam P, Aseer JR, et al. Self-reinforced polymer composites: an opportunity to recycle plastic wastes and their future trends. J Appl Polym Sci 2022;139(46):e53143. https://doi.org/10.1002/app.53143.

[7] Santos RAM, Gorbatikh L, Swolfs Y. Commercial self-reinforced composites: a comparative study. Compos B Eng 2021;223:109108. https://doi.org/10.1016/j.compositesb.2021.109108.

[8] Peijs T, Vanvught RJM, Govaert LE. Mechanical-properties of poly(vinyl alcohol) fibers and composites. Composites 1995;26(2):83–90. https://doi.org/10.1016/0010-4361(95)90407-q.

[9] Pegoretti A, Fabbri E, Migliaresi C, Pilati F. Intraply and interply hybrid composites based on E-glass and poly(vinyl alcohol) woven fabrics: tensile and impact properties. Polym Int 2004;53(9):1290–7. https://doi.org/10.1002/pi.1514.

[10] Zweben C. Flexural strength of aramid fiber composites. J Compos Mater 1978;12:422–30. https://doi.org/10.1177/002199837801200407.

[11] Zhang JM, Mousavi Z, Soykeabkaew N, Smith P, Nishino T, Peijs T. All-aramid composites by partial fiber dissolution. ACS Appl Mater Interfaces 2010;2(3):919–26. https://doi.org/10.1021/am900859c.

[12] Schaller R, Peijs T, Tervoort TA. High-performance liquid-crystalline polymer films for monolithic "composites". Compos Pt A-Appl Sci Manuf 2016;81: 296–304. https://doi.org/10.1016/j.compositesa.2015.11.024.
[13] Mugica JI, Aretxabaleta L, Ulacia I, Aurrekoetxea J. Rate-dependent phenomenological model for self-reinforced polymers. Compos Part A-Appl Sci Manufact 2016;84:96–102. https://doi.org/10.1016/j.compositesa.2016.01.002.
[14] Kelly A. Strong Solids. 2nd ed: Oxford: Clarendon Press; 1973.
[15] Papkov D, Zou Y, Andalib MN, Goponenko A, Cheng SZD, Dzenis YA. Simultaneously strong and tough ultrafine continuous nanofibers. ACS Nano 2013;7(4):3324–31. https://doi.org/10.1021/nn400028p.
[16] Sawai D, Fujii Y, Kanamoto T. Development of oriented morphology and tensile properties upon superdawing of solution-spun fibers of ultra-high molecular weight poly (acrylonitrile). Polymer 2006;47(12):4445–53. https://doi.org/10.1016/j.polymer.2006.03.067.
[17] Ahn H, Yeo SY, Lee B-S. Designing materials and processes for strong polyacrylonitrile precursor fibers. Polymers 2021;13(17):2863. https://doi.org/10.3390/polym13172863.
[18] Lefeuvre A, Bourmaud A, Morvan C, Baley C. Elementary flax fibre tensile properties: correlation between stress–strain behaviour and fibre composition. Ind Crop Prod 2014;52:762–9. https://doi.org/10.1016/j.indcrop.2013.11.043.
[19] Thuault A, Bazin J, Eve S, Breard J, Gomina M. Numerical study of the influence of structural and mechanical parameters on the tensile mechanical behaviour of flax fibres. J Ind Text 2014;44(1):22–39. https://doi.org/10.1177/1528083713481835.
[20] Trivaudey F, Placet V, Guicheret-Retel V, Boubakar ML. Nonlinear tensile behaviour of elementary hemp fibres. Part II: Modelling using an anisotropic viscoelastic constitutive law in a material rotating frame. Compos A Appl Sci Manuf 2015;68:346–55. https://doi.org/10.1016/j.compositesa.2014.10.020.
[21] Charlet K, Eve S, Jernot JP, Gomina M, Breard J. Tensile deformation of a flax fiber. Procedia Eng 2009;1(1):233–6. https://doi.org/10.1016/j.proeng.2009.06.055.
[22] Kulkarni A, Satyanarayana K, Sukumaran K, Rohatgi P. Mechanical behaviour of coir fibres under tensile load. J Mater Sci 1981;16:905–14. https://doi.org/10.1007/BF00542734.
[23] Lefeuvre A, Bourmaud A, Lebrun L, Morvan C, Baley C. A study of the yearly reproducibility of flax fiber tensile properties. Ind Crop Prod 2013;50:400–7. https://doi.org/10.1016/j.indcrop.2013.07.035.
[24] Vollrath F, Porter D, Dicko C. The structure of silk. In: Handbook of Textile Fibre Structure. Woodhead Publishing; 2009. p. 146–98. https://doi.org/10.1533/9781845697310.1.146.
[25] Gosline JM, DeMont ME, Denny MW. The structure and properties of spider silk. Endeavour 1986;10(1):37–43. https://doi.org/10.1016/0160-9327(86)90049-9.
[26] Bergmann F, Stadlmayr S, Millesi F, Zeitlinger M, Naghilou A, Radtke C. The properties of native Trichonephila dragline silk and its biomedical applications. Biomater Adv 2022;140:12. https://doi.org/10.1016/j.bioadv.2022.213089.
[27] Vehoff T, Glisovic A, Schollmeyer H, Zippelius A, Salditt T. Mechanical properties of spider dragline silk: humidity, hysteresis, and relaxation. Biophys J 2007;93 (12):4425–32. https://doi.org/10.1529/biophysj.106.099309.
[28] Heim M, Keerl D, Scheibel T. Spider silk: from soluble protein to extraordinary fiber. Angew Chem Int Ed 2009;48(20):3584–96. https://doi.org/10.1002/anie.200803341.
[29] Yang K, Wu Z, Zhou C, Cai S, Wu Z, Tian W, et al. Comparison of toughening mechanisms in natural silk-reinforced composites with three epoxy resin matrices. Compos A Appl Sci Manuf 2022;154:106760. https://doi.org/10.1016/j.compositesa.2021.106760.
[30] Wu C, Yang K, Gu Y, Xu J, Ritchie RO, Guan J. Mechanical properties and impact performance of silk-epoxy resin composites modulated by flax fibres. Compos A Appl Sci Manuf 2019;117:357–68. https://doi.org/10.1016/j.compositesa.2021.106760.
[31] Hsia Y, Gnesa E, Jeffery F, Tang S, Vierra C. Spider silk composites and applications. Metal, ceramic and polymeric composites for various uses 2011;2: 303–24. https://doi.org/10.5772/22894.
[32] Omrani F, Wang P, Soulat D, Ferreira M. Mechanical properties of flax-fibre-reinforced preforms and composites: influence of the type of yarns on multi-scale characterisations. Compos A Appl Sci Manuf 2017;93:72–81. https://doi.org/10.1016/j.compositesa.2016.11.013.
[33] Shah DU. Natural fibre composites: Comprehensive Ashby-type materials selection charts. Materials & Design (1980–2015) 2014;62:21–31. https://doi.org/10.1016/j.matdes.2014.05.002.
[34] Rozite L, Joffe R, Varna J, Nystrom B, Characterization and modeling of performance of Polymer Composites Reinforced with Highly Non-Linear Cellulosic Fibers. 6th EEIGM International Conference on Advanced Materials Research (AMR); 2011 Nov 07-08; European Sch Mat Engn (EEIGM), Nancy, FRANCE. BRISTOL: Iop Publishing Ltd; 2012. https://doi.org/10.1088/1757-899X/31/1/012005.
[35] Shamsuddin SR, Lee KY, Bismarck A. Ductile unidirectional continuous rayon fibre-reinforced hierarchical composites. Compos Pt A-Appl Sci Manuf 2016;90: 633–41. https://doi.org/10.1016/j.compositesa.2016.08.021.
[36] Lee WJ, Clancy AJ, Kontturi E, Bismarck A, Shaffer MSP. Strong and stiff: high-performance cellulose nanocrystal/poly(vinyl alcohol) composite fibers. ACS Appl Mater Interfaces 2016;8(46):31500–4. https://doi.org/10.1021/acsami.6b11578.
[37] Kafy A, Kim HC, Zhai L, Kim JW, Hai LV, Kang TJ, et al. Cellulose long fibers fabricated from cellulose nanofibers and its strong and tough characteristics. Sci Rep 2017;7(1):17683. https://doi.org/10.1038/s41598-017-17713-3.
[38] Mittal N, Ansari F, Gowda VK, Brouzet C, Chen P, Larsson PT, et al. Multiscale control of nanocellulose assembly: transferring remarkable nanoscale fibril mechanics to macroscale fibers. ACS Nano 2018;12(7):6378–88. https://doi.org/10.1021/acsnano.8b01084.
[39] Yadav MD, Dasgupta K, Patwardhan AW, Joshi JB. High Performance Fibers from Carbon Nanotubes: Synthesis, Characterization, and Applications in Composites: A Review. Ind Eng Chem Res 2017;56(44):12407–37. https://doi.org/10.1021/acs.iecr.7b02269.
[40] Wang F, Zhao S, Jiang Q, Li R, Zhao Y, Huang Y, et al. Advanced functional carbon nanotube fibers from preparation to application. Cell Rep Phys Sci 2022: 100989. https://doi.org/10.1016/j.xcrp.2022.100989.
[41] Boncel S, Sundaram RM, Windle AH, Koziol KKK. Enhancement of the mechanical properties of directly spun CNT fibers by chemical treatment. ACS Nano 2011;5 (12):9339–44. https://doi.org/10.1021/nn202685x.
[42] Lee WJ, Clancy AJ, Fernandez-Toribio JC, Anthony DB, White ER, Solano E, et al. Interfacially-grafted single-walled carbon nanotube / poly (vinyl alcohol) composite fibers. Carbon 2019;146:162–71. https://doi.org/10.1016/j.carbon.2019.01.075.
[43] Miaudet P, Badaire S, Maugey M, Derre A, Pichot V, Launois P, et al. Hot-drawing of single and multiwall carbon nanotube fibers for high toughness and alignment. Nano Lett 2005;5(11):2212–5. https://doi.org/10.1021/nl051419w.
[44] Lee WJ, Paineau E, Anthony DB, Gao Y, Leese HS, Sp R, et al. Inorganic nanotube mesophases enable strong self-healing fibers. ACS Nano 2020;14(5):5570–80. https://doi.org/10.1021/acsnano.9b09873.
[45] Lee D, Kim SG, Hong S, Madrona C, Oh Y, Park M, et al. Ultrahigh strength, modulus, and conductivity of graphitic fibers by macromolecular coalescence. Sci. Adv. 2022;8(16). https://doi.org/10.1126/sciadv.abn0939.
[46] Kim SG, Choi GM, Jeong HD, Lee D, Kim S, Ryu K-H, et al. Hierarchical structure control in solution spinning for strong and multifunctional carbon nanotube fibers. Carbon 2022;196:59–69. https://doi.org/10.1016/j.carbon.2022.04.040.
[47] Natarajan B. Processing-structure-mechanical property relationships in direct formed carbon nanotube articles and their composites: a review. Compos Sci Technol 2022;225:109501. https://doi.org/10.1016/j.compscitech.2022.109501.
[48] Fujimori T, Yamashita D, Kishibe Y, Sakai M, Inoue H, Onoki T, et al. One step fabrication of aligned carbon nanotubes using gas rectifier. Sci Rep 2022;12(1): 1285. https://doi.org/10.1038/s41598-022-05297-6.
[49] Bai Y, Zhang R, Ye X, Zhu Z, Xie H, Shen B, et al. Carbon nanotube bundles with tensile strength over 80 GPa. Nat Nanotechnol 2018;13(7):589–95. https://doi.org/10.1038/s41565-018-0141-z.
[50] Allaer K, De Baere I, Lava P, Van Paepegem W, Degrieck J. On the in-plane mechanical properties of stainless steel fibre reinforced ductile composites. Compos Sci Technol 2014;100:34–43. https://doi.org/10.1016/j.compscitech.2014.05.009.
[51] Callens MG, Gorbatikh L, Bertels E, Goderis B, Smet M, Verpoest I. Tensile behaviour of stainless steel fibre/epoxy composites with modified adhesion. Compos Pt A-Appl Sci Manuf 2015;69:208–18. https://doi.org/10.1016/j.compositesa.2014.11.022.
[52] Callens MG, De Cuyper P, Gorbatikh L, Verpoest I. Effect of fibre architecture on the tensile and impact behaviour of ductile stainless steel fibre polypropylene composites. Compos Struct 2015;119:528–33. https://doi.org/10.1016/j.compstruct.2014.09.028.
[53] Swolfs Y, De Cuyper P, Callens MG, Verpoest I, Gorbatikh L. Hybridisation of two ductile materials - Steel fibre and self-reinforced polypropylene composites. Compos Pt A-Appl Sci Manuf 2017;100:48–54. https://doi.org/10.1016/j.compositesa.2017.05.001.
[54] Hannemann B, Backe S, Schmeer S, Balle F, Breuer UP, Schuster J. Hybridisation of CFRP by the use of continuous metal fibres (MCFRP) for damage tolerant and electrically conductive lightweight structures. Compos Struct 2017;172:374–82. https://doi.org/10.1016/j.compstruct.2017.03.064.
[55] McBride AK, Turek SL, Zaghi AE, Burke KA. Mechanical Behavior of Hybrid Glass/Steel Fiber Reinforced Epoxy Composites. Polymers 2017;9(4):16. https://doi.org/10.3390/polym9040151.
[56] Zhang F, Lisle T, Curtin WA, Xia Z. Multiscale modeling of ductile-fiber-reinforced composites. Compos Sci Technol 2009;69(11):1887–95. https://doi.org/10.1016/j.compscitech.2009.04.006.
[57] Ahmed T. Hybrid composite structures: multifunctionality through metal fibres, PhD thesis. TU Delft; 2009. https://repository.tudelft.nl/islandora/object/uuid:85e91d70-dcf2-47c2-892a-cad116fe845f.
[58] Rizzo F, Pinto F, Meo M. Development of multifunctional hybrid metal/carbon composite structures. Compos Struct 2019;222:110907. https://doi.org/10.1016/j.compstruct.2019.110907.
[59] Gordon JE, Jeronimidis G. Composites with high work of fracture. Philos Trans R Soc A-Math Phys Eng Sci 1980;294(1411):545–50. https://doi.org/10.1098/rsta.1980.0063.
[60] Sun CT, Chen JL. A simple flow rule for characterizing nonlinear behavior of fiber composites. J Compos Mater 1989;23(10):1009–20. https://doi.org/10.1177/002199838902301004.
[61] Kellas S, Morton J, Jackson KE. An evaluation of the ±45 tensile test for the determination of the in-plane shear strength of composite materials. ICCM 8 - 8th International Conference on Composite Materials; Honolulu1991. https://iccm-central.org/Proceedings/ICCM8proceedings/papers/ICCM8_V4_69.pdf.
[62] Kellas S, Morton J, Jackson KE, editors. Damage and failure mechanisms in scaled angle-ply laminates: ASTM STP 1156; 1993. https://nam11.safelinks.protection.outlook.com/?url=https%3A%2F%2Fbooks.google.co.uk%2Fbooks%3Fhl%3Den%26lr%3D%26id%3DpXFdqSVTq9kC%26oi%3Dfnd%26pg%3DPA257%26dq%

3DKellas%2BS%2C%2BMorton%2BJ%2C%2BJackson%2BKE%2C%2Beditors.%2BDamage%2Band%2Bfailure%2Bmechanisms%2Bin%2Bscaled%2B%2Bangle-ply%2Blaminates%3A%2BASTM%2BSTP%2B1156%253B%2B1993.%2B%26ots%3DukZDXw3oSc%26sig%3DlG3hIRdsPH9tKNua_2_4sP8DmOI%23v%3Donepage%26q%26f%3Dfalse&data=05%7C02%7Ca.madhankumar%40elsevier.com%7Ce9fdfb1d56194d7d2db108dc4a9e4b3c%7C9274ee3f94254109a27f9fb15c10675d%7C0%7C0%7C638467290951009092%7CUnknown%7CTWFpbGZsb3d8eyJWIjoiMC4wLjAwMDAiLCJQIjoiV2luMzIiLCJBTiI6Ik1haWwiLCJXVCI6Mn0%3D%7C0%7C%7C%7C&sdata=ya2G5NlZlAQbkfvJCnkoLAT4qyHitzFVf1RrBl5I7rs%3D&reserved=0.

[63] Pozegic TR, Fotouhi M, Wu X, Hartley JW, Wisnom MR, Hamerton I. Pseudo-ductile behaviour in fibre reinforced thermoplastic angle-ply composites. Compos Sci Technol 2020;197:108261. https://doi.org/10.1016/j.compscitech.2020.108261.

[64] Moreno MCS, Munoz SH, Gutierrez AR, Rappold C, Vicente JLM, Morales-Rodriguez PA, et al. Pseudo-ductility in flexural testing of symmetric +/- 45 degrees angle-ply CFRP laminates. Compos Sci Technol 2018;156:8–18. https://doi.org/10.1016/j.compscitech.2017.12.015.

[65] Moreno MCS, Munoz SH. Pseudo-ductile effects in +/- 45 degrees angle-ply CFRP laminates under uniaxial loading: Compression and cyclic tensile test. Compos Pt B-Eng 2022;233:9. https://doi.org/10.1016/j.compositesb.2022.109631.

[66] Fuller JD, Wisnom MR. Pseudo-ductility and damage suppression in thin ply CFRP angle-ply laminates. Compos Part A-Appl Sci Manufact 2015;69:64–71. https://doi.org/10.1016/j.compositesa.2014.11.004.

[67] Wisnom MR. The effect of fiber rotation in +/-45-degrees tension tests on measured shear properties. Composites 1995;26(1):25–32. https://doi.org/10.1016/0010-4361(94)P3626-C.

[68] Fuller JD, Wisnom MR. Exploration of the potential for pseudo-ductility in thin ply CFRP angle-ply laminates via an analytical method. Compos Sci Technol 2015;112:8–15. https://doi.org/10.1016/j.compscitech.2015.02.019.

[69] Deng X, Hu JF, Wang WX, Matsubara T. A micromechanical model for the analysis of multidirectional fiber reinforced polymer laminates. Compos Struct 2019;208:507–16. https://doi.org/10.1016/j.compstruct.2018.10.019.

[70] Mizumoto K, Kanda Y, Isaki T, Sanada K, Nagata K, Miyata A, et al. Effect of fiber orientation on the tensile properties of cross-ply laminates of PP reinforced continuous carbon fiber. J Compos Mater 2021;55(24):3483–91. https://doi.org/10.1177/00219983211015720.

[71] Fuller JD, Wisnom MR. Ductility and pseudo-ductility of thin ply angle-ply CFRP laminates under quasi-static cyclic loading. Compos Part A-Appl Sci Manufact 2018;107:31–8. https://doi.org/10.1016/j.compositesa.2017.12.020.

[72] Vieille B, Taleb L. About the influence of temperature and matrix ductility on the behavior of carbon woven-ply PPS or epoxy laminates: Notched and unnotched laminates. Compos Sci Technol 2011;71(7):998–1007. https://doi.org/10.1016/j.compscitech.2011.03.006.

[73] Caminero MA, Rodriguez GP, Chacon JM, Garcia-Moreno I. Tensile and flexural damage response of symmetric angle-ply carbon fiber-reinforced epoxy laminates: Non-linear response and effects of thickness and ply-stacking sequence. Polym Compos 2019;40(9):3678–90. https://doi.org/10.1002/pc.25230.

[74] Yuan Y, Wang S, Yang H, Yao X, Liu B. Analysis of pseudo-ductility in thin-ply carbon fiber angle-ply laminates. Compos Struct 2017;180:876–82. https://doi.org/10.1016/j.compstruct.2017.08.070.

[75] Bergmann T, Heimbs S, Maier M. Mechanical properties and energy absorption capability of woven fabric composites under +/- 45 degrees off-axis tension. Compos Struct 2015;125:362–73. https://doi.org/10.1016/j.compstruct.2015.01.040.

[76] Kuo CM, Takahashi K, Chou TW. Effect of fiber waviness on the nonlinear elastic behavior of flexible composites. J Compos Mater 1988;22(11):1004–25. https://doi.org/10.1177/002199838802201101.

[77] Chun HJ, Shin JY, Daniel IM. Effects of material and geometric nonlinearities on the tensile and compressive behavior of composite materials with fiber waviness. Compos Sci Technol 2001;61(1):125–34. https://doi.org/10.1016/s0266-3538(00)00201-3.

[78] Diao H, Robinson P, Wisnom MR, Bismarck A. Unidirectional carbon fibre reinforced polyamide-12 composites with enhanced strain to tensile failure by introducing fibre waviness. Compos Part A-Appl Sci Manufact 2016;87:186–93. https://doi.org/10.1016/j.compositesa.2016.04.025.

[79] Dancila DS, Armanios EA. Energy-dissipating composite members with progressive failure: concept development and analytical modeling. AIAA J 2002;40(10):2096–104. https://doi.org/10.2514/2.1544.

[80] Dancila DS, Armanios EA. Energy-dissipating composite members with progressive failure: impulsive response and experimental verification. AIAA J 2010;48(4):728–37. https://doi.org/10.2514/1.39786.

[81] Pimenta S, Robinson P. Wavy-ply sandwich with composite skins and crushable core for ductility and energy absorption. Compos Struct 2014;116:364–76. https://doi.org/10.1016/j.compstruct.2014.05.020.

[82] Rosen BW. Mechanics of Composite Strengthening, Fibre Composite Materials. Metals Park Ohio, U.S.A.: ASM; 1965 [chapter 3].

[83] Zweben C. Tensile failure fiber composites. AIAA J 1968;6(12):2325–31. https://doi.org/10.2514/3.4990.

[84] Swolfs Y, McMeeking RM, Verpoest I, Gorbatikh L. The effect of fibre dispersion on initial failure strain and cluster development in unidirectional carbon/glass hybrid composites. Compos Pt A-Appl Sci Manuf 2015;69:279–87. https://doi.org/10.1016/j.compositesa.2014.12.001.

[85] Wisnom MR. On the high compressive strains achieved in bending tests on unidirectional carbon-fiber epoxy. Compos Sci Technol 1992;43(3):229–35. https://doi.org/10.1016/0266-3538(92)90093-i.

[86] Wisnom MR. The Relationship between Tensile and Flexural Strength of Unidirectional Composites. J Compos Mater 1992;26(8):1173–80. https://doi.org/10.1177/002199839202600805.

[87] Wisnom MR, Atkinson JW. Constrained buckling tests show increasing compressive strain to failure with increasing strain gradient. Compos Part A-Appl Sci Manufact 1997;28(11):959–64. https://doi.org/10.1016/s1359-835x(97)00067-5.

[88] De Luca F, Sernicola G, Shaffer MSP, Bismarck A. "Brick-and-mortar" nanostructured interphase for glass-fiber-reinforced polymer composites. ACS Appl Mater Interfaces 2018;10(8):7352–61. https://doi.org/10.1021/acsami.7b16136.

[89] De Luca F, Clancy AJ, Carrero NR, Anthony DB, De Luca HG, Shaffer MSP, et al. Increasing carbon fiber composite strength with a nanostructured "brick-and-mortar" interphase. Mater Horizons 2018;5(4):668–74. https://doi.org/10.1039/c7mh00917h.

[90] Magyar B, Czigany T, Szebenyi G. Metal-alike polymer composites: The effect of inter-layer content on the pseudo-ductile behaviour of carbon fibre/epoxy resin materials. Compos Sci Technol 2021;215:8. https://doi.org/10.1016/j.compscitech.2021.109002.

[91] Melaibari A, Wagih A, Basha M, Kabeel AM, Lubineau G, Eltaher MA. Bio-inspired composite laminate design with improved out-of-plane strength and ductility. Compos Part A-Appl Sci Manufact 2021;144:12. https://doi.org/10.1016/j.compositesa.2021.106362.

[92] Grail G, Pimenta S, Pinho ST, Robinson P. Exploring the potential of interleaving to delay catastrophic failure in unidirectional composites under tensile loading. Compos Sci Technol 2015;106:100–9. https://doi.org/10.1016/j.compscitech.2014.11.006.

[93] Hayashi TKK, Yamazaki A, Kihira M. Development of new material properties by hybrid composition. 2nd report Fukugo Zairyo (Composite Materials) 1972;1:21–5.

[94] Swolfs Y, Gorbatikh L, Verpoest I. Fibre hybridisation in polymer composites: a review. Compos Pt A-Appl Sci Manuf 2014;67:181–200. https://doi.org/10.1016/j.compositesa.2014.08.027.

[95] Bunsell AR, Harris B. Hybrid carbon and glass fibre composites. Composites 1974;4:157–64. https://doi.org/10.1016/0010-4361(74)90107-4.

[96] Aveston J, Sillwood JM. Synergistic fiber strengthening in hybrid composites. J Mater Sci 1976;11(10):1877–83. https://doi.org/10.1007/bf00708266.

[97] Aveston J, Kelly A. Theory of multiple fracture of fibrous composites. J Mater Sci 1973;8(3):352–62. https://doi.org/10.1007/bf00550155.

[98] Zhu H, Weitsman Y. The progression of failure mechanisms in unidirectionally reinforced ceramic composites. J Mech Phys Solids 1994;42(10):1601–32. https://doi.org/10.1016/0022-5096(94)90089-2.

[99] Sherman D, Lemaitre J, Leckie FA. The mechanical-behavior of an alumina carbon/epoxy laminate. Acta Metall Mater 1995;43(12):4483–93. https://doi.org/10.1016/0956-7151(95)00136-j.

[100] Bakis CE, Nanni A, Terosky JA, Koehler SW. Self-monitoring, pseudo-ductile, hybrid FRP reinforcement rods for concrete applications. Compos Sci Technol 2001;61(6):815–23. https://doi.org/10.1016/s0266-3538(00)00184-6.

[101] Cui YH, Tao J. A new type of ductile composite reinforcing bar with high tensile elastic modulus for use in reinforced concrete structures. Can J Civ Eng 2009;36(4):672–5. https://doi.org/10.1139/l09-012.

[102] Ali NM, Wang X, Wu ZS. Integrated Performance of FRP Tendons with Fiber Hybridization. J Compos Constr 2014;18(3):10. https://doi.org/10.1061/(asce)cc.1943-5614.0000427.

[103] Sihn S, Kim RY, Kawabe K, Tsai SW. Experimental studies of thin-ply laminated composites. Compos Sci Technol 2007;67(6):996–1008. https://doi.org/10.1016/j.compscitech.2006.06.008.

[104] Czél G, Wisnom MR. Demonstration of pseudo-ductility in high performance glass/epoxy composites by hybridisation with thin-ply carbon prepreg. Compos Part A-Appl Sci Manufact 2013;52:23–30. https://doi.org/10.1016/j.compositesa.2013.04.006.

[105] Czél G, Jalalvand M, Wisnom MR. Design and characterisation of advanced pseudo-ductile unidirectional thin-ply carbon/epoxy-glass/epoxy hybrid composites. Compos Struct 2016;143:362–70. https://doi.org/10.1016/j.compstruct.2016.02.010.

[106] Jalalvand M, Czél G, Wisnom MR. Numerical modelling of the damage modes in UD thin carbon/glass hybrid laminates. Compos Sci Technol 2014;94:39–47. https://doi.org/10.1016/j.compscitech.2014.01.013.

[107] Jalalvand M, Czél G, Wisnom MR. Damage analysis of pseudo-ductile thin-ply UD hybrid composites – a new analytical method. Compos Part A-Appl Sci Manufact 2015;69:83–93. https://doi.org/10.1016/j.compositesa.2014.11.006.

[108] Jalalvand M, Czél G, Wisnom MR. Parametric study of failure mechanisms and optimal configurations of pseudo-ductile thin-ply UD hybrid composites. Compos Pt A-Appl Sci Manuf 2015;74:123–31. https://doi.org/10.1016/j.compositesa.2015.04.001.

[109] Tavares RP, Melro AR, Bessa MA, Turon A, Liu WK, Camanho PP. Mechanics of hybrid polymer composites: analytical and computational study. Comput Mech 2016;57(3):405–21. https://doi.org/10.1007/s00466-015-1252-0.

[110] Guerrero JM, Mayugo JA, Costa J, Turon A. A 3D Progressive Failure Model for predicting pseudo-ductility in hybrid unidirectional composite materials under fibre tensile loading. Compos Pt A-Appl Sci Manuf 2018;107:579–91. https://doi.org/10.1016/j.compositesa.2018.02.005.

[111] Mesquita F, Swolfs Y, Lomov SV, Gorbatikh L. Ply fragmentation in unidirectional hybrid composites linked to stochastic fibre behaviour: a dual-scale model. Compos Sci Technol 2019;181:10. https://doi.org/10.1016/j.compscitech.2019.107702.

[112] Conde FM, Coelho PG, Tavares RP, Rodrigues HC, Guedes JM, Camanho PP. Optimization of the microstructure of unidirectional hybrid composites under uniaxial tensile loads. Compos Struct 2020. https://doi.org/10.1016/j.compstruct.2019.111795.

[113] Ribeiro F, Sena-Cruz J, Branco FG, Julio E, Castro F. Analytical hybrid effect prediction and evolution of the tensile response of unidirectional hybrid fibre-reinforced polymers composites for civil engineering applications. J Compos Mater 2020;54(22):3205–28. https://doi.org/10.1177/0021998320911956.

[114] Czél G, Jalalvand M, Wisnom MR, Czigany T. Design and characterisation of high performance, pseudo-ductile all-carbon/epoxy unidirectional hybrid composites. Compos Pt B-Eng 2017;111:348–56. https://doi.org/10.1016/j.compositesb.2016.11.049.

[115] Danzi F, Tavares RP, Xavier J, Fanteria D, Camanho pp.. Effects of hybridization and ply thickness on the strength and toughness of composite laminates. J Compos Mater 2021;55(30):4601–16. https://doi.org/10.1177/00219983211041762.

[116] Sapozhnikov SB, Swolfs Y, Lomov SV. Pseudo-ductile unidirectional high modulus/high strength carbon fibre hybrids using conventional ply thickness prepregs. Compos Pt B-Eng 2020;198:11. https://doi.org/10.1016/j.compositesb.2020.108213.

[117] Marino SG, Czél G. Improving the performance of pseudo-ductile hybrid composites by film-interleaving. Compos A Appl Sci Manuf 2021;142:106233. https://doi.org/10.1016/j.compositesa.2020.106233.

[118] Marino SG, Košťáková EK, Czél G. Development of pseudo-ductile interlayer hybrid composites of standard thickness plies by interleaving polyamide 6 nanofibrous layers. Compos Sci Technol 2023:109924. https://doi.org/10.1016/j.compscitech.2023.109924.

[119] Marino SG, Czél G. Development and characterisation of reparable, film-interleaved, pseudo-ductile hybrid composites. Compos A Appl Sci Manuf 2023:107496. https://doi.org/10.1016/j.compositesa.2023.107496.

[120] Burley A, Aitharaju V. Enhanced ductility in in-layer glass-carbon fiber/epoxy hybrid composites produced via tailored fiber placement. Compos A Appl Sci Manuf 2023:107488. https://doi.org/10.1016/j.compositesa.2023.107488.

[121] Huang C, Joosten MW. 3D printed continuous fibre-reinforced composites: Design and characterisation of advanced pseudo-ductile hybrid laminates. Compos Part A-Appl Sci Manufact 2021;146:10. https://doi.org/10.1016/j.compositesa.2021.106403.

[122] Ribeiro F, Sena-Cruz J, Branco FG, Julio E. Hybrid effect and pseudo-ductile behaviour of unidirectional interlayer hybrid FRP composites for civil engineering applications. Constr Build Mater 2018;171:871–90. https://doi.org/10.1016/j.conbuildmat.2018.03.144.

[123] Wisnom MR, Czél G, Swolfs Y, Jalalvand M, Gorbatikh L, Verpoest I. Hybrid effects in thin ply carbon/glass unidirectional laminates: accurate experimental determination and prediction. Compos Pt A-Appl Sci Manuf 2016;88:131–9. https://doi.org/10.1016/j.compositesa.2016.04.014.

[124] Wisnom MR, Czél G, Fuller JD, Jalalvand M. Taking advantage of the hybrid effect in thin-ply pseudo-ductile laminates. ECCM17 – 17th European Conference on Composite Materials, Munich, Germany, 26-30 June 2016 2016. http://real.mtak.hu/40438/1/Wisnom_ECCM17_2016.pdf.

[125] Parvizi A, Garrett KW, Bailey JE. Constrained cracking in glass fiber-reinforced epoxy cross-ply laminates. J Mater Sci 1978;13(1):195–201. https://doi.org/10.1007/bf00739291.

[126] Paris F, Velasco ML, Correa E. The scale effect in composites: an explanation physically based on the different mechanisms of damage involved in failure. Compos Struct 2021;257:19. https://doi.org/10.1016/j.compstruct.2020.113089.

[127] Wisnom MR, Fuller J, Suwarta P, Czél G. Repeated Tensile Loading of Thin-Ply Pseudo-Ductile Laminates. In: Xiao X, Loos A, Liu D, editors. Proceedings of the American Society for Composites: Thirtieth Technical Conference. Destech Publications, Inc; 2015. p. 2333–40. https://research-information.bris.ac.uk/ws/portalfiles/portal/74276863/Wisnom_ASC_2015_Pseudo_Ductile_Repeated_Loading.pdf.

[128] Fotouhi M, Suwarta P, Jalalvand M, Czél G, Wisnom MR. Acoustic emission monitoring of thin ply hybrid composites under repeated quasi-static tensile loading. FME Trans 2018;46(2):238–44. https://doi.org/10.5937/fmet1802238F.

[129] Ribeiro F, Sena-Cruz J, Vassilopoulos AP. Tension-tension fatigue behavior of hybrid glass/carbon and carbon/carbon composites. Int J Fatigue 2021;146:11. https://doi.org/10.1016/j.ijfatigue.2021.106143.

[130] Wisnom MR, Czél G. Compression Behaviour of Pseudo-Ductile Carbon/Glass Hybrid Laminates Pre-Fractured in Tension. In: Proceedings of the American Society for Composites—Thirty-fifth Technical Conference; 2020. https://www.dpi-proceedings.com/index.php/asc35/article/view/34932.

[131] Fotouhi M, Suwarta P, Jalalvand M, Czél G, Wisnom MR. Detection of fibre fracture and ply fragmentation in thin-ply UD carbon/glass hybrid laminates using acoustic emission. Compos Pt A-Appl Sci Manuf 2016;86:66–76. https://doi.org/10.1016/j.compositesa.2016.04.003.

[132] Ichenihi A, Li W, Gao YT, Rao YF. Feature selection and clustering of damage for pseudo-ductile unidirectional carbon/glass hybrid composite using acoustic emission. Appl Acoust 2021;182:10. https://doi.org/10.1016/j.apacoust.2021.108184.

[133] Czél G, Jalalvand M, Wisnom MR. Demonstration of pseudo-ductility in unidirectional hybrid composites made of discontinuous carbon/epoxy and continuous glass/epoxy plies. Compos A Appl Sci Manuf 2015;72:75–84. https://doi.org/10.1016/J.COMPOSITESA.2015.01.019.

[134] Yu H, Longana ML, Jalalvand M, Wisnom MR, Potter KD. Hierarchical pseudo-ductile hybrid composites combining continuous and highly aligned discontinuous fibres. Compos Pt A-Appl Sci Manuf 2018;105:40–56. https://doi.org/10.1016/j.compositesa.2017.11.005.

[135] Zhao C, Donough MJ, Prusty BG, Xiao J, Zhou L, An L. Pseudo-ductile fracture in grid stiffened structure by automated fibre placement. Compos Struct 2023:116694. https://doi.org/10.1016/j.compstruct.2023.116694.

[136] Jalalvand M, Czél G, Wisnom MR. Multi-directional hybrid laminates - studying the effect of fragmentation and dispersed delamination on stress-strain curves of unnotched laminates using analytical modelling. 20th International Conference on Composite Materials; Copenhagen2015. https://www.iccm-central.org/Proceedings/ICCM20proceedings/papers/paper-3317-2.pdf.

[137] Czél G, Rev T, Jalalvand M, Fotouhi M, Longana ML, Nixon-Pearson OJ, et al. Pseudo-ductility and reduced notch sensitivity in multi-directional all-carbon/epoxy thin-ply hybrid composites. Compos Part A-Appl Sci Manufact 2018;104:151–64. https://doi.org/10.1016/j.compositesa.2017.10.028.

[138] Jalalvand M, Fotouhi M, Wisnom MR. Orientation-dispersed pseudo-ductile hybrid composite laminates – a new lay-up concept to avoid free-edge delamination. Compos Sci Technol 2017;153:232–40. https://doi.org/10.1016/j.compscitech.2017.10.011.

[139] Fotouhi M, Jalalvand M, Wisnom MR. High performance quasi-isotropic thin-ply carbon/glass hybrid composites with pseudo-ductile behaviour in all fibre orientations. Compos Sci Technol 2017;152:101–10. https://doi.org/10.1016/j.compscitech.2017.08.024.

[140] Idarraga G, Fotouhi M, Jalalvand M, Wisnom M. Investigation of the hybrid effect in high performance quasi-isotropic thin-ply carbon/glass composites under tension. 22nd International Conference on Composite Materials (ICCM22), Melbourne, August. 2019. https://www.iccm-central.org/Proceedings/ICCM22proceedings/papers/ICCM22_Full_Paper_49.pdf.

[141] Fotouhi M, Jalalvand M, Saeedifar M, Xiao B, Wisnom MR. High performance quasi -isotropic thin -ply carbon/glass hybrid composites with pseudo -ductile behaviour loaded off -axis. Compos Struct 2020;247:9. https://doi.org/10.1016/j.compstruct.2020.112444.

[142] Kohler S, Cugnoni J, Amacher R, Botsis J. Damage mechanisms in thin-ply composites: Free edge/bulk measurements and multiscale modelling. 17th European Conference on Composite Materials, ECCM 2016; Munich2016. - https://www2.scopus.com/inward/record.uri?eid=2-s2.0-85018615965&partnerID=40&md5=c8b2c4362f4f726531a2c0b3e5cbf285.

[143] Czél G. Development of bi-directional pseudo-ductile glass/carbon-epoxy hybrid composites for improved safety in structural applications. Compos Pt B-Eng 2022;231:9. https://doi.org/10.1016/j.compositesb.2021.109546.

[144] Czél G, Jalalvand M, Wisnom MR. Hybrid specimens eliminating stress concentrations in tensile and compressive testing of unidirectional composites. Compos Pt A-Appl Sci Manuf 2016;91:436–47. https://doi.org/10.1016/j.compositesa.2016.07.021.

[145] Czél G, Suwarta P, Jalalvand M, Wisnom MR. Investigation of the compression performance and failure mechanism of pseudo-ductile thin-ply hybrid composites. 21st International Conference on Composite Materials; Xian2017. https://www.iccm-central.org/Proceedings/ICCM21proceedings/papers/3889.pdf.

[146] Suwarta P, Czél G, Fotouhi M, Rycerz J, Wisnom MR. Pseudo-ductility of unidirectional thin ply hybrid composites in longitudinal compression. ASC 33rd Technical Conference; Seattle2018. - https://www.researchgate.net/publication/328268733_Pseudo_ductility_of_Unidirectional_Thin_Ply_Hybrid_Composites_in_Longitudinal_Compression.

[147] Suwarta P. Pseudo-ductility of unidirectional thin-ply hybrid composites, PhD thesis. University of Bristol; 2020. https://research-information.bris.ac.uk/en/studentTheses/pseudo-ductility-of-unidirectional-thin-ply-hybrid-composites.

[148] Idarraga G, Jalalvand M, Fotouhi M, Meza J, Wisnom MR. Gradual failure in high-performance unidirectional thin-ply carbon/glass hybrid composites under bending. Compos Struct 2021;271:114128. https://doi.org/10.1016/j.compstruct.2021.114128.

[149] Suwarta P, Fotouhi M, Czél G, Longana M, Wisnom MR. Fatigue behaviour of pseudo-ductile unidirectional thin-ply carbon/epoxy-glass/epoxy hybrid composites. Compos Struct 2019;224:110996. https://doi.org/10.1016/j.compstruct.2019.110996.

[150] Fotouhi M, Suwarta P, Tabatabaeian A, Fotouhi S, Jenkin R, Jalalvand M, et al. Investigating the fatigue behaviour of quasi-isotropic pseudo-ductile thin-ply carbon/glass epoxy hybrid composites. Compos Pt A-Appl Sci Manuf 2022;163:11. https://doi.org/10.1016/j.compositesa.2022.107206.

[151] Fotouhi M, Fuller J, Longana M, Jalalvand M, Wisnom MR. The high strain rate tension behaviour of pseudo-ductile high performance thin ply composites. Compos Struct 2019;215:365–76. https://doi.org/10.1016/j.compstruct.2019.02.068.

[152] Czél G, Bugár-Mészáros M, Wisnom MR. Combined effect of moisture and test temperature on the pseudo-ductility of thin-ply carbon/epoxy-glass/epoxy hybrid composites. Compos A Appl Sci Manuf 2023;165:107353. https://doi.org/10.1016/j.compositesa.2022.107353.

[153] Mousavi-Bafrouyi SMS, Eslami-Farsani R, Geranmayeh A. The Temperature Effects on the Mechanical Properties of Pseudo-ductile Thin-ply Unidirectional Carbon-basalt Fibers/Epoxy Hybrid Composites with Different Stacking Sequences. Fiber Polym 2021;22(11):3162–71. https://doi.org/10.1007/s12221-021-1052-4.

[154] Fotouhi M, Jalalvand M, Prato A, Wisnom MR. Thin ply carbon/glass hybrid laminates to activate new damage mechanisms under indentation. ECCM18 – 18th European Conference on Composite Materials; Athens2018.
[155] Saleh Mousavi-Bafrouyi SM, Eslami-Farsani R, Geranmayeh A. Effect of stacking sequence on the mechanical properties of pseudo-ductile thin-ply unidirectional carbon-basalt fibers/epoxy composites. J Ind Text. 2022;51(2_suppl):2835S–52S. https://doi.org/10.1177/1528083720978400.
[156] Rev T, Jalalvand M, Fuller J, Wisnom MR, Czél G. A simple and robust approach for visual overload indication - UD thin-ply hybrid composite sensors. Compos Part A-Appl Sci Manufact 2019;121:376–85. https://doi.org/10.1016/j.compositesa.2019.03.005.
[157] Jalalvand M, Lok Wu HWM, Sheibanian F, Fotouhi M, Wisnom MR. Self-warning hybrid composite patches for repairing cracked aluminium panels. ECCM18 – 18th European Conference on Composite Materials; Athens2018.
[158] Wisnom MR, Jalalvand M, inventorsPatent: Sensor for indication of loading cycles of a structure patent PCT/GB2018/050144. 2018.
[159] Tabatabaeian A, Liu S, Harrison P, Schlangen E, Fotouhi M. A review on self-reporting mechanochromic composites: an emerging technology for structural health monitoring. Compos A Appl Sci Manuf 2022:107236. https://doi.org/10.1016/j.compositesa.2022.107236.
[160] Fotouhi S, Jalalvand M, Wisnom MR, Fotouhi M. Smart hybrid composite sensor technology to enhance the detection of low energy impact damage in composite structures. Compos A Appl Sci Manuf 2023. https://doi.org/10.1016/j.compositesa.2023.107595.
[161] Wisnom MR, Cantera MA, Czél G, Jalalvand M. New approaches to quantifying tensile strength variability and size effects in unidirectional composites. American Society for Composites 32nd Technical Conference; Purdue2017. - https://dpi-proceedings.com/index.php/asc32/article/view/15397.
[162] Czél G, Jalalvand M, Wisnom MR, Canal LP, Gonzalez CD, Llorca J. Novel experimental procedure and determination of full displacement fields of delaminating composite layer interfaces for evaluation of the mode II cohesive law. Eng Fract Mech 2015;149:326–37. https://doi.org/10.1016/j.engfracmech.2015.06.060.
[163] Jalalvand M, Czél G, Fuller JD, Wisnom MR, Canal LP, Gonzalez CD, et al. Energy dissipation during delamination in composite materials - an experimental assessment of the cohesive law and the stress-strain field ahead of a crack tip. Compos Sci Technol 2016;134:115–24. https://doi.org/10.1016/j.compscitech.2016.08.001.
[164] Jalalvand M, Fotouhi M, Wisnom MR. Effect of shear stresses on fibre direction tensile failure using a new simple and reliable test method with thin plies. Composites Part A: Applied Science and Manufacturing, in press. 2024.
[165] Rev T, Wisnom MR, Xu X, Czél G. The effect of transverse compressive stresses on tensile failure of carbon fibre/epoxy composites. Compos A Appl Sci Manuf 2022;156:106894. https://doi.org/10.1016/j.compositesa.2022.106894.
[166] Hine PJ, Bonner MJ, Ward IM, Swolfs Y, Verpoest I. The influence of the hybridisation configuration on the mechanical properties of hybrid self reinforced polyamide 12/carbon fibre composites. Compos Pt A-Appl Sci Manuf 2017;95:141–51. https://doi.org/10.1016/j.compositesa.2016.12.029.
[167] Swolfs Y, Shi J, Meerten Y, Hine P, Ward I, Verpoest I, et al. The importance of bonding in intralayer carbon fibre/self-reinforced polypropylene hybrid composites. Compos Pt A-Appl Sci Manuf 2015;76:299–308. https://doi.org/10.1016/j.compositesa.2015.06.017.
[168] Swolfs Y, Meerten Y, Hine P, Ward I, Verpoest I, Gorbatikh L. Introducing ductility in hybrid carbon fibre/self-reinforced composites through control of the damage mechanisms. Compos Struct 2015;131:259–65. https://doi.org/10.1016/j.compstruct.2015.04.069.
[169] Selezneva M, Swolfs Y, Katalagarianakis A, Ichikawa T, Hirano N, Taketa I, et al. The brittle-to-ductile transition in tensile and impact behavior of hybrid carbon fibre/self-reinforced polypropylene composites. Compos Pt A-Appl Sci Manuf 2018;109:20–30. https://doi.org/10.1016/j.compositesa.2018.02.034.
[170] Mencattelli L, Tang J, Swolfs Y, Gorbatikh L, Pinho ST. Bio-inspired design for enhanced damage tolerance of self-reinforced polypropylene/carbon fibre polypropylene hybrid composites. Compos Pt A-Appl Sci Manuf 2019;121:341–52. https://doi.org/10.1016/j.compositesa.2019.03.028.
[171] Hassani F, Martin PJ, Falzon BG. Progressive failure in interply hybrid composites of self-reinforced polypropylene and glass fibre. Polymer 2020;195:122411. https://doi.org/10.1016/j.polymer.2020.122411.
[172] Fuller JD, Jalalvand M, Wisnom MR. Combining fibre rotation and fragmentation to achieve pseudo-ductile CFRP laminates. Compos Struct 2016;142:155–66. https://doi.org/10.1016/j.compstruct.2016.01.073.
[173] Fuller J, Mitchell S, Pozegic T, Wu X, Longana M, Wisnom M. Experimental evaluation of hygrothermal effects on pseudo-ductile thin ply angle-ply carbon/epoxy laminates. Compos Pt B-Eng 2021;227:11. https://doi.org/10.1016/j.compositesb.2021.109388.
[174] Fuller JD, Jalalvand M, Wisnom MR, A pseudo ductile angle-ply sub-laminate approach for multidirectional thin ply CFRP laminates. 17th European Conference on Composite Materials, ECCM 2016; 2016; Munich. http://www.escm.eu.org/eccm16/assets/0120.pdf.
[175] Wu X, Fuller JD, Longana ML, Wisnom MR. Reduced notch sensitivity in pseudo-ductile CFRP thin ply angle-ply laminates with central 0 degrees plies. Compos Pt A-Appl Sci Manuf 2018;111:62–72. https://doi.org/10.1016/j.compositesa.2018.05.011.
[176] Prato A, Longana ML, Hussain A, Wisnom MR. Post-impact behaviour of pseudo-ductile thin-ply angle-ply hybrid composites. Materials 2019;12:579. https://doi.org/10.3390/ma12040579.
[177] Xiang HB, Zhang YX, Chen Y, Pagani A, Zhang C. A nonlinear analytical model for tensile failure prediction of pseudo-ductile composite laminates. Thin-Walled Struct 2022;179:13. https://doi.org/10.1016/j.tws.2022.109711.
[178] Wu X, Fuller JD, Wisnom MR. Role of fibre fragmentation on pseudo-ductility of thin-ply +/- 27(7)/0 (s) carbon fibre laminates with high modulus 0 degrees plies under compressive and flexural loading. Compos Sci Technol 2020;199:9. https://doi.org/10.1016/j.compscitech.2020.108377.
[179] Wu X, Fuller JD, Wisnom MR. An investigation into fatigue behaviour and damage progression in pseudo-ductile thin-ply angle-ply laminates. Compos Part A - Appl Sci Manufact 2021;149:11. https://doi.org/10.1016/j.compositesa.2021.106518.
[180] Tugyi P, Fuller J, Wisnom M, Rev T. Ductile Composite Longboard. 2017. https://www.youtube.com/watch?v=VvuPHESnIOA.
[181] Cox BN, Dadkhah MS, Morris WL. On the tensile failure of 3D woven composites. Compos Pt A-Appl Sci Manuf 1996;27(6):447–58. https://doi.org/10.1016/1359-835x(95)00053-5.
[182] Cox BN, Dadkhah MS, Inman RV, Morris WL, Zupon J. Mechanisms of compressive failure in 3D-composites. Acta Metall Mater 1992;40(12):3285–98. https://doi.org/10.1016/0956-7151(92)90042-d.
[183] Das S, Kandan K, Kazemahvazi S, Wadley HNG, Deshpande VS. Compressive response of a 3D non-woven carbon-fibre composite. Int J Solids Struct 2018;136:137–49. https://doi.org/10.1016/j.ijsolstr.2017.12.011.
[184] Grace NF, Ragheb WF, Abdel-Sayed G. Development and application of innovative triaxially braided ductile FRP fabric for strengthening concrete beams. Compos Struct 2004;64(3–4):521–30. https://doi.org/10.1016/j.compstruct.2003.09.051.
[185] Wehrkamp-Richter T, Hinterholz R, Pinho ST. Damage and failure of triaxial braided composites under multi-axial stress states. Compos Sci Technol 2017;150:32–44. https://doi.org/10.1016/j.compscitech.2017.07.002.
[186] Gautam M, Sivakumar S, Barnett A, Barbour S, Ogin SL, Potluri P. On the behaviour of flattened tubular Bi-axial and Tri-axial braided composites in tension. Compos Struct 2021;261:10. https://doi.org/10.1016/j.compstruct.2020.113325.
[187] Islam MH, Koncherry V, Wisnom MR, Potluri P. Pseudo-ductile composites with micro-wrapped hybrid tow. ASC 33rd Annual Technical Conference; Seattle2018. - https://www.scopus.com/inward/record.uri?eid=2-s2.0-85059437748&partnerID=40&md5=cfaf0a56f202598e1c5322571bdfb112.
[188] Del Rosso S, Iannucci L, Curtis PT. Experimental investigation of the mechanical properties of dry microbraids and microbraid reinforced polymer composites. Compos Struct 2015;125:509–19. https://doi.org/10.1016/j.compstruct.2015.02.036.
[189] Del Rosso S, Iannucci, L, Curtis PT, Robinson P. Hybrid UHMwPE/Carbon microbraids for ductile composites. 17th European Conference on Composite Materials; Munich2016.
[190] Barthelat F, Rabiei R. Toughness amplification in natural composites. J Mech Phys Solids 2011;59:829–40. https://doi.org/10.1016/j.jmps.2011.01.001.
[191] Zhang Q, Li H, Liu Y, Zhang Z, Yuan Y. Nacre-inspired topological design tuning the impact resistant behaviors of composite plates. Compos Struct 2022;299:116077. https://doi.org/10.1016/j.compstruct.2022.116077.
[192] Bullegas G, Pinho ST, Pimenta S. Engineering the translaminar fracture behaviour of thin-ply composites. Compos Sci Technol 2016;131:110–22. https://doi.org/10.1016/j.compscitech.2016.06.002.
[193] Malkin R, Yasaee M, Trask RS, Bond IP. Bio-inspired laminate design exhibiting pseudo-ductile (graceful) failure during flexural loading. Compos A Appl Sci Manuf 2013;54:107–16. https://doi.org/10.1016/J.COMPOSITESA.2013.07.008.
[194] Narducci F, Lee KY, Pinho ST. Realising damage-tolerant nacre-inspired CFRP. J Mech Phys Solids 2018;116:391–402. https://doi.org/10.1016/J.JMPS.2018.04.004.
[195] Such M, Ward C, Potter K. Aligned discontinuous fibre composites: a short history. Journal of Multifunctional Composites 2014;2:1995–8. https://doi.org/10.12783/issn.2168-4286/2/3/4.
[196] Wong KH, Turner TA, Pickering SJ, Warrior NA. The potential for fibre alignment in the manufacture of polymer composites from recycled carbon fibre. SAE Int J Aerosp 2010;2:225–31. https://doi.org/10.4271/2009-01-3237.
[197] Kelly A, Tyson WR. Tensile properties of fibre-reinforced metals: Copper/tungsten and copper/molybdenum. J Mech Phys Solids 1965;13:329–50. https://doi.org/10.1016/0022-5096(65)90035-9.

[198] Lee BJ, Argon AS, Parks DM, Ahzi S, Bartczak Z. Simulation of large strain plastic deformation and texture evolution in high density polyethylene. Polymer 1993;34 (17):3555–75. https://doi.org/10.1016/0032-3861(93)90039-D.
[199] Sorini C, Chattopadhyay A, Goldberg RK. An improved plastically dilatant unified viscoplastic constitutive formulation for multiscale analysis of polymer matrix composites under high strain rate loading. Compos B Eng 2020;184:107669. https://doi.org/10.1016/j.compositesb.2019.107669.
[200] Kravchenko SG, Sommer DE, Pipes RB. Uniaxial strength of a composite array of overlaid and aligned prepreg platelets. Compos A Appl Sci Manuf 2018;109: 31–47. https://doi.org/10.1016/j.compositesa.2018.02.032.
[201] Nishikawa M, Fukuzo A, Matsuda N, Hojo M. Evaluation of elastic-plastic response of discontinuous carbon fiber-reinforced thermoplastics: experiments and considerations based on load-transfer-based micromechanical simulation. Compos Sci Technol 2018;155:117–25. https://doi.org/10.1016/j.compscitech.2017.12.003.
[202] Piggott MR, Ko M, Chuang HY. Aligned short-fibre reinforced thermosets: Experiments and analysis lend little support for established theory. Compos Sci Technol 1993;48:291–9. https://doi.org/10.1016/0266-3538(93)90146-8.
[203] Yu H, Potter KD, Wisnom MR. A novel manufacturing method for aligned discontinuous fibre composites (High Performance-Discontinuous Fibre method). Compos A Appl Sci Manuf 2014;65:175–85. https://doi.org/10.1016/j.compositesa.2014.06.005.
[204] Yu H, Longana ML, Jalalvand M, Wisnom MR, Potter KD. Pseudo-ductility in intermingled carbon/glass hybrid composites with highly aligned discontinuous fibres. Compos A Appl Sci Manuf 2015;73:35–44. https://doi.org/10.1016/j.compositesa.2015.02.014.
[205] Henry J, Pimenta S. Semi-analytical simulation of aligned discontinuous composites. Compos Sci Technol 2017;144:230–44. https://doi.org/10.1016/j.compscitech.2017.01.027.
[206] Pimenta S, Robinson P. An analytical shear-lag model for composites with 'brick-and-mortar' architecture considering non-linear matrix response and failure. Compos Sci Technol 2014;104:111–24. https://doi.org/10.1016/j.compscitech.2014.09.001.
[207] Bullegas G, Moledo Lamela J, Pimenta S, Taveira PS. On the role of dynamic stress concentrations and fracture mechanics in the longitudinal tensile failure of fibre-reinforced composites. Eng Fract Mech 2020;228. https://doi.org/10.1016/j.engfracmech.2020.106920.
[208] Finley JM, Henry J, Shaffer MSP, Pimenta S. The influence of variability and defects on the mechanical performance of tailorable composites. J Compos Mater 2020;54:565–89. https://doi.org/10.1177/0021998319862855.
[209] Finley JM, Yu H, Longana ML, Pimenta S, Shaffer MSP, Potter KD. Exploring the pseudo-ductility of aligned hybrid discontinuous composites using controlled fibre-type arrangements. Compos A Appl Sci Manuf 2018;107:592–606. https://doi.org/10.1016/j.compositesa.2017.11.028.
[210] Czél G, Pimenta S, Wisnom MR, Robinson P. Demonstration of pseudo-ductility in unidirectional discontinuous carbon fibre/epoxy prepreg composites. Compos Sci Technol 2015;106:110–9. https://doi.org/10.1016/j.compscitech.2014.10.022.
[211] Taketa I, Okabe T, Kitano A. A new compression-molding approach using unidirectionally arrayed chopped strands. Compos A Appl Sci Manuf 2008;39: 1884–90. https://doi.org/10.1016/j.compositesa.2008.09.012.
[212] Li Y, Pimenta S, Singgih J, Nothdurfter S, Schuffenhauer K. Experimental investigation of randomly-oriented tow-based discontinuous composites and their equivalent laminates. Compos A Appl Sci Manuf 2017;102:64–75. https://doi.org/10.1016/j.compositesa.2017.06.031.
[213] Henry J, Pimenta S. Increasing damage tolerance in composites using hierarchical brick-and-mortar microstructures. J Mech Phys Solids 2018;118:322–40. https://doi.org/10.1016/j.jmps.2018.06.003.
[214] Rodríguez-García V, de Villoria RG. Automated manufacturing of bio-inspired carbon-fibre reinforced polymers. Compos. B. Eng. 2021;215:108795. https://doi.org/10.1016/J.COMPOSITESB.2021.108795.
[215] Begley MR, Philips NR, Compton BG, Wilbrink DV, Ritchie RO, Utz M. Micromechanical models to guide the development of synthetic 'brick and mortar' composites. J Mech Phys Solids 2012;60:1545–60. https://doi.org/10.1016/j.jmps.2012.03.002.
[216] Bachmann B, Maldonado J, Giger L, Masania K, Dransfeld C, Eguémann N. Experimental study of the stress transfer in discontinuous composites on the basis of a unit cell model. ICCM 20 - 20th International Conferences on Composite Materials; Copenhagen, Denmark2015. https://www.iccm-central.org/Proceedings/ICCM20proceedings/papers/paper-4113-3.pdf.
[217] Ravindran AR, Ladani RB, Wu S, Wang CH, Mouritz AP. Bioinspired design optimization for pseudo-ductility in platelet fibre laminates. Compos A Appl Sci Manuf 2023;168:107494. https://doi.org/10.1016/j.compositesa.2023.107494.
[218] Anthony DB, Bacarreza Nogales OR, Shaffer MSP, Bismarck A, Robinson P, Pimenta S. Pseudo-ductile failure mechanism introduced into finger jointed thermoplastic PES interleaved CFRC. ECCM 18 - 18th European Conference on Composite Materials; Athens, Greece2018. https://www.researchgate.net/publication/326232936_Pseudo-ductile_failure_mechanism_introduced_into_finger_jointed_thermoplastic_PES_interleaved_CFRC.
[219] Henry J, Pimenta S. Bio-inspired non-self-similar hierarchical microstructures for damage tolerance. Compos Sci Technol 2020:108374. https://doi.org/10.1016/j.compscitech.2020.108374.
[220] Sun J, Bacarreza O, Robinson P. Pseudo ductility in quasi-isotropic CFRP through ply weakening. ICCM 21 - 21st International Conferences on Composite Materials; Xi'an, China2017. https://www.iccm-central.org/Proceedings/ICCM21proceedings/papers/4101.pdf.
[221] Bacarreza O, Maidl S, Robinson P, Shaffer MSP. Exploring the use of friction to introduce ductility in composites. ICCM 21 - 21st International Conferences on Composite Materials; Xi'an, China2017. https://www.iccm-central.org/Proceedings/ICCM21proceedings/papers/3653.pdf.
[222] Ichenihi A, Li W, Gao Y. Damage analysis of combined continuous and discontinuous thin-ply carbon/glass hybrid composite using acoustic emission. Polym Compos 2021;42:6764–76. https://doi.org/10.1002/PC.26337.
[223] Ichenihi A, Li W, Zhe L. Numerical and digital image correlation analysis of tensile behavior of thin-ply hybrid laminates with discontinuous carbon sandwiched by continuous glass and carbon. J Compos Mater 2022;56:373–86. https://doi.org/10.1177/00219983211056560.
[224] Sanadi AR, Piggott MR. Interfacial effects in carbon-epoxies - Part 1 Strength and modulus with short aligned fibres. J Mater Sci 1985;20:421–30. https://doi.org/10.1007/BF01026510.
[225] University of Bristol. HiPerDiF (high performance discontinuous fibre) [Available from: https://www.bristol.ac.uk/composites/research/hiperdif/.
[226] Yu H, Potter KD, inventors Method and apparatus for aligning discontinuous fibres patent EP2986768B1. 2014.
[227] University of Delaware. TuFF - tailored universal feedstock for forming [Available from: https://www.ccm.udel.edu/research/program-highlights/tuff/.
[228] Tierney J, Vanarelli A, Heider D, Gillespie Jr JW, inventors Aligned discontinuous fiber preforms, composites and systems and processes of manufacture patent US10669659B2. 2020.
[229] Liu Z, Turner TA, Wong KH, Pickering SJ. Development of high performance recycled carbon fibre composites with an advanced hydrodynamic fibre alignment process. J Clean Prod 2021;278:123785. https://doi.org/10.1016/J.JCLEPRO.2020.123785.
[230] Yarlagadda S, Deitzel J, Heider D, Tierney J, Gillespie Jr JW. Tailorable Universal Feedstock for Forming (TUFF): Overview and Performance. SAMPE2019. https://sampe.knack.com/technical-papers#home/technicalpaperdetails/5cb7823171efac0cb6e45ab2/.
[231] Yu H, Longana ML, Grail G, Pimenta S, Robinson P, Wisnom MR, Potter KD. Aligned short fibre composites with nonlinear behaviour. ICCM 20 - 20th International Conferences on Composite Materials2015. https://www.iccm-central.org/Proceedings/ICCM20proceedings/papers/paper-4113-1.pdf.
[232] Kandemir A, Longana ML, Panzera TH, del Pino GG, Hamerton I, Eichhorn SJ. Natural Fibres as a Sustainable Reinforcement Constituent in Aligned Discontinuous Polymer Composites Produced by the HiPerDiF Method. Materials 2021;14(8):17. https://doi.org/10.3390/ma14081885.
[233] Nishikawa M, Okabe T, Takeda N. Periodic-cell simulations for the microscopic damage and strength properties of discontinuous carbon fiber-reinforced plastic composites. Adv Compos Mater 2009;18:77–93. https://doi.org/10.1163/156855108X399974.
[234] Okabe T, Motani T, Nishikawa M, Hashimoto M. Numerical simulation of microscopic damage and strength of fiber-reinforced plastic composites. Adv Compos Mater 2012;21:147–63. https://doi.org/10.1080/09243046.2012.688495.
[235] Henry J, Pimenta S. Virtual testing framework for hybrid aligned discontinuous composites. Compos Sci Technol 2018;159:259–72. https://doi.org/10.1016/j.compscitech.2017.12.007.
[236] Blaker JJ, Anthony DB, Tang G, Shamsuddin SR, Kalinka G, Weinrich M, et al. Property and Shape Modulation of Carbon Fibers Using Lasers. ACS Appl Mater Interfaces 2016;8:16351–8. https://doi.org/10.1021/acsami.6b05228.
[237] Parratt NJ, Potter KD. Mechanical behaviour of intimately-mixed hybrid composites. ICCM 3 - 3rd International Conferences on Composite Materials; Paris, France1980. https://iccm-central.org/Proceedings/ICCM3proceedings/papers/ICCM3_V1_24.pdf.
[238] Richter H. Single fibre and hybrid composites with aligned discontinuous fibres in polymer matrix. ICCM 3 - 3rd International Conferences on Composite Materials; Paris, France1980. https://iccm-central.org/Proceedings/ICCM3proceedings/papers/ICCM3_V1_29.pdf.
[239] Longana ML, Yu H, Lee J, Pozegic TR, Huntley S, Rendall T, et al. Quasi-isotropic and pseudo-ductile highly aligned discontinuous fibre composites manufactured with the HiPerDiF (High Performance Discontinuous Fibre) technology. Materials 2019;12. https://doi.org/10.3390/MA12111794.
[240] Yu H, Longana M, Swolfs Y, Wisnom M, Potter K. Hybrid effect of carbon/glass composites as a function of the strength distribution of aligned short carbon fibres. ECCM 17 - 17th European Conference on Composite Materials, Munich, Germany, 26-30 June2016. https://research-information.bris.ac.uk/en/publications/hybrid-effect-of-carbonglass-composites-as-a-function-of-the-stre.
[241] Henry J, Pimenta S. Modelling hybrid effects on the stiffness of aligned discontinuous composites with hybrid fibre-types. Compos Sci Technol 2017;152: 275–89. https://doi.org/10.1016/j.compscitech.2017.08.017.
[242] Jalalvand M. On the stiffness of intermingled discontinuous hybrid composites. Composites 2015: V ECCOMAS Thematic Conference on the Mechanical Response of Composites; Bristol, UK2015. https://research-information.bris.ac.uk/en/publications/on-the-stiffness-of-intermingled-discontinuous-hybrid-composites.
[243] Finley JM, Shaffer MSP, Pimenta S. Data-driven intelligent optimisation of discontinuous composites. Compos Struct 2020;243:112176. https://doi.org/10.1016/j.compstruct.2020.112176.
[244] Pimenta S, Henry J, Finley J. The effect of randomness at the micro-scale on failure of composites. ICCM 21 - 21st International Conferences on Composite Materials; Xi'an, China2017. https://www.iccm-central.org/Proceedings/ICCM21proceedings/papers/4289.pdf.
[245] Tang J, Swolfs Y, Longana ML, Yu HN, Wisnom MR, Lomov SV, et al. Hybrid composites of aligned discontinuous carbon fibers and self-reinforced

polypropylene under tensile loading. Compos A Appl Sci Manuf 2019;123: 97–107. https://doi.org/10.1016/j.compositesa.2019.05.003.
[246] Longana ML, Yu H, Jalalvand M, Wisnom MR, Potter KD. Aligned discontinuous intermingled reclaimed/virgin carbon fibre composites for high performance and pseudo-ductile behaviour in interlaminated carbon-glass hybrids. Compos Sci Technol 2017;143:13–21. https://doi.org/10.1016/j.compscitech.2017.02.028.
[247] Longana ML, Yu H, Hamerton I, Potter KD. Development and application of a quality control and property assurance methodology for reclaimed carbon fibers based on the HiPerDiF (High Performance Discontinuous Fibre) method and interlaminated hybrid specimens. Adv Manuf Polym Compos Sci 2018;4:48–55. https://doi.org/10.1080/20550340.2018.1456504.
[248] Longana M, Ondra V, Yu H, Potter K, Hamerton I. Reclaimed carbon and flax fibre composites: manufacturing and mechanical properties. Recycling 2018;3:52. https://doi.org/10.3390/recycling3040052.
[249] Jalalvand M, Czél G, Wisnom MR. Reducing the Notch Sensitivity of Quasi-Isotropic Layups using Thin-Ply Hybrid Laminates. In: Xiao X, Loos A, Liu D, editors. Proceedings of the American Society for Composites: Thirtieth Technical Conference; 8-10 September 2014.; San Diego: Destech Publications, Inc; 2015. p. 121-9. https://research-information.bris.ac.uk/ws/portalfiles/portal/71765404/MJalalvand_ASC_Notch_Sensitivity_Suppression_.pdf.
[250] Fotouhi M, Jalalvand M, Wisnom MR. Notch insensitive orientation-dispersed pseudo-ductile thin-ply carbon/glass hybrid laminates. Composites Part a-Applied Science and Manufacturing 2018;110:29–44. https://doi.org/10.1016/j.compositesa.2018.04.012.
[251] Sapozhnikov SB, Lomov SV, Swolfs Y, Carvelli V. Deformation and failure of pseudo-ductile quasi-isotropic all-carbon hybrid FRPS with an open hole under tension. Compos Pt B-Eng 2022;237:11. https://doi.org/10.1016/j.compositesb.2022.109870.
[252] Fotouhi M, Jalalvand M, Wu X, Wisnom MR. Bearing and bearing-bypass of pseudo-ductile thin-ply carbon/glass hybrids. ICCS21 2018.
[253] Fotouhi M, Jalalvand M, Xu X, Wisnom MR. Compact tension test behaviour of Pseudo-ductile thin-ply carbon/glass hybrids. In: 21st International Conference on Composite Structures: ICCS21; 2018.
[254] Nijs A, Selezneva M, Swolfs Y, Hirano N, Taketa I, Karaki T, et al. Notch-sensitivity of hybrid carbon-fibre/self-reinforced polypropylene composites. Compos Sci Technol 2020;200. https://doi.org/10.1016/j.compscitech.2020.108422.
[255] Wu X, Fuller JD, Wisnom MR. Open-hole response of pseudo-ductile thin-ply angle-ply laminates. 17th European Conference on Composite Materials (ECCM17); 26-30 June 2016; Munich2016. - https://www.scopus.com/inward/record.uri?eid=2-s2.0-84989353311&partnerID=40&md5=fae97f2d8aecb99855e2e9bde0485fba.
[256] Wu X, Fuller J, Fotouhi M, Wisnom M. Bearing failure of pseudo-ductile thin ply angle-ply laminates. 18th European Conference on Composite Materials (ECCM18); 24-28 June 2018; Athens, Greece2018.